WARNING
THIS IS
CITY PROPERTY
DO NOT DAMAGE OR STEAL

READ THE LAW
CALIFORNIA EDUCATION CODE
Section 23321
Form 170 3-49

JET PROPULSION

A publication of the
AMERICAN ROCKET SOCIETY
Research and Development

VOLUME 27 DECEMBER 1957 NUMBER 12

SPECIMEN

ANNUAL INDEX—Volume 27, January–December 1957 (see page 1268)

Optimum Burning Program as Related to Aerodynamic Heating for a Missile Traversing the Earth's Atmosphere . . . . . *Angelo Miele* 1231

The Mixing of Unbounded Coaxial Compressible Streams . . . . . *D. Roger Willis and Irvin Glassman* 1241

Solution of the Transient Heat-Conduction Equation for an Insulated, Infinite Metal Slab . . . . . *John H. Grover and William H. Holter* 1249

TECHNICAL NOTES

Hypersonic Conical Shocks for Dissociated Air in Thermodynamic Equilibrium . . . *Saul Feldman* 1253

Addendum to 'Stagnation Point Heat Transfer for Hypersonic Flow' . . . . *Mary F. Romig* 1255

Impact Points of Ballistic Rockets . . . . . *R. E. Roberson* 1256

Addendum to 'Heat Transfer to Satellite Vehicles Re-entering the Atmosphere' . . . . . *R. W. Detra, N. H. Kemp and F. R. Riddell* 1256

Studies in a New Type of Flat Flame Burner . . . . *William T. Biedler III and H. E. Hoelscher* 1257

Comments on the Powered Flight Trajectory of a Satellite . . . . . *Theodore N. Edelbaum* 1260

Some Decomposition Products of Normal Propyl Nitrate . . . *S. A. Greene and L. J. Gordon* 1261

Thermal Conductivity and Prandtl Numbers for Nonpolar Polyatomic Gases at High Temperatures . . . . . *Eldon L. Knuth* 1262

Optimal Rocket Trajectories . . . . . *D. F. Lawden* 1263

Note on 'Take-off From Satellite Orbit' . . . . . *J. B. Peterson* 1263

The Performance of a Rocket With Tapered Exhaust Velocity . . . . . *Howard S. Seifert* 1264

A Flow Reactor for High-Temperature Reaction Kinetics . . . . . *L. Crocco, I. Glassman and I. E. Smith* 1266

DEPARTMENTS

Book Reviews 1272 New Patents 1274 Technical Literature Digest 1278

rocket power
from reasoning power

A *reasoning* mind—man has always found this his most useful weapon when venturing into unknown fields. Today's frontier—one of the greatest unknowns ever faced by man—lies in outer space.

RMI, America's *first* rocket family, is uniquely qualified to help our country conquer the new frontier. For this project will require more powerful and more efficient rocket propulsion systems than any yet designed. And RMI's experience in the rocket power field extends back over 15 years . . . years in which RMI scientists and engineers pooled their reasoning power and knowledge to develop entirely new methods of propulsion and to produce rocket powerplants for dozens of military vehicles.

With this backlog of experience—and with an increasing staff of imaginative, reasoning engineers—RMI continues to blaze trails in many fields of rocket power: supersonic manned aircraft . . . versatile helicopters . . . catapults and test sleds . . . and missiles for defense and space exploration.

Engineers, Scientists—Perhaps you, too, can work with America's *first* rocket family. You'll find the problems challenging, the rewards great.

Power for Progress

RMI®

REACTION MOTORS, INC.

A MEMBER OF THE OMAR TEAM

DENVILLE, NEW JERSEY

4874

SCIENCE AND TECHNOLOGY
DEC 23 1957

LINO-WRIT® 4...

fastest | toughest | thinnest

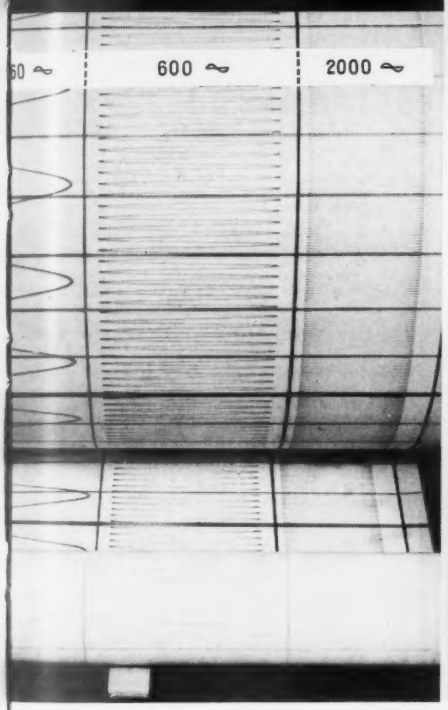

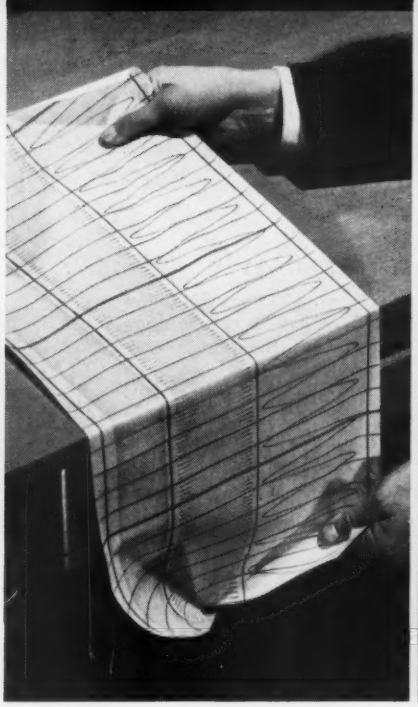

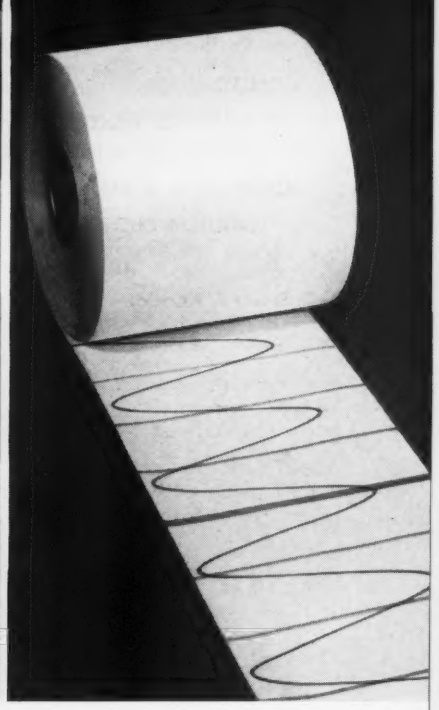

FASTEST—Lino-Writ 4 is the fastest oscillographic paper you can use—and the paper with the widest range. As shown by this photograph, you can record frequencies from 60 to 2000 cps *on the same roll.*

TOUGHEST—Snap it, crinkle it, bend it—and Du Pont Lino-Writ 4 springs back like new . . . with its valuable record intact! Its all-rag base not only makes it rugged, but also makes it *whitest,* easiest to read.

THINNEST—You get more paper on a standard roll. This roll holds 475 feet of Lino-Writ 4. Roll with same outside diameter holds only 250 feet of standard-weight paper. Translucence permits quick duplication in standard equipment.

SPLICE-FREE TOO!—Whatever speed you require, whatever thickness is best for you, whatever length roll you can use . . . you can get Lino-Writ splice-free, at no extra cost. Lino-Writ 1 for low frequency recording. Lino-Writ 2 for mid-range recording. Lino-Writ 3 for high frequency recording. New Lino-Writ 4, the fastest, toughest, thinnest photorecording paper you can use.

E. I. du Pont de Nemours & Co. (Inc.), Photo Products Dept., Wilmington 98, Delaware. In Canada: Du Pont Company of Canada (1956) Limited, Toronto.

DU PONT
REG. U. S. PAT. OFF.
Better Things for Better Living
. . . through Chemistry

DU PONT OSCILLOGRAPHIC PRODUCTS
for Functional Photography
Photography with a purpose . . . not an end in itself, but a means to an end.

JET PROPULSION

A publication of the

AMERICAN ROCKET SOCIETY

Research and Development

IRWIN HERSEY—DIRECTOR OF PUBLICATIONS

EDITOR MARTIN SUMMERFIELD

ASSISTANT EDITOR STANLEY BEITLER

ART EDITOR JOHN CULIN

ASSOCIATE EDITORS

ALI BULENT CAMBEL, *Northwestern University*
IRVIN GLASSMAN, *Princeton University*
M. H. SMITH, *Princeton University*

CONTRIBUTORS

MARSHALL FISHER, *Princeton University*
GEORGE F. McLAUGHLIN

ADVERTISING & PROMOTION MANAGER

WILLIAM CHENOWETH

ADVERTISING REPRESENTATIVES

D. C. Emery & Associates
155 East 42 St., New York, N. Y.
Telephone: Yukon 6-6855

James C. Galloway & Co.
6535 Wilshire Blvd., Los Angeles, Calif.
Telephone: Olive 3-3223

Jim Summers & Asssociates
35 E. Wacker Dr., Chicago, Ill.
Telephone: Andover 3-1154

R. F. and Larry Pickrell
318 Stephenson Bldg., Detroit, Mich.
Telephone: Trinity 1-0790

Harold Short
Holt Rd., Andover, Mass.
Telephone: Andover 2212

Louis J. Bresnick
304 Washington Ave., Chelsea 50, Mass.
Telephone: Chelsea 3-3335

AMERICAN ROCKET SOCIETY

Founded 1930

OFFICERS

President — Robert C. Truax
Vice-President — George P. Sutton
Executive Secretary — James J. Harford
Secretary — A. C. Slade
Treasurer — Robert M. Lawrence
General Counsel — Andrew G. Haley

BOARD OF DIRECTORS

Terms expiring on dates indicated

Krafft Ehricke, 1959
Andrew G. Haley, 1957
S. K. Hoffman, 1958
H. W. Ritchey, 1959
Milton W. Rosen, 1957
H. S. Seifert, 1958
John P. Stapp, 1959
K. R. Stehling, 1958

Wernher von Braun, 1957

TECHNICAL DIVISION CHAIRMEN

David G. Simons, Human Factors
John J. Burke, Instrumentation and Guidance
Edward N. Hall, Liquid Rocket
John F. Tormey, Propellants and Combustion
Brooks T. Morris, Ramjet
William L. Rogers, Solid Rocket

Krafft A. Ehricke, Space Flight

Scope of JET PROPULSION

This Journal is a publication of the American Rocket Society devoted to the advancement of the field of jet propulsion through the dissemination of original papers disclosing new knowledge or new developments. As used herein, the term "jet propulsion" embraces all engines that develop thrust by rearward discharge of a jet through a nozzle or duct, and thus it includes air-consuming engines and underwater systems as well as rockets. JET PROPULSION is open to contributions dealing not only with propulsion but with other aspects of jet-propelled flight, such as flight mechanics, guidance, telemetering, and research instrumentation. Increasing emphasis will be given to the scientific problems of extraterrestrial flight.

Information for Authors

Manuscripts must be as brief as the proper presentation of the ideas will allow. Exclusion of dispensable material and conciseness of expression will influence the Editors' acceptance of a manuscript. In terms of standard-size double-spaced typed pages, a typical maximum length is 22 pages of text (including equations), 1 page of references, 1 page of abstract, and 12 illustrations. Fewer illustrations permit more text, and vice versa. Greater length will be acceptable only in exceptional cases.

Short manuscripts, not more than one quarter of the maximum length stated for full articles, may qualify for publication as Technical Notes. They may be devoted either to new developments requiring prompt disclosure or to comments on previously published papers. Such manuscripts are usually published within two months of the date of receipt.

Sponsored manuscripts are published occasionally as an ARS service to the industry. A manuscript that does not qualify for publication according to the above-stated requirements as to subject scope or length, but which nevertheless deserves widespread distribution among jet propulsion engineers, may be printed as an extra part of the Journal or as a special supplement if the author or his sponsor will reimburse the Society for actual publication costs. Estimates are available on request. Acknowledgment of such financial sponsorship appears as a footnote on the first page of the article. Publication is prompt since such papers are not in the ordinary backlog.

Manuscripts must be double spaced on one side of paper only with wide margins to allow for instructions to printer. Include a 100 to 200 word abstract. State the authors' positions and affiliations in a footnote on the first page. Do not type equations; write them in ink. Identify unusual symbols or Greek letters for the printer. References are to be grouped at the end of the manuscript and are to be given as follows: for journal articles: authors first, then title, journal, volume, year, page numbers; for books: authors first, then title, publisher, city, edition, and page or chapter numbers. Line drawings must be clear and sharp to make clear engravings. Use black ink on white paper or tracing cloth. Lettering should be large enough to be legible after reduction. Photographs should be glossy prints, not matte or semi-matte. Each illustration must have a legend; legends should be listed in order on a separate sheet.

Manuscripts must be accompanied by written assurance as to security clearance in the event the subject matter lies in a classified area or if the paper originates under government sponsorship. Full responsibility rests with the author.

Submit manuscripts in duplicate (original plus first carbon, with two sets of illustrations) to the Editor, Martin Summerfield, Professor of Aeronautical Engineering, Princeton University, Princeton, N. J. Preprints of papers presented at ARS national meetings are automatically considered for publication.

JET PROPULSION is published monthly by the American Rocket Society, Inc., and the American Interplanetary Society at 20th & Northampton Sts., Easton, Pa., U. S. A. Editorial offices: 500 Fifth Ave., New York 36, N. Y. Price: $12.50 per year, $2.00 per single copy. Entered as second-class matter at the Post Office at Easton, Pa. Notice of change of address should be sent to the Secretary, ARS, at least 30 days prior to publication. Opinions expressed herein are the authors' and do not necessarily reflect the views of the Editors or of the Society.

© Copyright 1957 by the American Rocket Society, Inc.

This is

NATIONAL NORTHERN

...newest AP&CC division

Dedicated to research, development and production in

rocket power technology

Test a rocket motor's performance at 100,000 feet altitude... determine how extremes of temperature affect explosive and propellant charges... develop igniters of maximum sturdiness and reliability. These are typical activities at National Northern Division, West Hanover, Mass., latest addition to the AMERICAN POTASH family. Here, a qualified staff of scientists and technicians conducts research, development, field testing and production of propellants for rockets and missiles, explosives, pyrotechnics, detonators, igniters, squibs, gas generators, fuzes and other items.

Extreme environmental conditions are simulated in the laboratory or encountered in actual field tests on the firing range at West Hanover or the 1900-acre test range at Halifax, Mass. Here, too, AP&CC will extend its facilities for the investigation and development of TRONA* boron, lithium and perchlorate chemicals in high energy fuels.

For more than ten years National Northern has demonstrated its ability to work in close coordination with others. As an integral part of AMERICAN POTASH & CHEMICAL CORPORATION it is ready to go to work for you!

We invite inquiries leading to research and production contracts.

NATIONAL NORTHERN'S CURRENT FIELDS OF ACTIVITY:

ROCKET-MOTOR-IGNITER DEVELOPMENT • GAS GENERATORS • SURVEILLANCE TESTING OF EXPLOSIVES AND AMMUNITION • EFFECT OF ALTITUDE ON PERFORMANCE OF EXPLOSIVES, PROPELLANTS, TRACERS AND INCENDIARY ELEMENTS • DESIGN OF ELECTRIC DETONATORS AND SQUIBS • AIRCRAFT VULNERABILITY TESTS AND EVALUATION • EXPLOSIVE METAL FORMING

Also producers of:

...um & Potassium Chlorates
...ssium and Ammonium Perchlorates
...ental Boron
...um Nitrate
...um Perchlorate

TRONA

American Potash & Chemical Corporation

3030 WEST SIXTH STREET, LOS ANGELES 54, CALIFORNIA
99 PARK AVENUE, NEW YORK 16, NEW YORK
NATIONAL NORTHERN DIVISION

Where Miles are Measured in Thousandths of an Inch

As ballistic missiles go farther and faster, weight becomes an increasingly critical problem. Walls of rocket cases, for example, must be still stronger to withstand higher pressures, yet still thinner to cut "hardware" poundage to a minimum.

Obtaining optimum wall thinness throughout in rockets now being developed is one of M. W. Kellogg's current defense assignments. It is a complex engineering task and demands a highly specialized knowledge of metallurgy, metal fatigue, heat transfer, corrosion, weight-strength relationships, and welding techniques.

The M. W. Kellogg Company has been closely associated with the development and fabrication of rocket cases and components since 1947. Inquiries are invited from organizations wishing to put Kellogg's specialized background to work on specific problems.

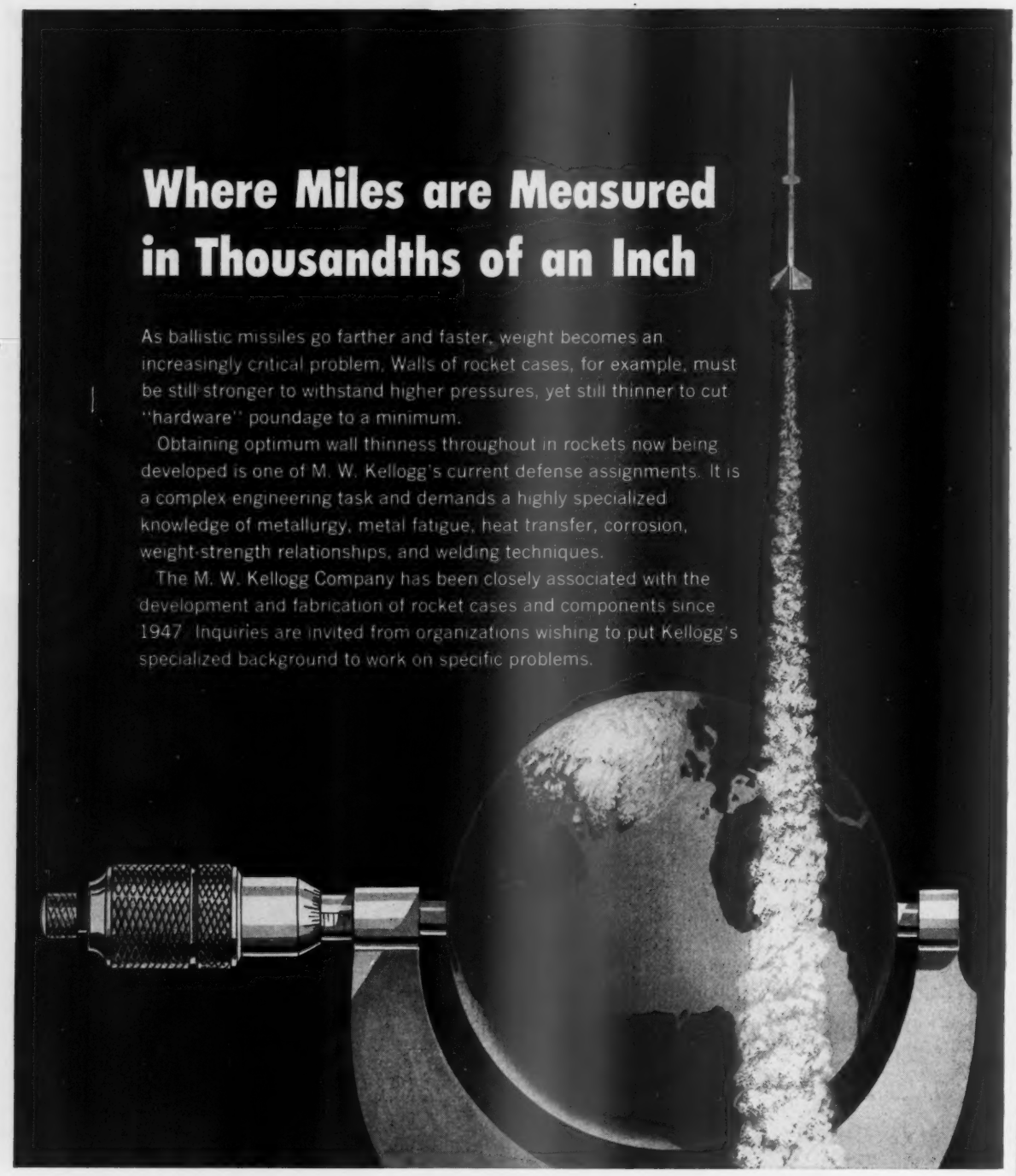

DEFENSE PRODUCTS DIVISION

THE M. W. KELLOGG COMPANY

711 THIRD AVENUE, NEW YORK 17, N. Y.

A SUBSIDIARY OF PULLMAN INCORPORATED

The Canadian Kellogg Company Limited, Toronto • Kellogg International Corporation, London
Companhia Kellogg Brasileira, Rio de Janeiro • Compania Kellogg de Venezuela, Caracas
Kellogg Pan American Corporation, New York • Societe Kellogg, Paris

M KELLOGG W

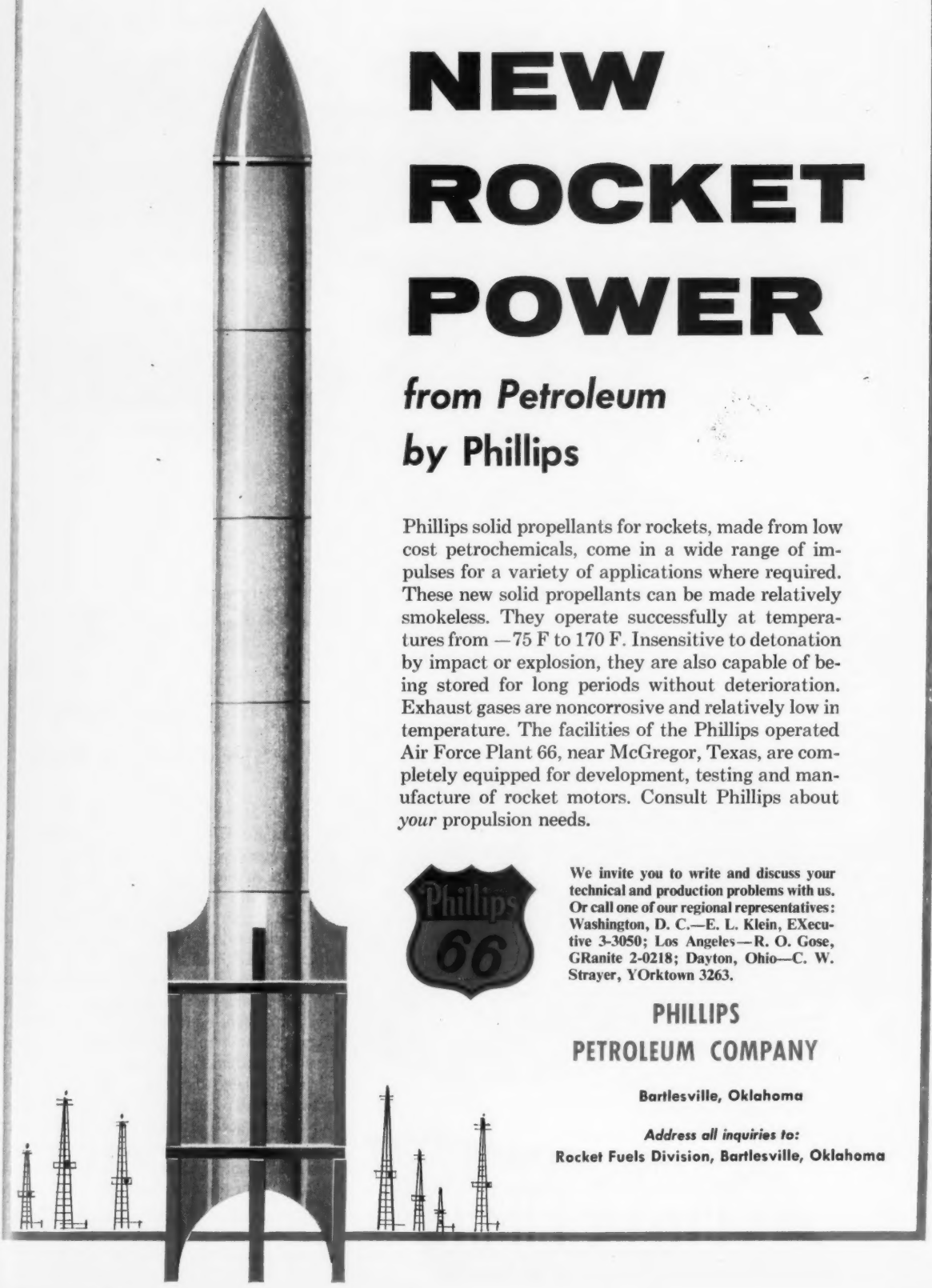

NEW ROCKET POWER

from Petroleum by Phillips

Phillips solid propellants for rockets, made from low cost petrochemicals, come in a wide range of impulses for a variety of applications where required. These new solid propellants can be made relatively smokeless. They operate successfully at temperatures from —75 F to 170 F. Insensitive to detonation by impact or explosion, they are also capable of being stored for long periods without deterioration. Exhaust gases are noncorrosive and relatively low in temperature. The facilities of the Phillips operated Air Force Plant 66, near McGregor, Texas, are completely equipped for development, testing and manufacture of rocket motors. Consult Phillips about *your* propulsion needs.

Phillips 66

We invite you to write and discuss your technical and production problems with us. Or call one of our regional representatives: Washington, D. C.—E. L. Klein, EXecutive 3-3050; Los Angeles—R. O. Gose, GRanite 2-0218; Dayton, Ohio—C. W. Strayer, YOrktown 3263.

PHILLIPS PETROLEUM COMPANY

Bartlesville, Oklahoma

Address all inquiries to:
Rocket Fuels Division, Bartlesville, Oklahoma

Propulsion Research
REFUELING PUMPS

provide dependable high-speed fuel flow

Today, in-flight refueling is the key to America's global air defense – saves time that can speed a plane to any possible target with the Sunday punch of retaliation, in the event of sneak attack. Where seconds can make the difference, America's fighting aircraft are being air-refueled in increasing numbers. At the Propulsion Research Division of Curtiss-Wright, highly trained and experienced specialists are developing a family of compact, high performance pump assemblies which can transfer fuel from tanker to striker aircraft at extremely high rates of speed. Units are available to meet a variety of fuel flow and pressure requirements. Refueling pumps are a good example of the contribution of the Propulsion Research Division to a wide variety of accessory power requirements for our air forces, and for industry.

PROPULSION RESEARCH DIVISION
CURTISS-WRIGHT
CORPORATION • SANTA MONICA, CALIFORNIA

Your Copy Ready Now

As prime producers of unsym-Dimethylhydrazine . . . under the tradename DIMAZINE . . . Westvaco has compiled and kept up-to-date all the data you need on the storage and handling of this advanced rocket fuel.

The third edition of this useful book is just off the press and available now. For your copy, return the coupon below.

DIMAZINE is Westvaco's trademark for unsym-Dimethylhydrazine

Gentlemen: Please forward a copy of your book, *Storage and Handling of Dimazine.*

NAME_____

TITLE_____

COMPANY_____

ADDRESS_____

CITY_____ P.O. ZONE____ STATE_____

fmc®
chemicals

Westvaco Chlor-Alkali Division
FOOD MACHINERY AND CHEMICAL CORPORATION

161 East 42nd Street, New York 17, New York

BECCO® peroxygen chemicals • FAIRFIELD® pesticide compounds • FMC® organic chemicals • NIAGARA® insecticides, fungicides and industrial sulphur • OHIO-APEX® plasticizers and resins • WESTVACO® alkalis, solvents, phosphates, barium and magnesium chemicals

PRECISION FORGINGS By WYMAN-GORDON

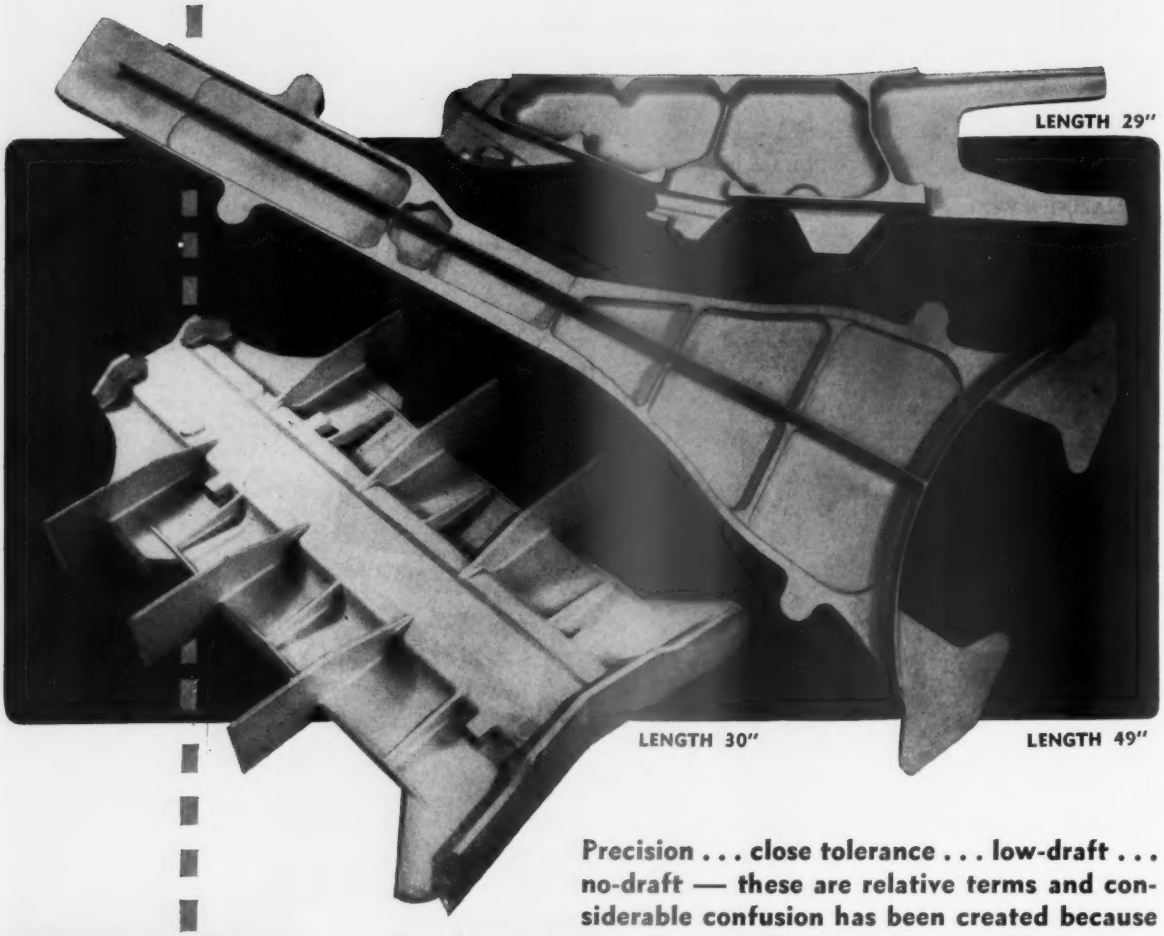

Precision . . . close tolerance . . . low-draft . . . no-draft — these are relative terms and considerable confusion has been created because they have been loosely used. Close tolerances on large forgings have been pioneered by Wyman-Gordon over the years. The degree of precision which is practical now becomes a question of economics.

The forgings illustrated are typical of Wyman-Gordon close tolerance forgings that have been produced in quantity. In solving problems of tolerances, design and metallurgical quality, there is no substitute for Wyman-Gordon experience.

WYMAN-GORDON COMPANY

Established 1883

FORGINGS OF ALUMINUM • MAGNESIUM • STEEL • TITANIUM

WORCESTER 1, MASSACHUSETTS

HARVEY, ILLINOIS • DETROIT, MICHIGAN

TECHNIQUES and DEVELOPMENTS
in oscillographic recording

FROM
SANBORN

CIRCUIT DESIGN AND TYPICAL USES OF THE "150" CARRIER PREAMPLIFIER

One of the most frequently used plug-in front ends for Sanborn 150 Series oscillographic recording systems is the Model 150-1100 Carrier Preamplifier, since with it a "150" system can record such variables as force, temperature, strain, pressure, displacement, velocity, flow, acceleration — or any variable which can be expressed as a suitable input signal by a transducer. The "1100 Carrier" will operate with a variety of different transducers and bridge circuits, which will be mentioned later on.

In the block diagram (Fig. 1), a push-pull oscillator provides an excitation voltage of about 5 v. to the transducer at a standard frequency of 2,400 cycles or optional frequencies of 600 and 1,200 cycles, using plug-in components. This excitation voltage also feeds the Balancing, Calibration and Zero Suppression circuits. (The Balancing controls allow correction of resistive and reactive signal leakage from the transducer, so that at zero load the net signal to the Preamplifier is zero. The Zero Suppression feature permits bucking out a large static load so that a small part of the load can be expanded over the full recording chart. The Gage Factor control allows the zero suppression range to be made equivalent to some convenient transducer load, or the full load rating of the transducer, and also causes the calibration signal to represent 2% of that load.) Transducer output is fed to the transformer through the Gage Factor potentiometer, across which the Balancing-Calibration-Zero Suppression circuits develop a voltage effectively in series with the transducer output. The mixer receives a suppressed carrier AM signal and re-inserts a carrier component, to make its output a conventional AM signal whose modulation represents the transducer load. The modulation signal (whose amplitude and polarity represent magnitude and direction of transducer output) is recovered by the demodulator and fed to the output amplifier, which in turn excites the Driver Amplifier and recording galvanometer of a "150" system.

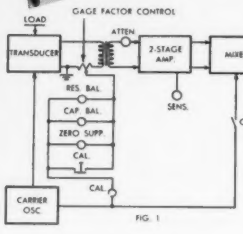

FIG. 1

Transducers which may be used with the Carrier Preamplifier include strain gage half-bridges or full-bridges, commercial resistance or reactance bridges, differential transformers and resistance thermometer bridges. The transducer chosen should provide at least 18.0 microvolts per volt of excitation at the minimum load to be recorded, for a one cm. deflection; impedance should be 100 to 1000 ohms. With strain gages, normal operation provides sensitivities of 50, 20 or 10 micro-inches per inch for each cm. on the recording, depending on the number of active gages. With resistance thermometers, if 1°C. or 2°F. per cm. stylus deflection is sufficient sensitivity, the user can construct his own resistance thermometer by including a 3 ohm coil of copper wire in one arm of an equal arm 100 ohm bridge.

Helpful information about the use of transducers with the 150-1100 Preamplifier is contained in the following Sanborn RIGHT ANGLE articles (reprints on request): Coupling Differential Transformers, Aug. and Nov. 1956; Filter Networks for use with Force Dynamometers, Nov. 1956; Calibration with 1-, 2- or 4-arm Strain Gage Bridges, Aug. 1955; Theoretical and Actual Applications of Bridge Circuits, May and Aug. 1954.

Wing flutter recording to infrared research . . . with the versatile "1100 Carrier"

Today, Carrier Preamp-equipped Sanborn "150" systems are being used for frequency response tests of process control system components; to record shaft deflections of fluid mixing equipment; in infrared research . . . vehicular traffic studies . . . submarine hull vibration measurements. Applications are limited only by the transducers available.

These are applications of only one "150" front-end; eleven more interchangeable, plug-in Preamplifiers increase the scope of Sanborn oscillographic recording systems to meet an almost infinite variety of research, production and field testing requirements. All Sanborn "150" direct writing systems record inkless traces in true rectangular coordinates; all provide 1% linearity; Basic Assemblies — equipped with your choice of Preamps — are available from one- to eight-channels, packaged in vertical cabinets, portable cases, or specially modified housings.

Technical data and help with your oscillographic recording problem are always available from Sanborn.

SANBORN COMPANY
INDUSTRIAL DIVISION
175 Wyman St., Waltham 54, Mass.

EXCELCO

BUILDERS OF MORE LARGE, THIN WALL, HIGH STRENGTH SOLID PROPELLANT ROCKET ENGINE CASES AND NOZZLES FOR DEVELOPMENT PURPOSES THAN ANY OTHER COMPANY IN AMERICA.

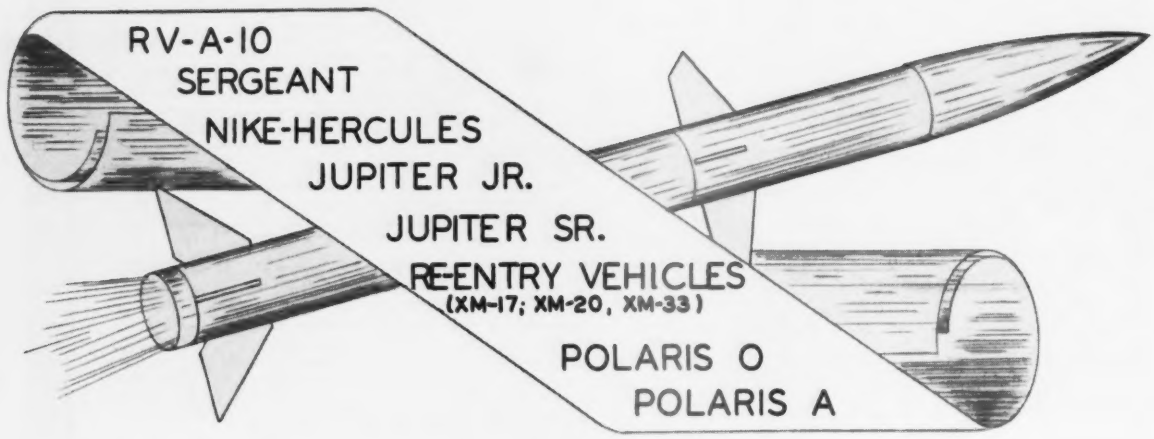

AND MANY OTHER CLASSIFIED PROJECTS

A SMALL EXPERIENCED ORGANIZATION GEARED TO HANDLE YOUR DEVELOPMENT AND PROTOTYPE REQUIREMENTS FOR STATIC AND FLIGHT TESTS IN THE SHORTEST POSS--IBLE TIME.

CALL OR WRITE

EXCELCO DEVELOPMENTS

MILL ST. PHONE 101

SILVER CREEK, NEW YORK

ROKIDE* Spray Coatings Protect the Widest Variety of Parts

Some of many possible applications

BAFFLE PLATES
BEARING SURFACES
CRUCIBLES
METAL ROLLS
FEED ROLLS
NOZZLES
PUMP SHAFTS
GAS TURBINE PARTS
DUCT LININGS
EXHAUST PORTS
THERMOCOUPLE TUBES
THERMOCOUPLE WIRE
GENERAL WIRE
MECHANICAL SEALS

Applying ROKIDE Coating to pump shaft.

The three types of ROKIDE spray coatings — "A" aluminum oxide, "ZS" zirconium silicate and "Z" zirconium oxide — are hard, adherent, crystalline refractory materials. They can be applied to underlying parts, particularly metals, of a wide variety of shapes and sizes.

Parts on which ROKIDE spray coatings are especially useful are those requiring thermal or electrical insulation . . . refractoriness . . . resistance to wear or corrosion . . . high melting points . . . excellent mechanical strength . . . dimensional stability . . . relative chemical inertness.

The coatings are proving their great protective values in a rapidly growing number of applications. Included are not only the newer fields, such as the manufacture of missiles, ram jets, nuclear reactors, etc. Industry in general, including foundries, metal melting, heat and power plants — plus makers of automotive engines, electrical and electronic products, heavy and light chemicals, ceramics, and pumps — are also safeguarding many different parts with these new Norton developments.

Facilities for applying ROKIDE coatings are maintained at Norton Company, Worcester, Mass., and at its plant 2555 Lafayette Street, Santa Clara, California.

For the latest ROKIDE Bulletin, write to NORTON COMPANY, 731 New Bond St., Worcester, Massachusetts.

NORTON
NEW PRODUCTS
Making better products . . . to make your products better

NORTON PRODUCTS
Abrasives • Grinding Wheels
Grinding Machines • Refractories

BEHR-MANNING DIVISION
Coated Abrasives • Sharpening Stones
Behr-cat Tapes

*Trade-Mark Reg. U. S. Pat. Off. and Foreign Countries

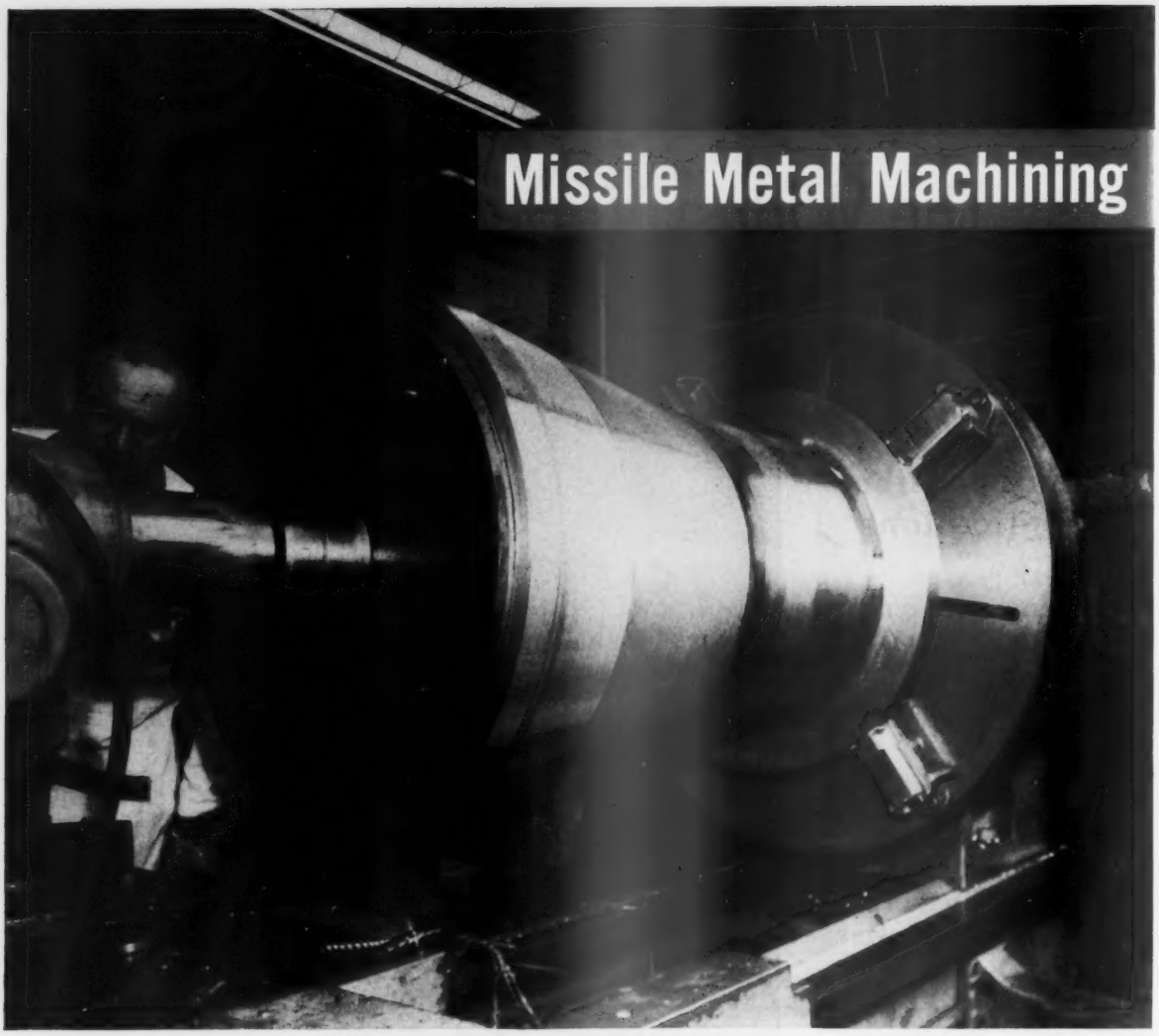

Big Nozzles for Big Rockets

Behind the tailstock you see a Diversey craftsman ready to take a cut that will trace the bottom flange and taper of the O.D. of the nozzle. As nozzles go, this one is big . . . real big. It is the nozzle for one of the large rocket motors.

At Diversey you have the LARGEST FACILITIES exclusively devoted to your missile metal machining problems. You work with fast, precise and progressive technical people who know what works and what won't. Bring your big missile problems to Diversey.

HYDROSPINNING NOW AVAILABLE

A new Hydrospinning Division has been formed at Diversey which uses the latest and largest equipment to produce intricate missile parts.

SEND FOR FREE BOOKLET

LEADERS IN CONTOUR MACHINING

Diversey ENGINEERING COMPANY

10550 WEST ANDERSON PLACE
FRANKLIN PARK, ILLINOIS • *A Suburb of Chicago*

FROM NOSE TO NOZZLE, FROM FIN TO FIN, CONTOUR TURNED PARTS—WITH PRECISION BUILT IN

Optimum Burning Program as Related to Aerodynamic Heating for a Missile Traversing the Earth's Atmosphere

ANGELO MIELE[1]

Douglas Aircraft Co., Inc., Santa Monica, Calif.

The burning program for a rocket-powered missile moving along a rectilinear path is investigated in the light of the thermal effects induced on the missile skin. Part 1 considers the problem of determining the thrust-time relationship which minimizes the difference ΔG between the final and initial values of an arbitrarily specified function $G(t, m, h, V, T)$ of time, mass, altitude, velocity and skin temperature, for the case where the so-called induced drag is negligible with respect to the zero-lift drag. It is shown that the totality of extremal arcs is composed of zero-thrust sub-arcs, sub-arcs to be flown with maximum engine output and variable-thrust sub-arcs. For problems not involving time, an explicit solution is obtained for the optimizing mass flow as a function of the local coordinates of the missile. In Part 2 closed form solutions are derived under the assumptions of isothermal atmosphere, negligible drag, negligible irradiation and constant Stanton number. Particular problems such as minimum increase in skin temperature are treated within the general frame of the present theory. The boundary value problem is investigated, and useful criteria are supplied for constructing extremal paths under various types of boundary conditions. Several numerical examples illustrate the effect of important design parameters on the physical nature of the optimum burning program.

Introduction

THE analysis of the optimum burning program for a rocket-powered vehicle has received considerable attention in recent years. The problem can be stated as follows: A rocket engine, capable of delivering a variable thrust, is applied to a vehicle of given configuration moving along a path of *prescribed* geometry. It is required to determine the thrust programming technique which minimizes the difference $\Delta G = G_f - G_i$ between the final and initial values of a specified function G of the coordinates of the vehicle.

Concerning vertical flight, previous investigations have been carried out by Hamel (1)[2] and by Tsien and Evans (2) for problems where $G = -m$. A broader treatment is due to Miele (3) for problems where $G = G(h,V,m,t)$. With regard to horizontal flight, the papers by Hibbs (4) and by Cicala and Miele (5) must be mentioned in connection with problems where $G = -X$, X denoting horizontal distance. More general questions, of the form $G = G(X,V,m,t)$, have been considered by the author in (6).

In all these investigations, an optimum burning program was determined regardless of thermal effects induced on the missile skin. Mathematically speaking, the only auxiliary conditions accounted for in the variational problem were the equations of motion.

Received July 1, 1957, and presented at the Eighth International Astronautical Congress, Barcelona, Spain, October 7–12, 1957.

[1] Engineering Consultant, Guided Missiles Division. Associate Professor of Aeronautical Engineering, Purdue University, Lafayette, Ind. Mem. ARS.

[2] Numbers in parentheses indicate References at end of paper.

It is to be noted, however, that in the upward flight phase of sounding rockets or of long-range ballistic rockets and, in general, for all vehicles traversing the earth's atmosphere at high speed, important heat transfer phenomena occur from and to the surrounding medium. Specifically, the missile skin receives heat energy from the boundary layer by convection, and from solar, terrestrial and interstellar sources by radiation; in turn, the skin emits radiant energy according to the well-known Stefan-Boltzmann law.

The increase in temperature of the skin is functionally related to the maneuver performed by the vehicle, i.e., functionally related to the thrust program for the case where the geometry of the flight path (or an equivalent condition) is prescribed. For missiles designed for very high Mach numbers, the temperature rise may be such as to dictate structural design, because of the loss of strength of materials. Thus, it becomes important to determine a thrust program which is optimum in the light of heat transfer phenomena. Mathematically speaking, the auxiliary conditions to be considered for the Mayer problem are the equations of motion *and* the heat balance equation (7).

Fundamental Hypotheses and Equations of Motion

The following hypotheses are used throughout the paper:

(a) The rocket-powered vehicle is ideally regarded as a particle of mass m variable with the time t.

(b) The thrust T_* is tangent to the flight path.

(c) The equivalent exit velocity V_e of the rocket engine is regarded as a constant, independent of the operational condition of the engine.

(d) The engine is capable of delivering all mass flows β bounded between a lower value $\beta = 0$ and an upper value $\beta = \beta_{max}$.

(e) The aerodynamic lag is disregarded; i.e., the aerodynamic forces are calculated as in unaccelerated flight.

(f) The acceleration of gravity is a constant.

(g) The trajectory is straight and inclined at an angle θ with respect to a horizontal plane.

(h) The "induced" drag is negligible with respect to the zero-lift drag.[3]

In view of the hypotheses (a, b, g and h) the dynamic behavior of the rocket-powered vehicle is represented with the following set of differential equations

$$J_1 \equiv \dot{m} + \beta = 0 \quad [1]$$

$$J_2 \equiv \dot{h} - V \sin\theta = 0 \quad [2]$$

$$J_3 \equiv \dot{V} + g \sin\theta + (D - T_*)/m = 0 \quad [3]$$

where h is the altitude, V the velocity, g the acceleration of gravity and D the drag. The dot denotes derivative with respect to time.

[3] Notice that the hypotheses (g and h) limit the applicability of the present theory to vertical or near-vertical trajectories, as is the case with a sounding rocket and with some types of ballistic missiles.

The Thrust Function

Because of hypothesis (c) the thrust T_* is expressed as a linear function of the mass flow β

$$T_* = \beta V_e \quad [4]$$

In turn, hypothesis (d) implies that the inequality

$$0 \leq \beta \leq \beta_{\max} \quad [5]$$

be satisfied by the class of all arcs investigated in the present analysis.

The limitation [5] which the size of the engine imposes on the mass flow β has a critical importance in determining the behavior of the solution, as has been recognized in (3, 5, 6). Several devices have been proposed in the literature in order to handle the above inequality. The one considered most appropriate is based on the idea of a parametric representation of the engine characteristics (3 and 6). Such a technique is developed in this article.

The mass flow β is represented as a function of a parameter α having the properties:

(a) For $-\infty \leq \alpha \leq \alpha_1$, the mass flow is $\beta = 0$.

(b) For $\alpha_2 \leq \alpha \leq +\infty$, the mass flow is $\beta = \beta_{\max}$.

(c) For $\alpha_1 \leq \alpha \leq \alpha_2$, a one-to-one correspondence is assumed between β and α.

With the above scheme, α is considered as the *independent parameter of the rocket engine* and is allowed to vary between $-\infty$ and $+\infty$. The mass flow β becomes a *dependent* quantity, varying between 0 and $\beta_{\max}$, according to the scheme of Fig. 1. In turn, the thrust T_* is limited between 0 and $T_{*\max}$ according to Equation [4] and Fig. 1. Notice that the condition $d\beta/d\alpha = 0$ represents either a coasting flight or a flight with maximum engine output. On the other hand, $d\beta/d\alpha \neq 0$ represents any other operating condition of the engine intermediate between the two limiting ones. Notice also that α is *only* a parameter and that there is no necessity of attributing to it any special physical meaning.

Atmospheric Properties

In Part 1 it is assumed that the absolute temperature τ of the atmosphere in which the missile is flying is an arbitrarily specified function of the altitude h. The distribution of static pressure p and speed of sound a vs. altitude are consequently determined. The particular sub-case of an isothermal medium is considered in Part 2.

The Drag Function

Because of the hypothesis (h) the total drag of the missile D is identical with the zero-lift drag. The latter can be decomposed into pressure drag and friction drag. The pressure drag depends on velocity and altitude, even accounting for compressibility and viscosity effects. The friction drag, in turn, depends on velocity, altitude, and on the distribution of skin temperature of the missile. In the present analysis the effects of variations of frictional drag caused by variations in the distribution of skin temperature are neglected. As a consequence, the drag function is represented as

$$D = D(V, h) \quad [6]$$

Heat Transfer Equation

In accordance with the established practice, the calculation of the transient temperature at a point of the missile skin is carried out by assuming that heat transfer is polarized, in the sense that the speed of propagation of thermal effects is infinite in the direction normal to the skin and zero in any direction tangential to the skin.

In the light of the above hypotheses, a one-dimensional analysis becomes possible for *each point* of the missile skin, according to the differential equation

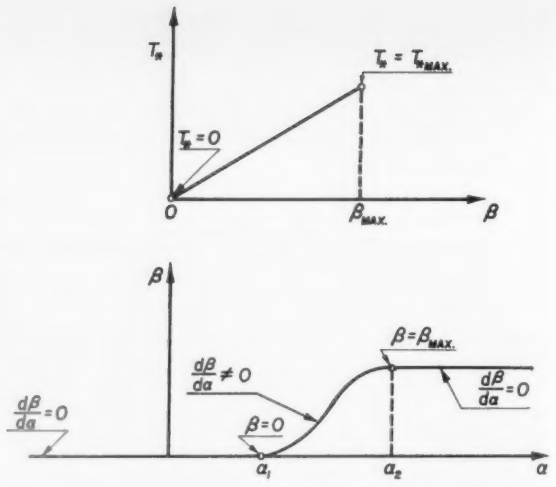

Fig. 1 Parametric representation of the engine characteristics

$$C_s \rho_s \delta_s \dot{T} = Q + \epsilon G_* - \epsilon \sigma_* T^4 \quad [7]$$

where the first member denotes heat gained by the unit area of missile skin per unit time. Terms appearing on the right have the following significance: Q is the heat transferred from boundary layer to skin per unit time and unit area; ϵG_* is the heat received by the skin per unit time and unit area because of irradiation associated with solar, terrestrial and interstellar sources; $\epsilon \sigma_* T^4$ is the radiant heat emitted by the missile skin per unit time and unit area.[4]

In Equation [7], T is the skin temperature; $C_s = C_s(T)$, ρ_s and δ_s are, respectively, the specific heat (referred to the unit mass), density and thickness of the skin; $\epsilon = \epsilon(T)$ is the emissivity, assumed equal to the absorptivity; σ_* is the Stefan-Boltzmann radiation constant; G_* is the incident irradiation associated with solar, terrestrial and interstellar sources and depends, in general, on the altitude h and on the angle of incidence between surface and solar rays. For a given missile design and for a given point of the missile skin, the parameter Q is a complicated function of free-stream Reynolds number, free-stream Mach number and ratio of wall temperature to free-stream temperature. Since the Reynolds number and the Mach number depend on velocity V and altitude h only, one concludes that, for the present problem, Equation [7] has the form

$$J_4 \equiv \dot{T} + \varphi(h, V, T) = 0 \quad [8]$$

$$\varphi = \frac{\epsilon(\sigma_* T^4 - G_*) - Q}{c_s \rho_s \delta_s} \quad [9]$$

A given point of the missile skin is considered in this article, and Equation [8] is applied to determine the transient temperature at such a point. In the case in which the location in question is the one where the most unfavorable thermal effects are expected, it may be anticipated that the predicted skin temperature is higher than the actual one. In fact, the one-dimensional hypothesis embodied in Equation [8] rules out any alleviation effect which the most critical parts of the missile skin may receive from the surrounding elements of matter.

[4] Equation [7] neglects heat transfer phenomena between the skin and other components of the missile.

PART 1. Generalized Solutions

In this section of the paper, the optimum burning program is studied in connection with an arbitrary distribution of atmospheric temperature τ vs. altitude h, a drag function of the form $D = D(V,h)$ and a thermal function of the form $\varphi = \varphi(h,v,T)$.

Variational Approach

The set of differential equations [1–3, 8] is now considered, where $T_* = \beta V_e$, $\beta = \beta(\alpha)$ and $D = D(V,h)$. The time t is assumed as the independent variable. The dependent variables are the mass m, the altitude h, the velocity V, the skin temperature T and the engine parameter α. The number of differential equations is four while the number of unknown functions is five. One degree of freedom is left and an optimum requirement can be, therefore, imposed.

After prescribing the initial coordinates $t_i = 0$, $m_i = m(0)$, $h_i = h(0)$, $V_i = V(0)$, $T_i = T(0)$, and some, but not all, of the final coordinates t_f, m_f, h_f, V_f, T_f, the variational problem, of Mayer type, is stated as follows: Among all sets of functions $m(t)$, $h(t)$, $V(t)$, $T(t)$, $\alpha(t)$ satisfying Equations [1–3, 8] and the prescribed end-conditions, to determine the special set which minimizes the difference ΔG between the final and the initial value of an arbitrarily specified function $G = G(t,m,h,V,T)$ of the coordinates of the missile. Particular cases of this general problem are, for instance, the case $G = T$, minimizing the increase in skin temperature; and the case $G = -m$, minimizing the propellant consumption.

Euler Equations

A set of variable Lagrange multipliers $\lambda_1(t)$, $\lambda_2(t)$, $\lambda_3(t)$, $\lambda_4(t)$ is introduced and the following expression formed

$$F = \sum_{k=1}^{4} \lambda_k J_k \qquad [10]$$

where J_1, J_2, J_3, J_4 denote, respectively, the first members of Equations [1–3, 8]. Since the unknown functions are five in number, one must write five Euler equations. These are written

$$\frac{d}{dt}\left[\frac{\partial F}{\partial \dot{z}_J}\right] = \frac{\partial F}{\partial z_J} \qquad (J = 1, \ldots, 5) \qquad [11]$$

where $z_1 = m$, $z_2 = h$, $z_3 = V$, $z_4 = T$, $z_5 = \alpha$. The explicit form of Equation [11] is

$$\dot{\lambda}_1 = \frac{V_e\beta - D}{m^2}\lambda_3 \qquad [12]$$

$$\dot{\lambda}_2 = \lambda_3 \frac{D_h}{m} + \lambda_4\varphi_h \qquad [13]$$

$$\dot{\lambda}_3 = -\lambda_2 \sin\theta + \lambda_3 \frac{D_v}{m} + \lambda_4\varphi_v \qquad [14]$$

$$\dot{\lambda}_4 = \lambda_4\varphi_T \qquad [15]$$

$$0 = \frac{d\beta}{d\alpha}\left[\lambda_1 - \lambda_3 \frac{V_e}{m}\right] \qquad [16]$$

$$D_h = \frac{\partial D}{\partial h}, \qquad D_v = \frac{\partial D}{\partial V} \qquad [17]$$

$$\varphi_h = \frac{\partial \varphi}{\partial h}, \qquad \varphi_v = \frac{\partial \varphi}{\partial V}, \qquad \varphi_T = \frac{\partial \varphi}{\partial T} \qquad [18]$$

First Integral

Since the fundamental function F, given by Equation [10], is formally independent of the time, the following first integral holds

$$-\lambda_1\beta + \lambda_2 V \sin\theta + \lambda_3\left[\frac{V_e\beta - D}{m} - g\sin\theta\right] - \lambda_4\varphi = C_1 \qquad [19]$$

where C_1 is an integration constant.

Discontinuity of the Eulerian Solution

The Euler Equation [16] is particularly interesting because it shows that the extremal arc is discontinuous, being generally composed of sub-arcs of equation

$$\frac{d\beta}{d\alpha} = 0 \qquad [20]$$

and sub-arcs of equation

$$\lambda_1 - \lambda_3 \frac{V_e}{m} = 0 \qquad [21]$$

According to the parametric representation indicated in Fig. 1, Equation [20] represents either a coasting flight or a flight with maximum engine output. Equation [21], on the other hand, represents a flight condition with a continuous variable-thrust, as shown in the following sections.

Erdmann-Weierstrass Corner Conditions

In view of the discontinuous character of the solution, the Erdmann-Weierstrass corner conditions (8) must be applied. These are continuity conditions to be satisfied *at every corner* of the discontinuous extremal solution by the six quantities

$$\frac{\partial F}{\partial \dot{m}}, \frac{\partial F}{\partial \dot{h}}, \frac{\partial F}{\partial \dot{V}}, \frac{\partial F}{\partial \dot{T}}, \frac{\partial F}{\partial \dot{\alpha}}, \sum_{J=1}^{5} \frac{\partial F}{\partial \dot{z}_J}\dot{z}_J - F \qquad [22]$$

Since F is independent of $\dot{\alpha}$, the continuity of $\partial F/\partial\dot{\alpha}$ is inherently verified at all corner points. The analogous requirement for the remaining five quantities [22] leads to

$$(\lambda_k)_- = (\lambda_k)_+ \qquad [23]$$

$$(C_1)_- = (C_1)_+ \qquad [24]$$

where the subscript $(-)$ denotes a condition *immediately before* the junction and the subscript $(+)$, a condition immediately after the junction. The Erdmann-Weierstrass conditions require, therefore, (a) that the multipliers $\lambda_k (k = 1,2,3,4)$ be *continuous* at all junction points, and (b) that the integration constant C_1 be the *same* for all sub-arcs of the discontinuous extremal solution; this circumstance implies that the quantity $\lambda_1 - (\lambda_3 V_e/m)$ be *zero* immediately before and immediately after *each* junction point.

Boundary Conditions[5]

For the problem under consideration, the boundary conditions include a number of fixed end-point conditions plus a number of natural conditions. The latter must be obtained from the following general *transversality condition*, which is to be *identically satisfied* (8) for all systems of variations $(\delta t, \delta z_J)$ consistent with the prescribed end-conditions

$$[\delta G + \lambda_1\delta m + \lambda_2\delta h + \lambda_3\delta V + \lambda_4\delta T - C_1\delta t]_1^f = 0 \qquad [25]$$

Closed Form Expressions for the Distribution of Lagrange Multipliers

As the analysis of (9) shows, closed form expressions can be derived, yielding the Lagrange multipliers $\lambda_k (k = 1 \ldots 4)$ at all points of the variable-thrust sub-arc, defined by Equation

[5] The present article is a condensed form of the investigation described in (9), where more extensive analytical details are available.

[21]. In this connection, extensive manipulations yield the following results

$$\frac{\lambda_1}{C_2} = V_e \exp\left(\frac{V + gt\sin\theta}{V_e}\right) \quad \ldots\ldots [26]$$

$$\frac{\lambda_2}{C_2} =$$

$$\frac{\frac{C_1}{C_2}\varphi_v + \left[\varphi_v (D + mg\sin\theta) - \varphi\left(\frac{D}{V_e} + D_v\right)\right]\exp\left(\frac{V + gt\sin\theta}{V_e}\right)}{(V\varphi_v - \varphi)\sin\theta} \quad \ldots\ldots [27]$$

$$\frac{\lambda_3}{C_2} = m\exp\left(\frac{V + gt\sin\theta}{V_e}\right) \quad \ldots\ldots [28]$$

$$\frac{\lambda_4}{C_2} =$$

$$\frac{\frac{C_1}{C_2} + \left[D + mg\sin\theta - V\left(\frac{D}{V_e} + D_v\right)\right]\exp\left(\frac{V + gt\sin\theta}{V_e}\right)}{V\varphi_v - \varphi} \quad \ldots\ldots [29]$$

where C_2 is an integration constant. Notice that these equations hold regardless of the boundary conditions and whatever the shape of the function G whose difference ΔG is to be minimized.

Problems Where No Time Condition Is Imposed

For the particular case where the G-function has the form $G = G(m,h,V,T)$ and the final time instant is free of choice ($\delta t_f \equiv$ arbitrary), the transversality condition [25] yields $C_1 = 0$.

Problems Not Involving Heat Transfer

If the G-function has the form $G = G(t,m,h,V)$ and the final temperature is free of choice ($\delta T_f \equiv$ arbitrary), the transversality condition [25] yields $\lambda_{4f} = 0$. Because of this condition at the final point, the Euler equation [15] leads to $\lambda_4 \equiv 0$, at all instants of time. As a consequence, Equation [29] reduces to

$$D + mg\sin\theta - V\left(\frac{D}{V_e} + D_v\right) + \frac{C_1}{C_2}\exp\left[-\frac{V + gt\sin\theta}{V_e}\right] = 0 \quad \ldots [30]$$

and therefore yields, for $\theta = \pi/2$, a result already obtained by the writer in (3).

Problems Not Involving Heat Transfer Where No Time Condition Is Imposed

For the sub-case where the G-function has the form $G = G(m,h,V)$ and both the final skin temperature T_f and the final time instant t_f are free of choice, the simultaneous conditions $\lambda_4 = 0$ and $C_1 = 0$ must be applied. As a consequence, Equation [30] leads to

$$D + mg\sin\theta - V\left(\frac{D}{V_e} + D_v\right) = 0 \quad \ldots\ldots [31]$$

For $\theta = \pi/2$, Equation [31] supplies a result which is implied in the equations already derived by Tsien and Evans (2), for one particular set of boundary conditions.

Optimum Mass Flow for Problems Where No Time Condition Is Imposed

An explicit expression for the optimum acceleration (or for the optimum thrust) can be obtained if the Lagrange multipliers are eliminated. In this connection, Equations [15, 29] yield for $C_1 = 0$

$$\frac{\dot{V}}{g} = \frac{\psi_1 + \psi_2}{\psi_3 + \psi_4} \equiv \psi \quad \ldots\ldots [32]$$

$$\psi_1 = -\sin\theta\,\frac{V(D + V_eD_v) + \frac{V_eV}{g}\,[VD_h + VV_eD_{vh} - V_eD_h]}{V(D + V_eD_v) - V_e[D + mg\sin\theta]} \quad \ldots [33]$$

$$\psi_2 = \frac{VV_e}{g}\,\frac{(\varphi_h - V\varphi_{vh})\sin\theta + \varphi\varphi_{vT} - \varphi_v\varphi_T}{\varphi - V\varphi_v} \quad \ldots [34]$$

$$\psi_3 = V\,\frac{D + 2V_eD_v + V_e^2D_{vv}}{V(D + V_eD_v) - V_e(D + mg\sin\theta)} \quad \ldots [35]$$

$$\psi_4 = VV_e\,\frac{\varphi_{vv}}{\varphi - V\varphi_v} \quad \ldots\ldots [36]$$

$$D_{vv} = \frac{\partial^2 D}{\partial V^2};\ D_{vh} = \frac{\partial^2 D}{\partial V\partial h} \quad \ldots\ldots [37]$$

$$\varphi_{vv} = \frac{\partial^2\varphi}{\partial V^2};\ \varphi_{vh} = \frac{\partial^2\varphi}{\partial V\partial h};\ \varphi_{vT} = \frac{\partial^2\varphi}{\partial V\partial T} \quad \ldots\ldots [38]$$

The drag D and its derivatives depend on velocity and altitude only. In turn, the thermal function φ and its derivatives depend on velocity, altitude and skin temperature. As a consequence, it is concluded that the ψ-function has the form $\psi = \psi(m,h,V,T)$. The instantaneous mass flow at points of the variable-thrust sub-arc of the extremal solution is consequently given by

$$\frac{V_e\beta}{mg} = \sin\theta + \frac{D}{mg} + \psi(m, h, V, T) \quad \ldots\ldots [39]$$

In conclusion, the optimizing mass flow β can either be $\beta = 0$ or $\beta = \beta_{max}$ or can have the value which satisfies Equation [39]. The latter holds whatever be the distribution of atmospheric properties vs. altitude, the drag function D and the thermal function φ; it also holds for all G-functions of the form $G = G(m,h,V,T)$ provided the final time instant is free of choice.

PART 2. Closed Form Solutions

In Part 1, an explicit solution has been obtained for the optimum mass flow. For the variable-thrust sub-arc, this optimum mass flow is defined by Equations [32–39]. Its form, however, is such that analytical solutions of the system composed of heat transfer equation and equations of motion are out of reach. Numerical analyses are in order and digital computers must be used. Prior to any attack of the problem with digital computing equipment, however, it appears desirable to achieve some qualitative understanding of the physical nature of the optimum thrust program, even if drastic hypotheses are necessary to attain such an objective.

Additional Hypotheses

In the following section, closed form solutions are derived for problems where $G = G(m,h,V,T)$. The following hypotheses are used in combination with those previously listed:

(a) An ideally isothermal atmosphere is assumed, i.e., an atmosphere where the speed of sound is constant.

(b) The drag of the missile is considered negligible with respect to thrust and weight ($D = 0$).

(c) Irradiation terms are neglected in the heat balance equation.

(d) Use is made of a *modified* Stanton number St, based on free stream density ρ, free stream velocity V and on a conventional adiabatic wall temperature T_a corresponding to free-stream conditions; such a Stanton number[6] is regarded as a constant; moreover, constant values are also assumed for the thermal properties of air and skin and for the recovery factor r.

In view of hypothesis (a) the distribution of relative density σ vs. altitude h is given by

$$\sigma = \rho/\rho_0 = \exp(-\gamma\bar{h}) \quad [40]$$

$$\bar{h} = gh/a^2 \quad [41]$$

where $\bar{h}$ is a nondimensional altitude, ρ is the absolute density of air at altitude h, and ρ_0 is the absolute density at sea level. Because of the neglect of irradiation terms, the thermal function φ takes the form

$$\varphi = -\frac{Q}{C_s\rho_s\dot{\delta}_s} \quad [42]$$

where Q is the heat input from boundary layer to skin per unit time and unit wetted area. The latter can be rewritten as

$$\frac{Q}{C_p\rho V(T_a - T)} = St \quad [43]$$

$$T_a = \tau\left(1 + \frac{\gamma - 1}{2} rM^2\right) \quad [44]$$

where M is the free-stream Mach number, τ the free-stream temperature and γ the ratio of specific heat at constant pressure C_p to specific heat at constant volume C_v. Simple manipulations yield the following useful form for the thermal function

$$\varphi = K_1\sigma M\left[\frac{T}{\tau} - 1 - K_2M^2\right] \quad [45]$$

$$K_1 = \frac{C_p}{C_s}\frac{\rho_0}{\rho_s}\frac{a}{\delta_s}\tau St \quad [46]$$

$$K_2 = \frac{\gamma - 1}{2} r \quad [47]$$

Integration of the Equations of Motion

Sub-Arc Flown With Maximum Engine Output

Because of the hypotheses of the previous paragraph the sub-arc $\beta = \beta_{max}$ is identified by

$$M + \bar{t} + u\log\bar{m} = C_3 \quad [48]$$

$$\frac{\bar{m}u}{K_3} + \bar{t} = C_4 \quad [49]$$

$$\bar{h} + \frac{\bar{t}^2}{2} + \frac{u^2}{K_3}\bar{m}(1 - \log\bar{m}) = C_5 \quad [50]$$

where $\bar{m} = m/m_i$ is a nondimensional mass, $M = V/a$ the Mach number, $u = V_e/a$ the ratio of exit velocity to atmospheric speed of sound, and $\bar{t} = tg\sin\theta/a$ a nondimensional time. The terms appearing on the right of Equations [48–50] are integration constants and

$$K_3 = \frac{V_e\,\beta_{max}}{gm_i\sin\theta} \quad [51]$$

For the ideal case of a pulse-burning sub-arc ($K_3 = \infty$) Equations [48–50] imply the constancy of the three quantities, $\bar{h}$, $\bar{t}$, and $M + u\log\bar{m}$.

Coasting Sub-Arc

For $\beta = 0$ the equations of motion yield the obvious results

$$\bar{m} = C_6 \quad [52]$$

$$M^2 + 2\bar{h} = C_7 \quad [53]$$

$$\bar{t} + M = C_8 \quad [54]$$

where C_6, C_7, C_8 are integration constants.

Variable Thrust Sub-Arc

For the variable thrust sub-arc, the optimum acceleration reduces to

$$\frac{\dot{V}}{g} = \frac{\gamma\sin\theta}{3}M^2[1 - 3K_4\sigma] \quad [55]$$

$$K_4 = \frac{C_p}{C_s}\frac{\rho_0}{\rho_s}\frac{a^2}{g\dot{\delta}_s}\frac{St}{3\gamma\sin\theta} \quad [56]$$

At this point a change of independent variable is operated in the sense that the relative density σ is now assumed as the new independent variable. Equation [55] is rewritten as

$$\frac{dM}{M} = \left(K_4 - \frac{1}{3\sigma}\right)d\sigma \quad [57]$$

admitting, therefore, the general integral

$$M = C_9\frac{\exp(K_4\sigma)}{\sqrt[3]{\sigma}} \quad [58]$$

where C_9 is a constant. The differential relationship between time and relative density is stated as

$$d\bar{t} = -C_{10}\frac{d\sigma}{\sigma^{2/3}\exp(K_4\sigma)} \quad [59]$$

$$C_{10} = \frac{1}{\gamma C_9} \quad [60]$$

The integration process for Equation [59] leads to[7]

$$\bar{t} = C_{11} - C_{10}A(\sigma) \quad [61]$$

$$A(\sigma) = 3\sqrt[3]{\sigma}\sum_0^\infty(-1)^n\frac{(K_4\sigma)^n}{n!(3n+1)} \quad [62]$$

where C_{11} is a constant. The distribution of mass along the variable-thrust sub-arc is calculated from

$$\bar{m} = C_{12}\exp\left(-\frac{M + \bar{t}}{u}\right) \quad [63]$$

where C_{12} is a constant.

[6] For a given missile design and for a given point of the missile skin, the Stanton number St is a complicated function of free-stream Reynolds number Re, free-stream Mach number M and ratio of wall temperature T to free-stream temperature τ. In spite of this, the following sections of this paper refer to the ideal case where the Stanton number is a constant, independent of M, Re and T/τ. It cannot be denied that the above hypothesis is quite drastic in its nature. Nevertheless, the writer feels that the essential facts of the mechanism of heat transfer are retained in the present idealized scheme. The latter, on the other hand, has the merit of leading to closed form solutions and therefore to clear-cut information on the qualitative nature of the optimum burning program. Moreover, as the subsequent analysis shows, the optimum burning program is affected only in a minor way by the hypothesis concerning the Stanton number.

[7] A discussion of the manipulations leading to Equations [61, 62] can be found in (9). In many practical cases, the term $K_4\sigma$ is at most of order one. As a consequence, no appreciable error is introduced into the results by neglecting the terms of exponent larger than 3 in the expression for $A(\sigma)$.

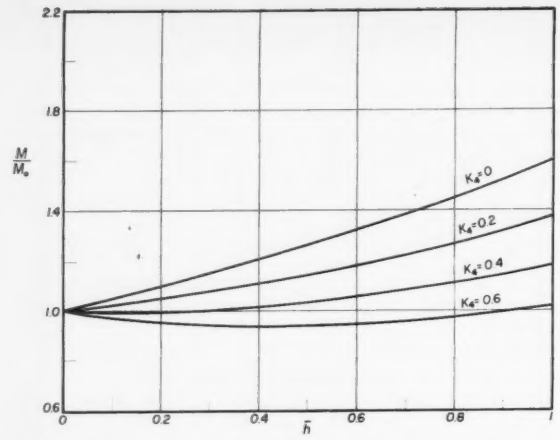

Fig. 2 Mach number-altitude relationship along the variable-thrust sub-arc

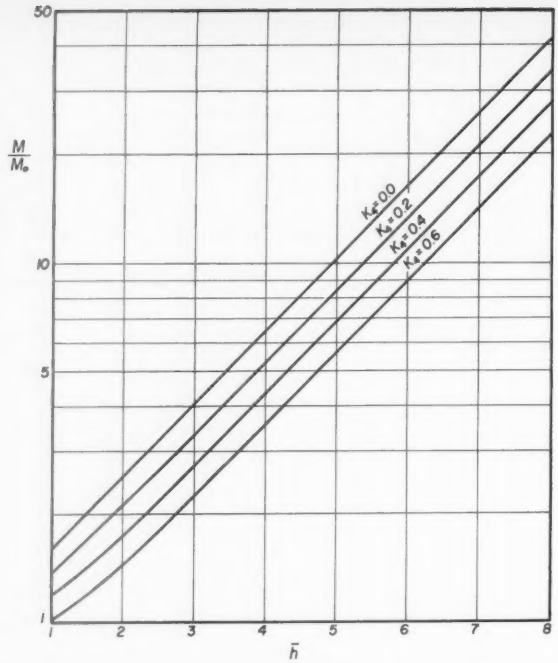

Fig. 3 Mach number-altitude relationship along the variable-thrust sub-arc

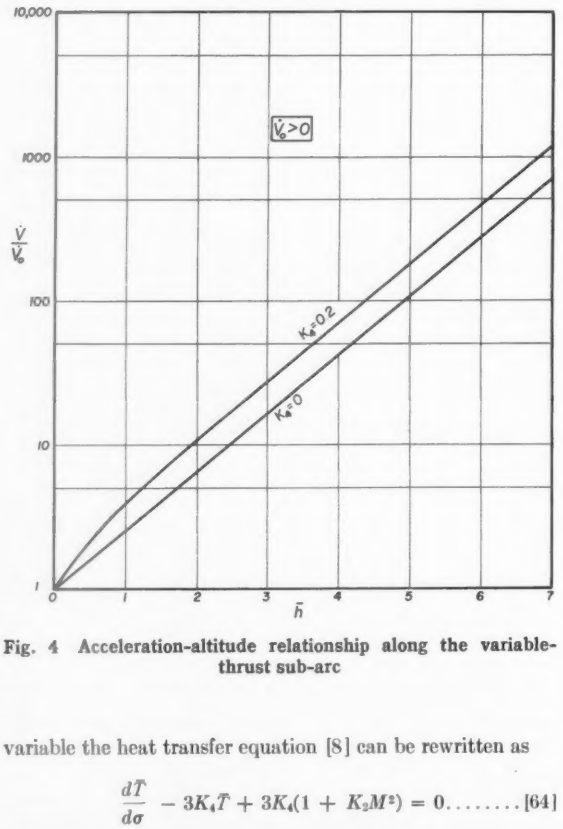

Fig. 4 Acceleration-altitude relationship along the variable-thrust sub-arc

Discussion of Results

As the previous analysis shows, the thermal parameter K_4, defined by Equation [56], is systematically present in the solutions. Such a parameter depends on the thermal properties of air and skin and on the Stanton number, which characterizes the convective process from boundary layer to skin. The lowest value for the above thermal parameter is $K_4 = 0$: It corresponds to the ideal case of a skin of infinite thermal capacity. Increasing values of K_4 are associated with decreasing thickness of skin.

Mach Number-Altitude Relationship

The ratio M/M_0 of Mach number at altitude to Mach number at sea-level is plotted in Figs. 2 and 3 as a function of the nondimensional altitude $\bar{h}$, and of the thermal parameter K_4. For $K_4 < \frac{1}{3}$ (skin of relatively high thermal capacity) the Mach number increases monotonically as the altitude increases. On the other hand, for $K_4 > \frac{1}{3}$ (skin of relatively low thermal capacity) the Mach number initially decreases, has a minimum at the altitude where $\sigma = 1/(3K_4)$ and afterwards increases as the altitude increases; in other words after entering the variable-thrust sub-arc, the velocity of the missile must be decreased to limit the amount of heat transferred from boundary layer to skin in the low altitude region.

Acceleration-Altitude Relationship

The ratio $\dot{V}/\dot{V}_0$ of optimum acceleration at altitude to optimum acceleration at sea level is indicated in Fig. 4 as a function of the altitude $\bar{h}$, for two values of the thermal parameter K_4. The diagram shows that the acceleration increases with such rapidity, as $\bar{h}$ increases, that there is a very definite altitude above which the optimum burning program may become impractical from a structural standpoint. Consider, for instance, a missile whose thermal constant is $K_4 = 0.2$ and assume that the initial acceleration is $\dot{V}_0/g = 0.5$. Assume also that the maximum permissible acceleration is $(\dot{V}/g)_{max} = 15$. As Fig. 4 shows, the optimum burning program can only be used at altitudes below[8] approximately 100,000 ft. Analogously, if it is assumed that the maximum permissible acceleration is $(\dot{V}/g)_{max} = 40$, one concludes that the optimum burning program can only be used at altitudes[8] below 130,000 ft.

Integration of the Heat Transfer Equation

After assuming the relative density σ as the independent variable the heat transfer equation [8] can be rewritten as

$$\frac{d\bar{T}}{d\sigma} - 3K_4\bar{T} + 3K_4(1 + K_2M^2) = 0 \quad \ldots\ldots [64]$$

where $\bar{T} = T/\tau$ is the ratio of skin temperature to free-stream temperature and K_4 is defined by Equation [56]. For a prescribed Mach number-density relationship $M(\sigma)$, the above

[8] The figure in question is based on an ideal isothermal atmosphere where $a = 1000$ ft sec^{-1}.

equation can be regarded as linear in the unknown function $\bar{T}(\sigma)$, yielding the following general integral

$$\bar{T} = 1 + [\text{const} - 3K_2K_4 \int M^2 \exp(-3K_4\sigma)d\sigma] \exp(3K_4\sigma) \quad [65]$$

Sub-Arc Flown With Maximum Engine Output

For this type of sub-arc the temperature equation must be dealt with, in general, by approximate methods. An important exception is represented by the pulse-burning case in which Equation [65] reduces to

$$\bar{T} = C_{13} \quad [66]$$

where C_{13} is a constant.

Coasting Sub-Arc

For the coasting sub-arc, Equation [65] yields

$$\bar{T} = 1 + K_2C_7 + C_{14} \exp(3K_4\sigma) + \frac{2}{\gamma} K_2 C(\sigma) \quad [67]$$

$$C(\sigma) = \log \sigma + [\log(3K_4) - Ei(-3K_4\sigma)] \exp(3K_4\sigma) \quad [68]$$

where C_{14} is a constant and $Ei(-3K_4\sigma)$ is the so-called exponential-integral function, defined as

$$Ei(-3K_4\sigma) = \int_{\infty}^{3K_4\sigma} \frac{\exp(-x)}{x} dx =$$

$$0.5772 + \log(3K_4\sigma) + \sum_{1}^{\infty} (-1)^n \frac{(3K_4\sigma)^n}{n!n} \quad [69]$$

Variable-Thrust Sub-Arc

For the variable-thrust sub-arc the skin temperature-density relationship is supplied by

$$\bar{T} = 1 + [C_{15} - 3K_2K_4C_9^2A(\sigma)] \exp(3K_4\sigma) \quad [70]$$

where C_{15} is an integration constant.

An Upper Limit for the Increase in Skin Temperature

As the subsequent analysis shows, an upper limit can be detected for the increase in skin temperature of a missile which flies according to the optimum burning program. Assume, for instance, that at the moment of entering the variable-thrust sub-arc, the flight condition is represented by $\bar{h} = 0$, $\sigma = 1$, $M = M_0$, $\bar{T} = 1$. The integration constants C_9 and C_{15} are subsequently calculated and Equation [70] rewritten as

$$\frac{\bar{T} - 1}{K_2M_0^2} = 3K_4[A(1) - A(\sigma)] \exp[K_4(3\sigma - 2)] \quad [71]$$

To investigate whether Equation [71] has any stationary points, the condition $d\bar{T}/d\sigma = 0$ is imposed, yielding

$$3K_4\sigma^{3/4} \exp(K_4\sigma)[A(1) - A(\sigma)] = 1 \quad [72]$$

Equation [72] is plotted in Fig. 5 from which the following conclusions are drawn:

(a) For a thermal constant $K_4 < 0.99$ the skin temperature is a monotonically increasing function of the altitude. As a consequence, an upper limit to the skin temperature is supplied by the ideal condition which the missile would attain should the optimum burning program be continued up to $\bar{h} = \infty$, i.e., $\sigma = 0$

$$\frac{\bar{T} - 1}{K_2M_0^2} = 3K_4 A(1) \exp(-2K_4) \quad [73]$$

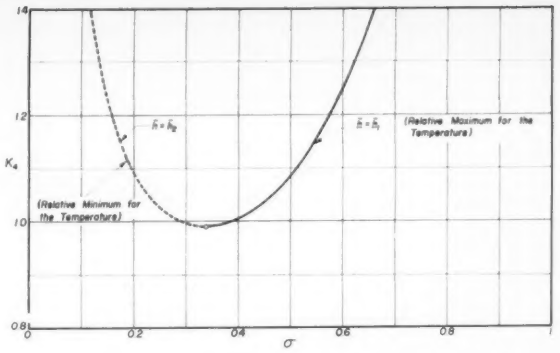

Fig. 5 Altitude where the skin temperature is stationary (variable-thrust sub-arc)

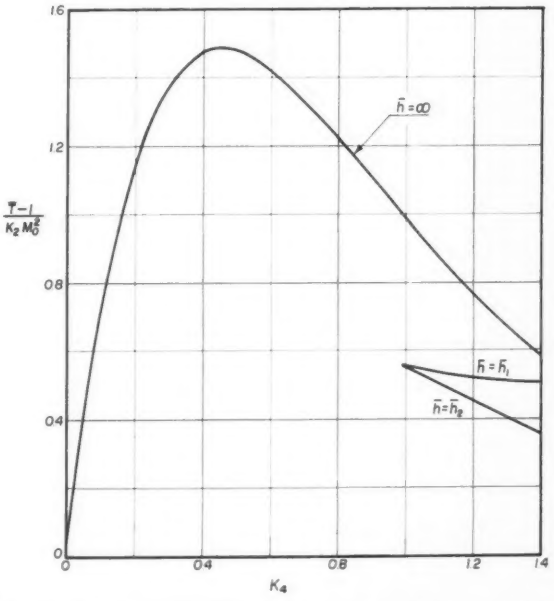

Fig. 6 Skin temperature at $\bar{h} = \infty$ and at stationary points (variable-thrust sub-arc)

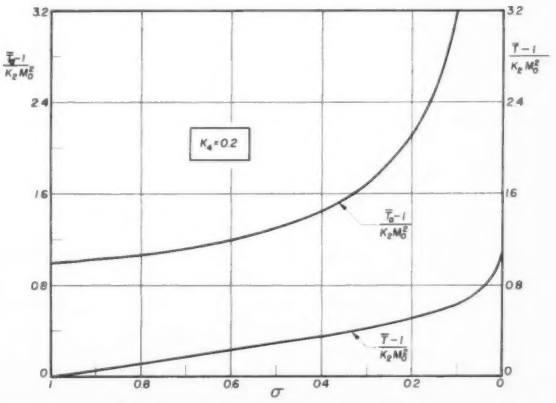

Fig. 7 Adiabatic wall temperature and skin temperature at points of the variable-thrust sub-arc

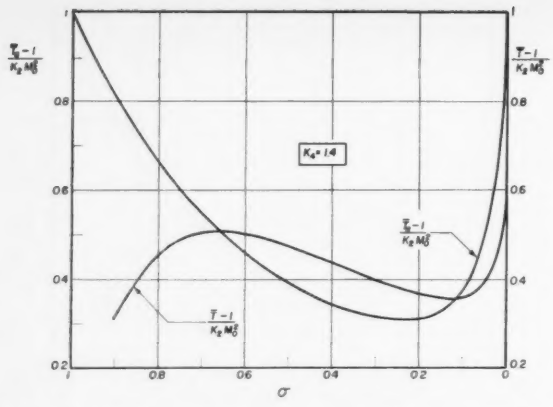

Fig. 8 Adiabatic wall temperature and skin temperature at points of the variable-thrust sub-arc

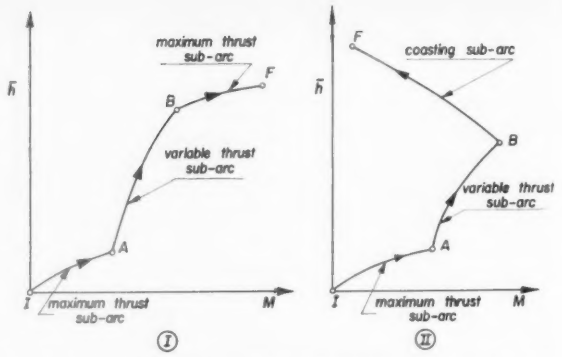

Fig. 9 Combination of sub-arcs for minimum increase in skin temperature

(b) For a thermal constant $K_4 > 0.99$ there are two altitudes at which the skin temperature is stationary, the lower altitude $\bar{h}_1$ corresponding to a relative maximum for the temperature $\bar{T}_1$, the higher altitude $\bar{h}_2$ to a relative minimum $\bar{T}_2$. The temperature rise between sea level and the altitude defined by Equation [72] is supplied by

$$\frac{\bar{T} - 1}{K_2 M_0^2} = \sigma^{-2/3} \exp\,[2K_4(\sigma - 1)] \quad \ldots\ldots\ldots [74]$$

where the density σ is to be consistent with Equation [72].

In Fig. 6 the temperatures defined by Equations [73, 74] are plotted as a function of the thermal constant K_4. As the graph indicates, for $0.99 < K_4 < 1.4$, the stationary condition reached at $\bar{h} = \bar{h}_1$ is not critical and the absolute maximum for the temperature is reached at $\bar{h} = \infty$. To emphasize the significance of the above results, Figs. 7 and 8 have been prepared. They yield the nondimensional skin temperature $\bar{T} = T/\tau$ and boundary layer temperature $\bar{T}_a = T_a/\tau$ as a function of the relative density σ at points of the variable-thrust sub-arc. For a thermal constant $K_4 < \frac{1}{3}$ (for instance $K_4 = 0.2$) the optimum Mach number is a monotonically increasing function of the altitude (Figs. 2 and 3). As a consequence, the boundary layer temperature $\bar{T}_a$ increases with the altitude: Heat energy is continuously transferred from boundary layer to missile skin, as shown in Fig. 7. On the other hand, for a thermal constant $K_4 > 0.99$, i.e., for a skin of relatively low thermal capacity, the Mach number-altitude diagram presents a minimum point. The diagram of the boundary layer temperature, therefore, has also a minimum point. The skin temperature rise becomes such that an *inversion* occurs in the heat transfer process. This interesting phenomenon is shown in Fig. 8 which refers to a thermal constant $K_4 = 1.4$: Heat energy is released from *skin to boundary layer* in the altitude interval where $0.112 < \sigma < 0.657$.

Solution of the Boundary Value Problem

In the previous sections, general solutions have been derived for the problem of minimizing the difference ΔG between the final and the initial value of an arbitrarily specified function $G = G(m,h,V,T)$. It has been shown that the extremal arc is composed of sub-arcs $\beta = 0$, sub-arcs $\beta = \beta_{max}$ and sub-arcs to be flown with regulated thrust.

Now a particular form of the G-function is considered, namely, $G = T$ (minimum increase in skin temperature). In this connection, the boundary value problem is investigated: It consists of determining the special combination of sub-arcs which satisfy a set of prescribed end-conditions, more specifically: $\bar{t}_i = 0, \bar{m}_i = 1, \bar{h}_i = 0, M_i = 0, \bar{T}_i = 1$; $\bar{m}_f \equiv$ given, $M_f \equiv$ given, $\bar{h}_f \equiv$ given.

Two main types of extremal trajectories may exist (9). They are indicated in Fig. 9 with the roman numerals I and II. The trajectories of type I include: An initial sub-arc IA flow with maximum thrust, a central sub-arc AB flown with variable thrust, and a final sub-arc BF flown with maximum thrust. The trajectories of type II differ from the previous ones in so far as the final sub-arc BF involves a coasting flight.

In the following sections the ideal case of an engine capable of delivering all mass flows between 0 and ∞ is considered, for simplicity. The reader, however, may find an extensive treatment in (9), for the case where the maximum thrust is finite.

The ω Function

The following function of the local coordinates of the missile is now defined

$$\omega = \frac{\exp\,(K_4\sigma)}{\sqrt[3]{\sigma}}\,[A(\sigma) - A(1)] - \gamma M[M + u \log \bar{m}] \quad \ldots [75]$$

Let the symbol ω_f denote the value of ω calculated at the final point. As the analysis of (9) points out, the final point F must be reached: (a) With a coasting flight if $\omega_f < 0$; (b) with engine operating at maximum output if $\omega_f > 0$; (c) with regulated thrust if $\omega_f = 0$.

Determination of Corner Points

A fundamental aspect of the boundary value problem is to determine the corner points A and B of the extremal solution. In general, an indirect procedure must be used (9). For the particular case $\beta_{max} = \infty$, however, a direct approach is possible.

Case (I)—The Final Sub-Arc BF Is Flown With Maximum Engine Output

As the analysis of (9) points out, the Mach numbers at points A and B are supplied by

$$M_A = \frac{\exp\,(K_4)}{\gamma}\,\frac{A(\sigma_f) - A(1)}{M_f + u \log m_f} \quad \ldots\ldots [76]$$

$$M_B = \frac{1}{\gamma}\,\frac{A(\sigma_f) - A(1)}{M_f + u \log \bar{m}_f}\,\frac{\exp\,(K_4\sigma_f)}{\sqrt[3]{\sigma_f}} \quad \ldots\ldots [77]$$

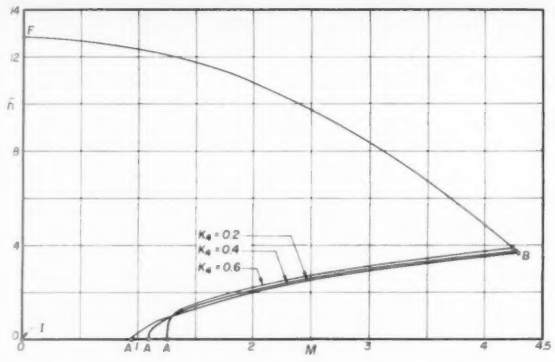

Fig. 10 **Extremal trajectories of type II for different values of the thermal parameter K_4**

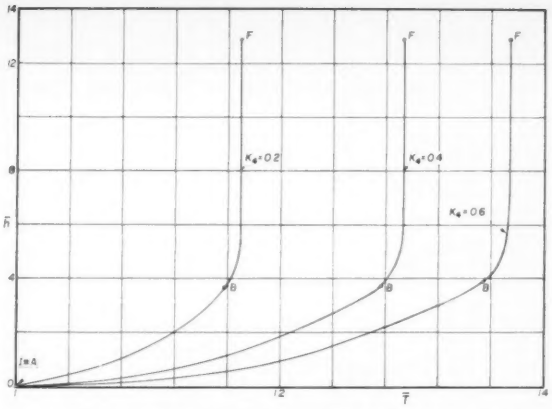

Fig. 11 **Extremal trajectories of type II for different values of the thermal parameter K_4**

Case (II)—The Final Sub-Arc BF Is Flown With Engine Shut-Off

As it is shown in (9) the following transcendental equation determines the relative density at point B

$$-\gamma\sqrt{M_f^2+\frac{2}{\gamma}\log\frac{\sigma_B}{\sigma_f}}\left[u\log\bar{m}_f+\sqrt{M_f^2+\frac{2}{\gamma}\log\frac{\sigma_B}{\sigma_f}}\right]+[A(\sigma_B)-A(1)]\frac{\exp(K_4\sigma_B)}{\sqrt[3]{\sigma_B}}=0 \quad [78]$$

Once σ_B is known, the Mach numbers at points A and B are determined from

$$M_A=\sqrt{M_f^2+\frac{2}{\gamma}\log\frac{\sigma_B}{\sigma_f}}\sqrt[3]{\sigma_B}\exp[K_4(1-\sigma_B)] \quad [79]$$

$$M_B=\sqrt{M_f^2+\frac{2}{\gamma}\log\frac{\sigma_B}{\sigma_f}} \quad [80]$$

Numerical Examples

With the object of illustrating the previous approximate theory, several numerical examples have been carried out. These examples are now described.

Burning Program for Minimum Temperature Increase in a Sounding Rocket for Several Values of K_4

The problem of minimizing the temperature increase in a sounding rocket is now considered in connection with the following set of conditions

$$\bar{m}_i=1, \quad \bar{h}_i=0, \quad \bar{T}_i=1, \quad M_i=0$$

$$\bar{m}_f=0.4, \quad \bar{h}_f=12.88, \quad M_f=0 \quad [81]$$

$$K_2=0.19, \quad u=7,$$

Several values are considered for the thermal parameter K_4, namely, $K_4=0.2$, $K_4=0.4$ and $K_4=0.6$. The first step is to determine the sign of the function ω, defined by Equation [75], at the final point. Due to the fact that $\omega_f<0$, one concludes that the final point is to be reached with a coasting flight. The second step is to determine the altitude $\bar{h}_B$ where the transition from regulated thrust to coasting occurs. In this connection, the transcendental Equation [78] must be solved. The Mach numbers M_A and M_B are calculated from Equations [79 and 80].

The subsequent step is to determine the distribution of Mach number, mass, time and temperature with the equations of paragraphs under "Integration of the Equations of Motion" and "Integration of the Heat Transfer Equation." The Eulerian paths include a pulse-burning sub-arc IA a central sub-arc AB flown with regulated thrust and a final coasting sub-arc BF, and are described in Fig. 10, from which the following conclusion is drawn: *The optimum burning program is quite insensitive to changes in the thermal properties of air and skin.* The temperature rise $\bar{T}-1$, on the contrary, strongly depends on the value of the thermal parameter K_4 (Fig. 11).

In the light of this statement, the writer feels that the hypothesis of constancy of the Stanton number is well-justified from the point of view of predicting the optimizing mass flow β as a function of the time t. The errors introduced by the Stanton number hypothesis in the calculation of skin temperatures, however, should be corrected. In this connection, the following iterative procedure appears to be logical: (a) Calculate the optimum burning program in the $(\bar{h},M,\bar{m},\bar{t})$ space by assuming a constant value for the parameter K_4; (b) determine the distribution of temperatures $\bar{T}(\bar{h})$ for constant value of K_4; (c) starting from (a) and (b), calculate the true distribution of Stanton numbers $St(\bar{h})$, as supplied by the boundary layer theory; (d) integrate the temperature equation by approximate methods.

Effect of the Propellant Mass on the Temperature at Final Point in a Sounding Rocket

The problem of a sounding rocket is now considered in connection with the set of conditions

$$\bar{m}_i=1, \quad \bar{h}_i=0, \quad \bar{T}_i=1, \quad M_i=0 \quad [82]$$

$$\bar{h}_f=12.88, \quad M_f=0,$$

$$K_4=0.20, \quad K_2=0.19, \quad u=7$$

The extremal path includes a pulse-burning sub-arc IA, a central sub-arc AB flown with regulated thrust and a final coasting sub-arc BF, and is shown in Fig. 12 for several values of the ratio of propellant mass to take-off mass. Inspection of Fig. 12 shows that an increase in propellant mass causes a shifting of the optimum distribution of speeds toward the region of lower velocities. As a consequence, lower final temperatures must be expected when $\bar{m}_p=1-\bar{m}_f$ increases. This effect is clearly shown in Fig. 13.

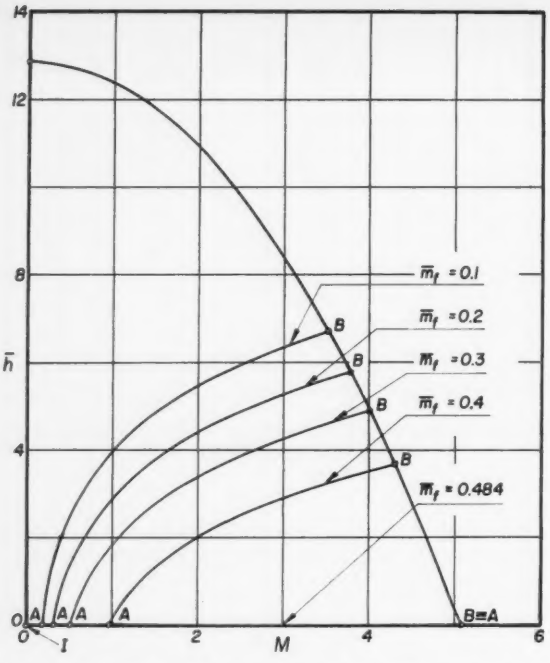

Fig. 12 Extremal trajectories of type II for different values of the propellant mass

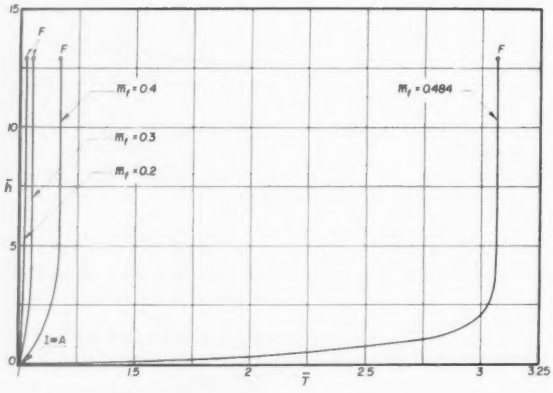

Fig. 13 Extremal trajectories of type II for different values of the propellant mass

The particular trajectory associated with $\bar{m}_f = 0.484$ (Fig. 12) has the property of minimizing the propellant consumption for the case where the drag is ideally zero and no condition of a thermal nature is imposed. The temperature rise associated with such a trajectory, however, is considerable (Fig. 13). In this connection, Fig. 13 points out one important concept: A slight increase in propellant mass over the minimum value necessary to reach the prescribed altitude $\bar{h}_f$ determines a sharp decrease in the skin temperature at final point. The use of extra amounts of propellant, therefore, may be an effective means for preventing the occurrence of undesirable effects due to aerodynamic heating.

Conclusions and Recommendations for Further Research

The burning program minimizing an arbitrarily specified function of the final values of time, mass, altitude, velocity and skin temperature is investigated. For problems where no time condition is imposed, explicit solutions are obtained for the optimizing mass flow as a function of the local coordinates of the missile. Closed form solutions are derived under the assumption of isothermal atmosphere, negligible drag, negligible irradiation and constant Stanton number. Numerical examples show that the Stanton number hypothesis originates only minor errors in the prediction of the optimum burning program.

Due to the approximate character of the theory developed in Part 2, further research is necessary to reach a full understanding of the problem of the optimum burning program. Because of the practical impossibility of obtaining closed form solutions for the general case, two lines of approach should be explored. In the first place, digital computing equipment should be used to integrate the equations of the optimum path by accounting for the effects of the aerodynamic drag (neglected in Part 2) for irradiation phenomena and by lifting the hypotheses of constancy of the Stanton number and the assumption of isothermal atmosphere. In the second place, an approach should be undertaken with the so-called direct methods of the calculus of variations, such as, for instance, the Rayleigh-Ritz method. In this connection, the writer feels that much can be done by exploring the class of arcs composed of sub-arcs $\beta = 0$, sub-arcs $\beta = \beta_{max}$ and sub-arcs where the acceleration is assumed to be proportional to some power of the Mach number.

References

1 Hamel, G., "Über eine mit dem Problem der Rakete Zusammenhängende Aufgabe der Variationsrechnung," *ZAMM*, vol. 7, Dec. 1927, pp. 451–452.

2 Tsien, H. S., and Evans, R. C., "Optimum Thrust Programming for a Sounding Rocket," *Journal of the American Rocket Society*, vol. 21, Sept. 1951, pp. 99–107.

3 Miele, A., "Generalized Variational Approach to the Optimum Thrust Programming for the Vertical Flight of a Rocket, Part I, Necessary Conditions for the Extremum," Purdue University, School of Aeronautical Engineering, Report A-57-1, March 1957 (AFOSR-TN-57-173).

4 Hibbs, A. R., "Optimum Burning Program for Horizontal Flight," *Journal of the American Rocket Society*, vol. 22, July-Aug. 1952, pp. 206–212.

5 Cicala, P., and Miele, A., "Generalized Theory of the Optimum Thrust Programming for the Level Flight of a Rocket-Powered Aircraft," JET PROPULSION, vol. 26, June 1956, pp. 443–455.

6 Miele, A., "An Extension of the Theory of the Optimum Burning Program for the Level Flight of a Rocket-Powered Aircraft," Purdue University, School of Aeronautical Engineering, Report A-56-1, June 1956 (AFOSR-TN-56-302).

7 Abraham, L. H., "Structural Analysis of High Speed Vehicles," Douglas Aircraft Co., Inc., Report SM-18375, June 1954.

8 Bliss, G. A., "Lectures on the Calculus of Variations," The University of Chicago Press, Chicago, 1946.

9 Miele, A., "Optimum Burning Program as Related to Aerodynamic Heating for a Missile Traversing the Earth's Atmosphere," Douglas Aircraft Co., Inc., Report SM-27236, April 1957.

The Mixing of Unbounded Coaxial Compressible Streams[1]

D. ROGER WILLIS[2] and IRVIN GLASSMAN[3]

Princeton University, Princeton, N. J.

An investigation was made of the over-all characteristics associated with unbounded mixing of axially symmetric compressible coaxial air streams. Experiments were performed to determine the effects of what are considered the fundamental parameters of the problem (the initial Mach numbers and initial stagnation temperature ratio of the streams). Included in the range of experiments were primary Mach numbers of 2.60, 0.97 and 0.68, secondary Mach numbers of 0.45, 0.25 and 0.00, and stagnation temperature ratios of 1.00 and 1.429. Mass flows in the mixing region, and hence mixing rates were computed from the experimental data for the range of parameters tested.

The experimental (and to a lesser extent the analytical) results exhibited a very marked effect of the secondary Mach number. This effect was greatest for the subsonic primary Mach numbers. The over-all spreading was less for $M_1 = 2.60$ and the effect of the secondary Mach number was less pronounced. The effect of increased temperature ratio was to increase the over-all spreading.

A practical correlation between the spreading rates was found for the subsonic Mach numbers. For a constant primary Mach number the spreading angle of the mixing region seems to depend linearly on the secondary Mach number.

Nomenclature

x	=	axial distance from nozzle
r	=	radial distance from axis
u	=	velocity in axial direction
v	=	velocity in radial direction
M	=	Mach number
T	=	temperature
ρ	=	density
$b(x)$	=	mixing width $= (r_j - r_i)$
r_0	=	primary nozzle radius
q	=	spreading angle
τ	=	shear stress
m	=	mass flow

Subscripts

1	=	primary stream
a	=	secondary stream
s	=	stagnation
i	=	edge of core region
j	=	outside edge of mixing region

Superscripts

—	=	time mean
$'$	=	difference from mean value
$*$	=	arbitrary integration limit

Introduction

THE mixing of two unbounded coaxial compressible streams, which are turbulent, is of considerable interest in such problems as the spreading of turbojet or rocket engine exhausts in flight, and it is the simplest logical extension of free jet mixing, a case which has been examined quite extensively (1–7).[4]

The present investigation was not concerned with the details of the turbulence, but rather with the over-all effects on the mixing of varying the initial Mach numbers and stagnation temperature ratio. An understanding of this mixing process should assist in the analysis of the more complex problem of mixing in a duct.

Work has been performed on the problem of mixing in a duct (8–11). There are several significant differences between these investigations and the unbounded mixing studied here. In the duct there can be no radial inflow of mass and the axial static pressure can vary appreciably. The bounded data which have been presented were either for low Mach numbers (0.1–0.2) or were difficult to interpret close to the nozzle exit, due to shocks or excessive boundary layers. The various relative dimensions of the nozzles and ducts used by different investigators made correlation of their data difficult. The nozzles used at this laboratory have unusually large dimensions which minimize the boundary layer effects. They were carefully designed and gave to a very good degree shock-free parallel flow. Schlieren techniques were employed to check

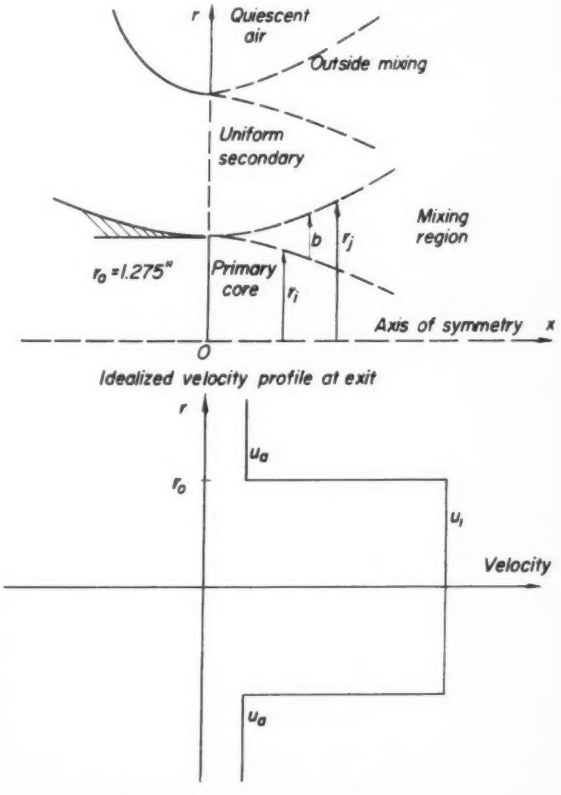

Fig. 1 Schematic of flow regions

Received March 11, 1957.

[1] This work was sponsored by Project SQUID which is supported by the Office of Naval Research under Contract N6-ori-105, T.O. 111, NR-098-038. Reproduction in full or part is permitted for any use of the United States Government.

[2] Assistant in Research, Department of Aeronautical Engineering.

[3] Assistant Professor, Department of Aeronautical Engineering. Mem. ARS.

[4] Numbers in parentheses indicate References at end of paper.

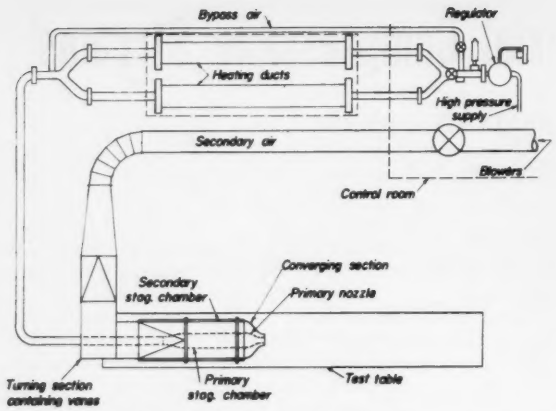

Fig. 2 Schematic of apparatus

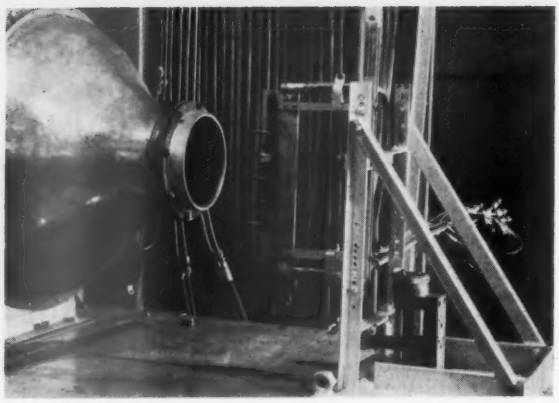

Fig. 3 Photograph of pressure-temperature probe showing micrometer adjustment mechanism

this condition (7). In the idealized problem, used for the analytical developments, the secondary stream is infinite and the velocity has a "step" profile at the nozzle exit as shown in Fig. 1. The secondary stream is in practice finite, and is eventually destroyed by outside mixing. However, all the data presented are for points upstream of this interference, and it is therefore believed that they will approximate closely those with an infinite secondary stream. The primary nozzle radius is now the only physical dimension of the apparatus involved and hence the data presented should have wide application.

Analytical approaches to the mixing problem started with Tollmein in 1926 (1). Two basic approaches exist; the first attempts to solve the differential equations of motion, the second uses a Kármán-type momentum integral with an explicit assumption for the velocity profile. Both methods assume similarity of velocity profiles. Different assumptions regarding the shear stress have been used. These include Prandtl's mixing length model, Taylor's vorticity transfer model and the assumption of a constant exchange coefficient across the mixing region. No single method appears to correlate all the practical data well, although one method may work well in one practical case, and another method in another case. A detailed discussion has been given in (12), which also contains a selective bibliography.

In this paper a turbulent Prandtl number of unity is assumed throughout. The energy equation is eliminated by means of the Crocco integral which relates density to velocity. The momentum equations then reduce to a single integral equation in u, $\rho(u)$, x, r and $\overline{u'v'}$. An attempt to find consistent similar velocity profiles and shear stress expressions led to an equation having no physically correct solutions. The correct qualitative trends were given by a simple Kármán-type approach using a linear velocity profile and the assumption that at $u = (u_1 + u_a)/2$, $\overline{u'v'} = k(u_1 - u_a)^2$ where k is constant.

The main emphasis of this paper is to present what are believed to be new data on unbounded compressible axisymmetric mixing, where clean exit conditions allow significant measurements to be taken in the core region.

Experimental Apparatus and Procedures

Air Supply System

A schematic of the experimental apparatus is shown in Fig. 2. The primary air is stored in high pressure bottles at 3000 psig. It passes through regulating valves, heating ducts, and the primary stagnation chamber and exhausts through the primary nozzle. The stagnation temperature is altered by allowing a controlled amount of the air to bypass the heating ducts. The stagnation chamber is insulated with internal and external ceramic liners to reduce heat transfer between the streams, and is provided with screens to insure uniform low intensity turbulence at the nozzle exit. Two nozzles, one for $M_1 = 2.60$ and one for subsonic Mach numbers, were designed, the former by the Foelsch method (13) corrected for boundary layers (14), to give parallel shock free flow at the exit. Both nozzles have exit diameters of 2.55 in.

The secondary air is supplied from two centrifugal blowers with rated mass flows at 2800 c.f.m. each at standard conditions. The maximum flow from the blowers for the 107.5 sq in. annulus corresponds to $M_a = 0.50$. Normal techniques such as turning vanes, egg-crates and screens are employed to assure uniform secondary flow. The converging section was designed to give a linear change of area with axial distance and had a radius of 6 in. at its exit. The temperature of the secondary air can be varied in the range 80 to 160 F but the control response is sluggish, and the temperature cannot be varied appreciably during a test run.

Pressure and Temperature Measuring System

Profiles in the mixing region were taken using a combination total-profile, total-temperature probe, positioned directly by a micrometer thread (Fig. 3). This arrangement allowed swift and accurate positioning of the probe, which was critical with mixing regions of the order of 0.2 in. The impact tubes were of normal design. The total temperature tubes, consisting of copper-constantan thermocouples enclosed by stainless steel radiation shields, gave high recovery factors, better than 95 per cent.

Both stagnation chambers contained static pressure taps and thermocouples. (Flow velocities in the stagnation chambers were sufficiently low for these readings to approximate closely the values corresponding to the stagnation conditions.)

Pressures were measured with mercury manometers or Bourdon gages, and stagnation temperatures with recording potentiometers.

Unlike free jet ($M_a = 0.00$) experiments where the temperature T_{sa} is fixed, variations in T_{sa} may occur during a test run with secondary air flow. It is therefore desirable to have a direct record of the ratio (T_{s_1}/T_{sa}) available during an experimental run. To this end a servomechanism was designed which utilized the recording potentiometers' property of transforming a d-c signal linearly into a mechanical displacement, and a direct reading of T_{s_1}/T_{sa} was obtained.

Range of Experimental Data

Surveys were taken across the jet at 0, 1, 2, 3 and 4 primary nozzle diameters downstream. Total pressure and, where applicable, total temperature measurements were taken for various combinations of $M_1 = 2.60, 0.97$ and 0.68, $M_a = 0.45$,

0.25 and 0.00, and T_{s1}/T_{sa} = 1.00 and 1.429. A value of T_{s1}/T_{sa} = 1.429 corresponds to over 200 F difference in temperature between the streams. The pressure readings were recorded photographically and mixing boundaries estimated from the profiles. Check runs were carried out to test the repeatability and over-all accuracy of the data.

In the case of zero secondary flow comparative tests were made with the outside of the nozzle lagged with insulating material. With $M_a \neq 0.00$ it was of course not feasible to insulate the nozzle without disturbing the secondary flow.

The effect of disturbing the boundary layers on the inside and outside of the primary nozzle was also investigated. Simple spoilers made of cotton thread were glued to the nozzle 1.5 in. from the exit. The thickness of the spoilers was 0.02 in. compared with an estimated 0.05 in. for the boundary layer. Significantly thicker spoilers were found to affect the uniform primary stream at exit, presumably due to separation of the boundary layer. Profile checks were carried out at 3 diameters and compared with the previous data. These results are reported in the following section.

When tests were run with M_a = 0.00, the secondary converging section was removed so that data could be compared with the previous work using this apparatus (6). There appeared to be a small but significant effect of the configuration just outside the primary nozzle, presumably due to differences in the induced flows. A systematic study of these effects was outside the scope of the present investigation but might be of interest in the future.

Accuracy of the Experimental Data

The pressures and temperatures were recorded to a high degree of accuracy by the manometers and thermocouples, respectively. The position of the probe was known to 0.003 in. and normally better. In reading the photographs of the manometers errors of $\pm\frac{1}{20}$ in. Hg could occur. The chief source of error arose when estimating the mixing boundaries from the pressure and temperature profiles. Close to a boundary a small error in temperature or pressure reading can alter the estimate of the width of the region appreciably.

For the isoenergetic case up to four tests were performed with the same initial parameters. Two values of the mixing width are obtained from each test as measurements were taken above and below the axis of symmetry. (Traverses were made in a vertical plane.) The values reported are mean quantities from these repeated tests. An idea of the over-all accuracy of the data may be obtained by studying the variations in the values of the spreading widths. The expected errors as a percentage of the mean spreading width were at worst 8 per cent for a single estimate, and 4 per cent for the mean estimate with M_a = 0.00, and 5.0 and 1.6 per cent, respectively, for $M_a \neq 0.00$. Most of the errors were considerably less than these extreme values.

Results[5]

Isoenergetic Mixing Data

The subsonic isoenergetic mixing cases were used to test the repeatability of the data. The values presented are the means of several tests and form a basis for comparison with the other data.

Figs. 4 to 8 show typical total pressure profiles for various axial distances and initial Mach number combinations. They represent only a few of the many similar curves obtained in over 200 test runs. Fig. 4 demonstrates the high degree of uniformity achieved in both primary and secondary streams at the nozzle exit. Also clearly indicated in this figure are the small relative dimensions of the boundary layers compared with the uniform regions.

Figs. 5 and 7 depict over-all total pressure profiles. In each

[5] More detailed data are reported in (15).

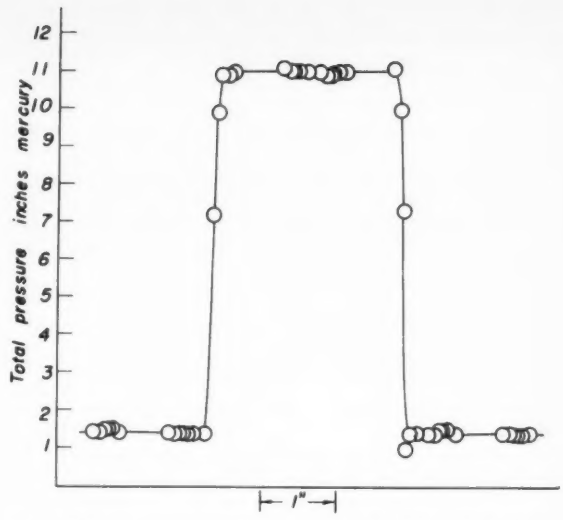

Fig. 4 Total pressure profile at nozzle exit—M_1 = 0.68, M_a = 0.25, T_{s1}/T_{sa} = 1.00

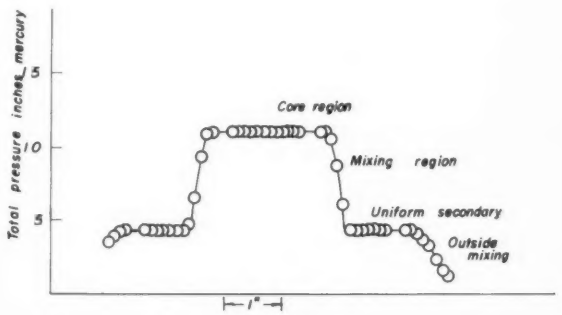

Fig. 5 Over-all total pressure profile—x = 4 radii, M_1 = 0.68, M_a = 0.45

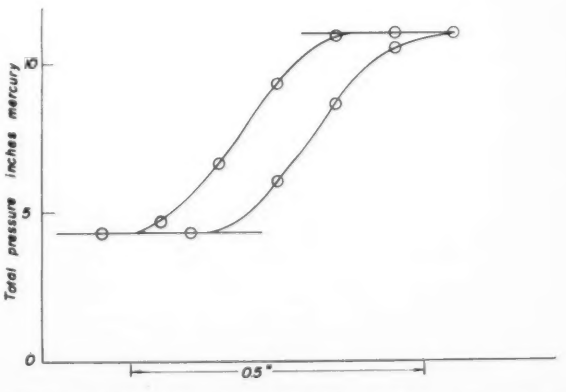

Fig. 6 Detailed total pressure mixing profiles—x = 4 radii, M_1 = 0.68, M_a = 0.45, T_{s1}/T_a = 1.00

can be seen clearly the uniform primary and secondary regions, the mixing zone, and the effect of outside mixing destroying the uniform secondary region. At $x = 8$ (primary nozzle) radii the uniform secondary region has shrunk considerably. For $M_1 = 0.97$ and $M_a = 0.25$ it was in fact so small that no attempt was made to estimate the mixing boundaries at this point. No data were taken for x greater than 8 radii.

The mixing regions on both sides of the jet axis are shown in more detail in Figs. 6 and 8. The degree of symmetry of the mixing is readily demonstrated with this method of presentation. Fairing in the profiles up to the limiting values of the uniform regions required a certain amount of individual discretion. Radial distances were measured with respect to the test table. The position of the axis of symmetry was determined by taking the average value of the distances to the four mixing boundaries, two above and two below the axis. The values of r_i and r_j were then obtained except in the case $M_1 = 2.60$ when r_i was not estimated as the weak shock structure made this impractical.

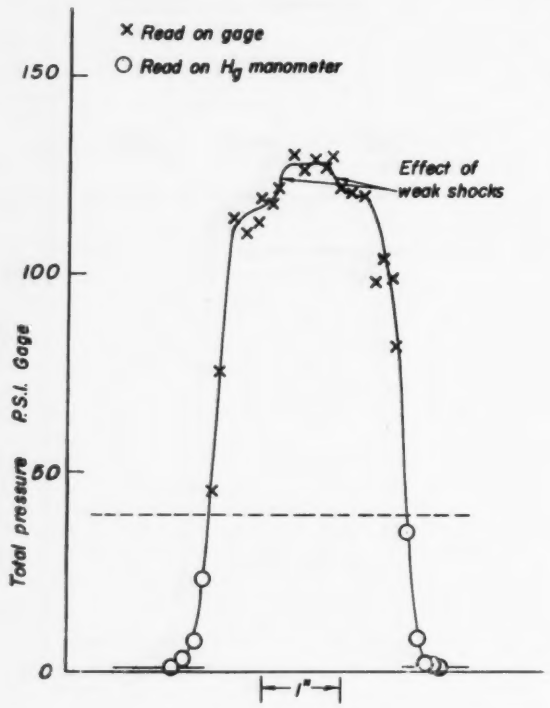

Fig. 7 Over-all total pressure profile, $\frac{1}{M}$ $x = 6$ radii, $M_1 = 2.60$, $M_a = 0.25$, T_{s1}/T_{sa} 1.00

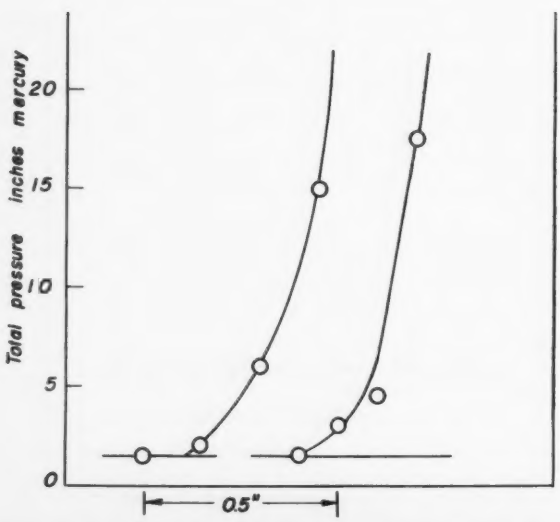

Fig. 8 Detailed total pressure profile—$x = 6$ radii, $M_1 = 2.60$, $M_a = 0.25$, $T_{s1}/T_{sa} = 1.00$

The major experimental results are reported in Figs. 9 and 10. Fig. 9 is a typical example of the several cross plots that can be drawn (15). The dependence of the mixing boundaries on the initial Mach numbers is clearly demonstrated. For a constant M_1 increasing M_a decreases the spreading angles and the over-all spreading decreases with increasing M_1. There is a marked effect of the secondary Mach number. For $M_a = 0.00$, the spreading decreases with increasing M_1. For $M_a = 0.25$, the spreading is a very weak function of M_1, increasing slightly with increasing M_1. For $M_a = 0.45$, the spreading definitely increases with M_1. On the hypothesis that the mixing is primarily determined by momentum transfer this phenomena can be rationalized as follows:

A larger velocity difference between the streams causes higher shear stress and a greater momentum difference. The former effect tends to increase the spreading, and the latter to have the reverse effect. At $M_a = 0$ it appears that the first effect predominates but as M_a increases the second effect becomes more important and is eventually the determining factor. A simple Kármán-type approach, described in the Appendix, also gives this same inversion effect. The relative positions of the outer mixing boundaries (for simplicity the inner boundaries are omitted) are shown in Fig. 10 for the complete spectrum of initial Mach numbers.

The data are correlated by assuming the spreading linear with axial distance. The lines were chosen to give best agreement with the mass flows in the mixing regions as described below.

Mass Flow in Mixing Region

It is of considerable interest to determine the mass flow in the mixing region. As there is no experimental measurement of the density in the mixing region, it is necessary to make some assumption regarding the variation of density with velocity.

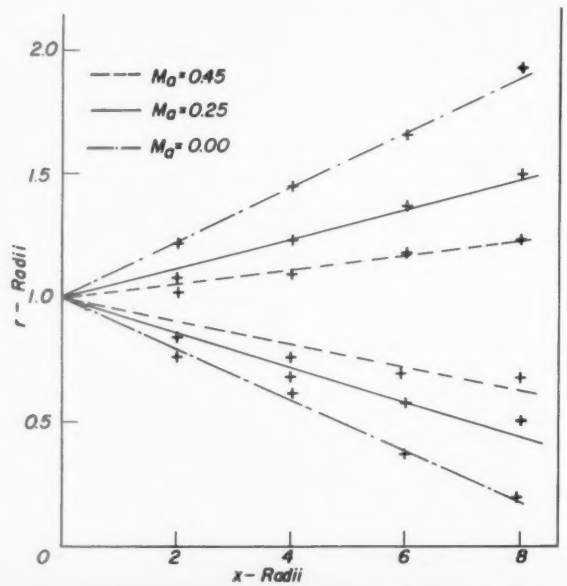

Fig. 9 Momentum mixing boundaries—$M_1 = 0.68$, $T_{s1}/T_{sa} = 1.00$

Table 1 Comparison of methods for determining mass flow in mixing region

	Run 1		Run 2		Run 3	
M_1	0.68		0.97		0.97	
M_a	0.45		0.25		0	
	A	B	A	B	A	B
x = 2 radii	0.270	0.307	0.321	0.325	0.423	0.332
x = 4 radii	0.478	0.496	0.701	0.656	0.830	0.586
x = 6 radii	0.680	0.708	0.956	0.890	1.19	0.810
x = 8 radii	0.950	0.958			1.47	0.942

The Crocco integral is again used. The velocity ratio u/u_1 is a known function of total pressure (assuming constant atmospheric pressure). Hence density, and the integral $m = \int_{r_i}^{r_j} \rho u r \, dr$ may be evaluated. This method, designated method A, involves lengthy and tedious calculation. If it could be assumed that both primary and secondary streams flow axially up to the mixing region, the integral could be evaluated simply as

$$m = \int_{r_i}^{r_j} \rho u r \, dr = \rho_1 u_1 (r_0^2 - r_i^2) + \rho_a u_a (r_j^2 - r_0^2)$$

This method, designated method B, would require only trivial computation as r_j, r_i have already been determined. The values of $m/\frac{1}{2}\rho_1 u_1 r_0^2$ calculated by these two methods were compared for three experimental runs, shown in Table 1.

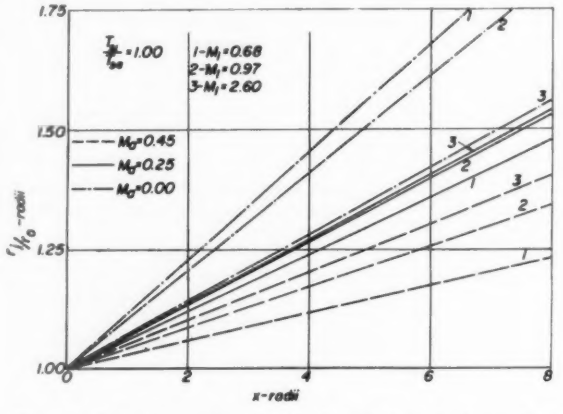

Fig. 10 Outer momentum mixing boundaries of primary jet

For $M_a = 0.25$ and 0.45 methods A and B do not disagree by more than 10 per cent. As there is no evidence that the Crocco integral is valid to greater accuracy than this, there is little point in using the much longer and more tedious method A. For $M_a = 0.00$, however, considerable disagreement occurs. This is not surprising, as the assumption in method B is obviously bad for this case when there is in fact a small but appreciable inflow of mass radially.

The mean mass flows, where method A is used for $M_a = 0.00$, and method B for $M_a = 0.45$ and $M_a = 0.25$, are depicted in Fig. 11. Here also a strong dependence on M_a can be seen.

The linear boundaries of the mixing regions were now calculated by making the sums $\Sigma(r_j^2 - r_0^2)$ and $\Sigma(r_0^2 - r_i^2)$, taken over x = 2, 4, 6 and 8 radii, equal for the practical points, and for the points on the straight lines $r_j = r_0 + q_j x$ and $r_i = r_0 - q_i x$, respectively. For comparison purposes values of q_i, q_j and $q_i + q_j$ appear in Table 2.

The spreading angle of the mixing region $b(x)/x$, or $q_i + q_j$, appears to be a linear function of M_a for a given value of M_1 (Fig. 12); $b(x)$ is assumed zero for $M_1 = M_a$ to give two more points on the lines. If the variation of spreading angle with M_1 is known for the free jet case it should then be possible, for subsonic Mach numbers at least, to predict the spreading angle for $M_a \neq 0$ according to the formula

$$\frac{b(x)}{M_1}\text{ free jet} = \frac{b(x)}{M_1 - M_a}$$

If the extrapolation of the experimental points to $M_1 = M_a$ is truly linear as would appear from the experimental results, then a very interesting conclusion would be drawn, i.e., two high velocity concentric air streams whose Mach numbers are close but different mix very slowly. Another interesting observation which can be made from Fig. 12 is that the crossover of the constant M_1 lines gives some idea where the changeover of the importance of momentum effects to shear effects takes place for jets in the Mach number range covered. The posi-

Table 2 Linear spreading rates

			Momentum boundaries		
M_1	M_a	T_{s1}/T_{sa}	$\frac{r_j - r_0}{x}$	$\frac{r_0 - r_i}{x}$	$\frac{b(x)}{x}$
0.68	0.00	1.000	0.1150	0.1010	0.2160
0.68	0.25	1.000	0.0604	0.0694	0.1298
0.68	0.45	1.000	0.0295	0.0446	0.0741
0.97	0.00	1.000	0.1040	0.0928	0.1968
0.97	0.25	1.000	0.0682	0.0739	0.1421
0.97	0.45	1.000	0.0434	0.0552	0.0986
2.60	0.00	1.000	0.0710	..	..
2.60	0.25	1.000	0.0672	..	..
2.60	0.45	1.000	0.0509	..	..
0.68	0.25	1.429	0.0639	0.0764	0.1403
0.68	0.45	1.429	0.0299	0.0537	0.0836
0.97	0.25	1.429	0.0807	0.0848	0.1655
0.97	0.45	1.429	0.0552	0.0714	0.1266

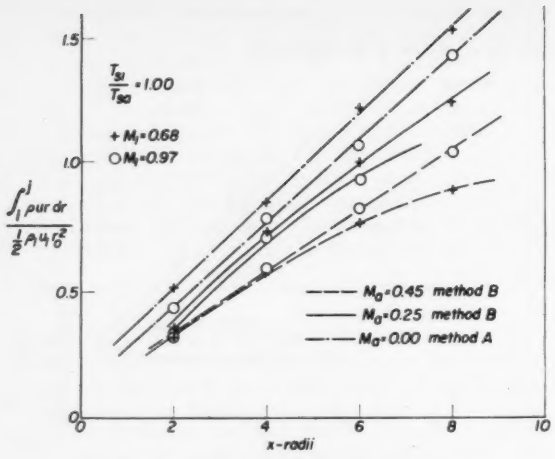

Fig. 11 Mass flow in mixing region

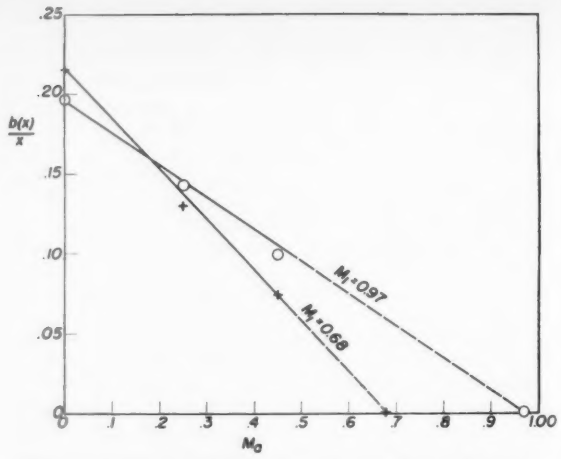

Fig. 12 Spreading angle vs. secondary Mach number

tion of the $M_a = 0$ points for other Mach numbers would follow the trend shown, the lower the M_1 the larger $b(x)/x$. Warren (6) has shown that the data given in this report so correlates with that of other investigators. Since the $b(x)/x$ given here is different from the spreading angles correlated by Warren, the raw data of the other investigators would be required to plot their M_1, $M_a = 0$ results in Fig. 12. Unfortunately, these data were not available.

Heated Stream Data $T_{s1}/T_{sa} = 1.429$

These data are presented in similar fashion to the isoenergetic data in Figs. 13, 14 and 15. It is necessary here to estimate both the momentum and energy boundaries. It appears from recent data for $M_1 = 2.60$, $M_a = 0.00$ and $T_{s1}/T_{sa} = 1.00$ that turbulence and conduction due to the large difference of static temperature may be responsible for this lack of definition. For the subsonic Mach numbers and $T_{s1}/T_{sa} = 1.429$ the momentum boundaries spread faster than with $T_{s1}/T_{sa} = 1.00$, the percentage change in $b(x)/x$ being larger for $M_1 = 0.97$ than $M_1 = 0.68$. The energy boundaries spread faster than the momentum boundaries which is in agreement with previous observation on lower speed jets (4). If the primary stream has a very high Mach number or is very cold so that $T_a > T_1$ it appears that this may not be the case and the energy core may be longer than the momentum core, due to turbulence and the conduction of heat toward the axis being appreciable. Indeed stagnation temperatures higher than T_{s1} have been recorded beyond the core for $T_{s1} = T_{sa}$, $M_1 = 2.60$, $M_a = 0.00$, and the term isoenergetic appears somewhat of a misnomer in this case.

Effect of Disturbing Boundary Layer and Lagging Nozzle

Though small, velocity and temperature boundary layers do exist at the nozzle exit. If the mixing were largely determined by either of these, then the data presented would depend on the physical dimensions of the apparatus used and would have far less general application. Profile checks carried out as described in the previous section revealed that within the limits of experimental accuracy no change in the over-all mixing could be detected with either boundary layer change. Small changes may occur at 1 or even 2 radii downstream, but were not detected in the over-all mixing further downstream. It is therefore thought that the data presented are to a very good measure independent of the apparatus used.

Conclusions

The dependence of momentum boundaries on initial parameters can be satisfactorily attributed to two opposing effects of increased velocity difference between the streams; namely, increase in momentum difference and increase in shear stress. For secondary Mach numbers close to zero (<0.25) the latter effect is stronger, but the former dominates at higher secondary Mach numbers. The isoenergetic subsonic data shows a linear dependence of spreading angle on $M_1 - M_a$ for a given M_1. Heating the primary jet confirmed the results of previous lower speed work in that the momentum boundaries spread faster.

The relative positions of the energy and momentum boundaries appear to depend on both total and static temperature ratios (and/or differences) between the streams and upon turbulence effects. For the subsonic heated cases where $T_{s1} > T_{sa}$ and $T_1 > T_a$ the energy boundaries spread faster than the corresponding momentum boundaries. However, for $M_1 = 2.60$ where $T_{s1} \geqslant T_{sa}$ but $T_1 < T_a$ the reverse holds at the core boundary, and the energy core extends beyond the momentum core. (This could be significant in, for example, positioning JATO units.)

Analysis of the problem using a Kármán-type approach was only qualitatively successful as indicated by the prediction of an inversion effect discussed. For any good quantitative agreement, a more realistic treatment of the nonsimilar velocity profiles, and a better understanding of the turbulent shear will probably be needed.

The experimental conditions were such that they closely approximated those of idealized mixing with an infinite stream, and thus the results presented are thought to be essentially a new contribution to the turbulent mixing field.

Acknowledgment

The advice given during the course of this study by Luigi Crocco is most gratefully acknowledged. The study was a part of a larger program in supersonic and subsonic mixing carried out at Princeton University. The original phases of the program were under the direction of J. V. Charyk. Walter E. Warren was instrumental in the development of the experimental apparatus. J. E. A. John and A. Bozowski assisted in performing a large part of the tests.

References

1 Tollmein, W., "Berechnung der Turbulenten Ausbreitungs Vorgänge, *ZAMM*, vol. 4, 1926, p. 486. Translated as NACA TM 1085, 1945.

2 Kuethe, A. M., "Investigation of the Turbulent Mixing Regions Formed by Jets," *Journal of Applied Mechanics*, vol. 2, 1935, pp. 87–95.

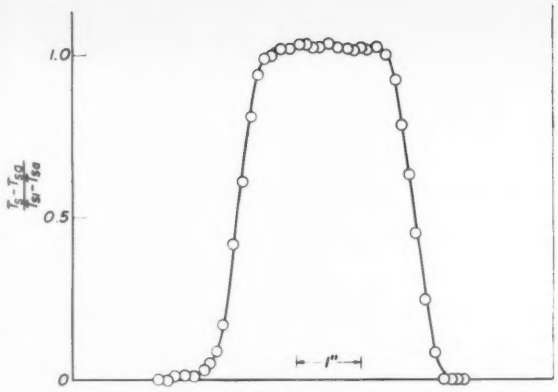

Fig. 13 Temperature mixing profile, $x = 4$ radii, $M_1 = 0.97$, $M_a = 0.25$, $T_{s1}/T_{sa} = 1.429$

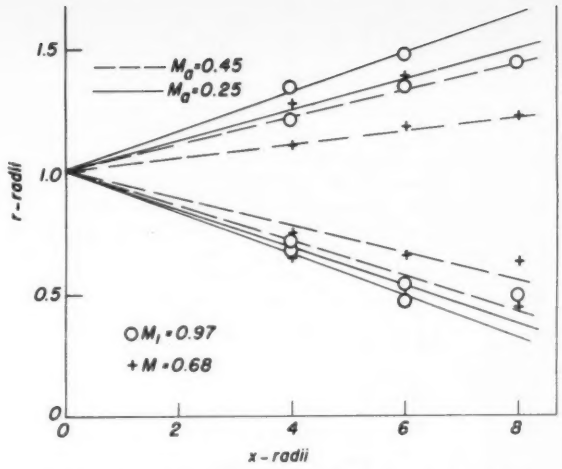

Fig. 14 Momentum mixing boundaries, $T_{s1}/T_{s_a} = 1.429$

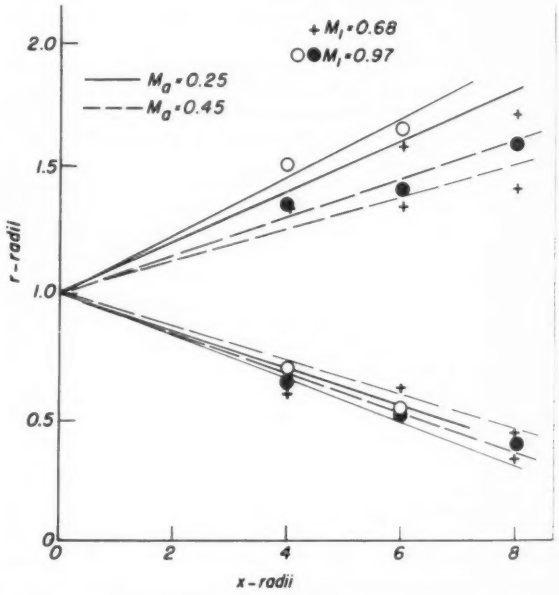

Fig. 15 Energy mixing boundaries, $T_{s1}/T_{s_a} = 1.429$

3 Abramovich, G. N., "The Theory of a Free Jet of a Compressible Gas," NACA TM 1058, 1944.

4 Corrsin, S., and Uberoi, M. S., "Further Experiments on the Flow and Heat Transfer in a Heated Turbulent Air Jet," NACA Report 998, 1950.

5 Alexander, L. G., Baron, T., Comings, E. W., "Transport of Momentum, Mass and Heat in Turbulent Jets," Contract N6-ori-71 (11), ONR, Engineering Expt. Station, University of Illinois, Bulletin Series 413, 1953.

6 Warren, W. R., Jr., "An Analytical and Experimental Investigation of Compressible Free Jets," Ph.D. Thesis, Dept. of Aeronautical Engineering, Princeton University, 1957.

7 Pitkin, E. T., "An Experimental Investigation of an Axially Symmetric Supersonic Jet Mixing with Free Air," Princeton University Aeronautical Engineering Lab Report 243, Aug. 1953.

8 Szablewski, W., "Die Ausbreitung eines Heissluttstrahlesin Bewegter Luft," GDC/2460, Sept. 1946. Translated as NACA TM 1288, 1950.

9 Pabst, O., "Die Austreitung Heisser Gasstrahlen in Bewegter Luft, I. Teil, Versuche im Kerugebiet,: Deytsche Luft fahrtforschung, Untersuchs-Mitteilunger," no. 8004, 11. Teil, Untersuchs-Mitteilunger, no. 8007, 1944.

10 Alexander, L. G., Comings, E. H., Grimmett, H. L., and White, E. A., "Transfer of Momentum in a Jet of Air Issuing into a Tube," Engineering Experiment Station, University of Illinois, Tech. Report 11, May 1, 1952.

11 Forstall, W., Jr., and Shapiro, A. H., "Momentum and Mass Transfer in Coaxial Gas Jets," *Journal of Applied Mechanics*, vol. 10, 1950, pp. 399–408.

12 Pai, S. I., "Fluid Dynamics of Jets," D. Van Nostrand, 1954.

13 Foelsch, K., "The Analytical Design of an Axially Symmetric Laval Nozzle for a Parallel and Uniform Jet," *Journal of the Aeronautical Sciences*, vol. 16, 1949, pp. 161–167.

14 Puckett, A. E., "Final Report on Model Supersonic Wind Tunnel Project," O.S.R.D. Report 3569, April 30, 1944.

15 Willis, D. R., "The Mixing of Unbounded Axially Symmetric Turbulent Compressible Jets," M.S.E. Thesis, Princeton University Aeronautical Engineering Lab Report 352, 1956.

APPENDIX

Summary of Analytic Approaches

Despite considerable researches (1–11), the field of turbulent mixing is still very much open, particularly in the compressible case. It seems unlikely that any one of the several theories expounded will be suitable for all cases of turbulent mixing. However, in specific problems, one or more of the theories may give a good correlation with the practical data.

No attempt was made to evolve a new theory, but to adapt an existing theory to the problem of axisymmetric compressible dual stream mixing. Any method that gives a good correlation with existing data, allows easy inter- and extrapolation, uses reasonable assumptions and does not involve excessive computation will be considered satisfactory.

The following assumptions are used throughout:

1) normal assumptions for jets, small angles, p constant

2) the density variation can be represented by a Crocco integral of the type $T_s = T + u^2/2c_p = A' + B'u$ giving $\rho/\rho_1 = 1/(D + Eu + Fu^2)$ (turbulent $Pr = 1$)

3) the velocity profiles in the mixing region are similar for given M_1, M_a, T_{s_1}/T_a settings, i.e.

$$\frac{u - u_a}{u_1 - u_a} = f\left[\frac{r - r_i(x)}{b(x)}\right] = f(\xi)$$

4) $\overline{u'v'}$ may be expressed in terms of the mean quantities in the form $h(\xi)$. It will be seen that the following expressions fall into this category

$$b(x)\left(\frac{\partial u}{\partial r}\right),\ ub(x)\left(\frac{\partial u}{\partial r}\right),\ b^2(x)\left(\frac{\partial u}{\partial r}\right)^2$$

With Assumptions 1 and 2 the equation of motion becomes

$$\frac{\partial}{\partial x}\int_0^{r^*} \rho u^2 r\, dr - u^* \frac{\partial}{\partial x}\int_0^{r^*} \rho u r\, dr = -(r^* \rho \overline{u'v'})^* \ldots [1]$$

Using Assumptions 3 and 4, an equation in ξ and x results. The first method tried to find what $h(\xi)$, $f(\xi)$, $b(x)$ and $r_i(x)$ will satisfy this. By assuming power law relations $b(x) = \beta x^m$ and $r_i - r_0 = \alpha x^n$ it is found that $m = n = 1$ are the only consistent values. By equating coefficients of x^0 and x^1 two equations in $f(\xi)$ and $h(\xi)$ are obtained; $h(\xi)$ is easily eliminated giving one equation in $f(\xi)$. Assuming a McLaurin series for $b(x)$ and $r_i(x) - r_0$ would also lead to the same two equations by equating coefficients of x^0 and x^1. Very similar equations may also be obtained using $\overline{u'V'} = h(\xi)/b(x)$ and power law relations for $b(x)$ and $r_0 - r_i(x)$, when $m = n = \frac{1}{2}$ are found to be the only consistent solutions. The two equations may be written

$$\text{coeff } x^0\, h(\xi) = P_0(f(\xi), \xi) \ldots [2]$$

$$\text{coeff } x^1\, h(\xi) = P_1(f(\xi), \xi) \ldots [3]$$

Elimination of $h(\xi)$ gives an equation in $f(\xi)$ and ξ. It can be proved that (regrettably) this equation has no solution satisfying the physical boundary conditions on f. It therefore appears that one at least of the assumptions used is incorrect.

For x small it may well be argued that Equation [2] is of prime importance. The equation is indeed the one that would arise in the corresponding two-dimensional problem under similar assumptions. To solve this equation it is necessary to make a further assumption upon the explicit form of $h(\xi)$. None of the more common expressions for shear stress led to an equation which could be immediately solved. With $\rho = \rho_1 = \text{const}$ the problem reduces to Tollmein's equation with $\tau \sim kb^2(x)(\partial u/\partial r)^2$. This solution could be extended numerically to cover a given case when $\rho/\rho_1 = 1/(a + bf + cf^2)$. The method did not give better correlations than the simplified model used below and, as it was tedious, effort in this direction was discontinued. Details of the various methods will be found in Appendix B of (15).

The second method is essentially an engineering approach. An explicit form of the shear stress at the point where $u - u_a = (\frac{1}{2})(u_i - u_a)$, and a velocity profile $f(\xi)$ are assumed. Integration of the fundamental equations with $r^* = \infty$ and $r^* = r_i + b/2$ gives two equations which can be solved for r_i and b. As such methods have been found to be insensitive to assumed velocity profile (7), a linear profile is selected on grounds of simplicity. For the shear stress at the half velocity point the assumption used was $\overline{u'V'} = k(u_1 - u_a)^2$. This result would be derived from several functional forms in the velocity for example

$$\overline{u'V'} = k\left|u_{\max} - u_{\min}\right| b(x)\frac{\partial u}{\partial r} \text{ (Ref. 8)}$$

$$\overline{u'V'} = k\, b^2(x)\left(\frac{\partial u}{\partial r}\right)^2$$

$$\overline{u'V'} = k\left|u - u_{\min}\right| b(x)\left(\frac{\partial u}{\partial r}\right)$$

It is known from practice that at the half velocity point the velocity profile is nearly linear. It would therefore appear reasonable that at this point the shear stress is a function primarily of the velocity gradient, and any terms involving $\partial^2 u/\partial r^2$, etc., would be small at this point.

On solving the equations (see Appendix B of (15) for details), it is found that to a close approximation $r_i - r_0$ and b are both proportional to x. These results cannot be foreseen and were only discovered on substituting numerical values in the equations.

The values of $b(x)/kx$ found by this method are given in Table 3.

Table 3 Values of $b(x)/kx$

M_1/M_a	0.45	0.25	0.00
2.60	8.69	11.63	14.20
0.97	5.40	9.00	15.88
0.68	3.10	7.13	15.92

It will be seen that for a given M_1 or M_a the correct dependence on M_a or M_1 is predicted. The actual numbers, however, are not simply connected with the experimental values for spreading rates. The use of an exponential velocity profile, which approximated the actual profiles more closely, also gave the same trends. The effect of M_1 for $M_a = 0.00$ was more pronounced however.

It is considered that probably the poorest of the several assumptions used in these approaches is that of similarity of the velocity profiles. The Crocco integral reduces to the believable hypothesis of constant stagnation temperature for $T_{s_1} = T_{s_a}$. The assumed expression for shear stress at the half velocity point is consistent with forms that have proved satisfactory in similar jet mixing problems with similarity well established.

Solution of the Transient Heat-Conduction Equation for an Insulated, Infinite Metal Slab[1]

JOHN H. GROVER[2] and WILLIAM H. HOLTER[3]

Atlantic Research Corp., Alexandria, Va.

The transient equation for the transfer of heat from hot combustion gases to an insulated, infinite metal slab has been solved. A graphical representation of the generalized solution has been prepared, as well as a graphical representation of a simplified, approximate solution of sufficient accuracy for engineering use. From these curves, the insulation required to protect a metal slab from hot gases can be determined. An illustrative example is given.

Nomenclature

a_i = positive roots of $\tan a_i l = (bg - a_i^2)/(b + g)a_i$
b = h/k
C = heat capacity of insulating slab
C_m = heat capacity of metal slab
g = $\rho C/\rho_m C_m l_m$
h = coefficient of heat transfer between heating or cooling fluid (hot gases) and surface of insulating slab
k = thermal conductivity of insulating slab
l = thickness of insulating slab
l_m = thickness of metal slab
m = k/hl = dimensionless resistance ratio
n = $\rho_m C_m l_m/\rho C l$ dimensionless heat-capacity ratio
T = temperature at position x at time θ
T_m = temperature of metal slab = temperature of insulation at position l at time θ
T' = temperature of heating or cooling fluid (hot gases)
T_0 = initial temperature of insulating slab
X = $\alpha\theta/l^2$ = dimensionless time parameter
x = normal distance from surface to point
Y = $(T' - T_m)/(T' - T_0)$ dimensionless temperature-difference ratio
α = $k/\rho C$ = thermal diffusivity of slab (insulation)
β_i = $a_i l$
θ = time from start of heating or cooling
ρ = density of insulating slab
ρ_m = density of metal slab

Introduction

CONSIDER a metal slab separated from a transient flow of hot gases by a layer of insulation. This paper presents a new method for predicting the temperature-time history of the metal slab as a function of the pertinent variables. The results are presented as a family of curves which interrelate certain dimensionless parameters. These curves are similar to those developed by various authors (3, 7)[4] for the heating of slabs, cylinders, spheres and other shapes.

The curves were developed primarily for use in calculating the amount of insulation necessary to protect rocket motor walls from being overheated by hot combustion gases. However, they may also be used to determine the insulation needed to protect thin-skinned missiles from aerodynamic heating. In addition, the curves could be used to solve many transient heating problems where undirectional flow of heat can be assumed and nearly all of the heat transferred to the metal is conducted through the insulation.

A solution has been developed with appropriate boundary conditions for an infinite slab of insulation with finite thermal conductivity, in contact at one surface with a slab of metal of infinite thermal conductivity and in contact at the other surface with hot flowing gases. Additional assumptions include: (a) Conduction of heat only in the direction normal to the plane of the slabs, (b) an initially uniform temperature throughout the slabs, (c) no heat transferred to the metal slab except by conduction through the insulation, (d) no thermal resistance between the two slabs, (e) a finite thermal film resistance between the hot flowing gases and the insulation, (f) temperature of the flowing gases does not decrease in the direction of flow and (g) thermal diffusivity, $k/\rho C$, of the insulation is invariant with temperature.

The basic equation of heat conduction

$$k\frac{\partial^2 T}{\partial x^2} = \rho C\frac{\partial T}{\partial \theta} \quad \ldots\ldots\ldots\ldots [1]$$

has been solved for numerous conditions (1); however, no analytical solution has been found for the boundary conditions inherent in the above assumptions.[5] Jaeger (4) has solved the equation for heat transfer through a hollow cylinder with very general boundary conditions. Although his solution may be modified to yield the conditions of this problem, the numerical solution of the equation is cumbersome and time consuming. It is also possible to solve the equation graphically by the method of Schmidt (6). However, this method is also very laborious and a simpler method was sought.

Solution of Equation

A solution of the basic equation of heat conduction was developed, through the use of Laplace transforms with the boundary conditions

$$T = T_0 \text{ at } \theta = 0 \quad \ldots\ldots\ldots\ldots [2]$$

$$T \to T' \text{ as } \theta \to \infty \quad \ldots\ldots\ldots\ldots [3]$$

$$-k\frac{\partial T}{\partial x} = h(T' - T) \text{ at } x = 0 \quad \ldots\ldots\ldots\ldots [4]$$

$$-k\frac{\partial T}{\partial x} = \rho_m C_m l_m \frac{\partial T_m}{\partial \theta} \text{ at } x = l \quad \ldots\ldots\ldots\ldots [5]$$

The solution obtained was

$$\frac{T' - T}{T' - T_0} = \sum_{i=1}^{\infty} \frac{2be^{-\alpha a_i^2 \theta}(a_i^2 + g^2)(b \sin a_i x + a_i \cos a_i x)}{a_i\{[(bg - a_i^2)^2 + a_i^2(b + g)^2]l + (bg + a_i^2)(b + g)\}} \quad \ldots [6]$$

Received Dec. 11, 1956.

[1] The figures and equations presented in this paper were prepared under the sponsorship of the Navy Bureau of Ordnance.

[2] Chemical Engineer. Mem. ARS.

[3] Mathematician.

[4] Numbers in parentheses indicate References at end of paper.

[5] It was later found that the solution given by Mayer (5) for the heating of a composite slab can be reduced to the one given here.

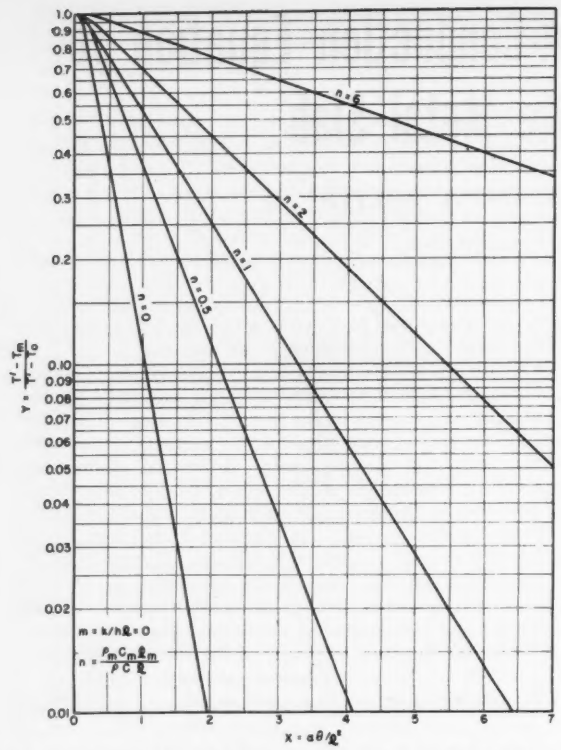

Fig. 1 Dimensionless plot of temperature rise vs. heating time for an insulated, infinite metal slab

where

$$a_i = \text{positive roots of } \tan a_i l = \frac{bg - a_i^2}{(b + g)a_i} \quad [7]$$

$$b = h/k \quad [8]$$

$$g = \rho C/\rho_m C_m l_m \quad [9]$$

$$\alpha = k/\rho C \quad [10]$$

The temperature of the metal is obtained by letting x equal l in Equation [6] to yield

$$\frac{T' - T}{T' - T_0} = \sum_{i=1}^{\infty} \times \frac{2be^{-\alpha a_i^2 \theta}(a_i^2 + g^2)(b \sin a_i l + a_i \cos a_i l)}{a_i\{[(bg - a_i^2)^2 + a_i^2(b + g)^2]l + (bg + a_i^2)(b + g)\}} \quad [11]$$

Equation [11] may be rearranged in terms of the dimensionless parameters X, Y, m, n and β_i to give

$$Y = \sum_{i=1}^{\infty} \frac{2e^{-X\beta_i^2}(1 + m^2\beta_i^2)(1 + n^2\beta_i^2)\cos \beta_i}{\beta_i^2(m + n)\{(1 + m^2\beta_i^2)(1 + n^2\beta_i^2) + n(1 + m^2\beta_i^2) + m(1 + n^2\beta_i^2)\}} \quad [12]$$

where

$$m = \frac{1}{bl} = \frac{k}{hl} \quad [13]$$

$$n = \frac{1}{gl} = \frac{\rho_m C_m l_m}{\rho C l} \quad [14]$$

$$X = \frac{\alpha\theta}{l^2} \quad [15]$$

$$Y = \frac{T' - T_m}{T' - T_0} \quad [16]$$

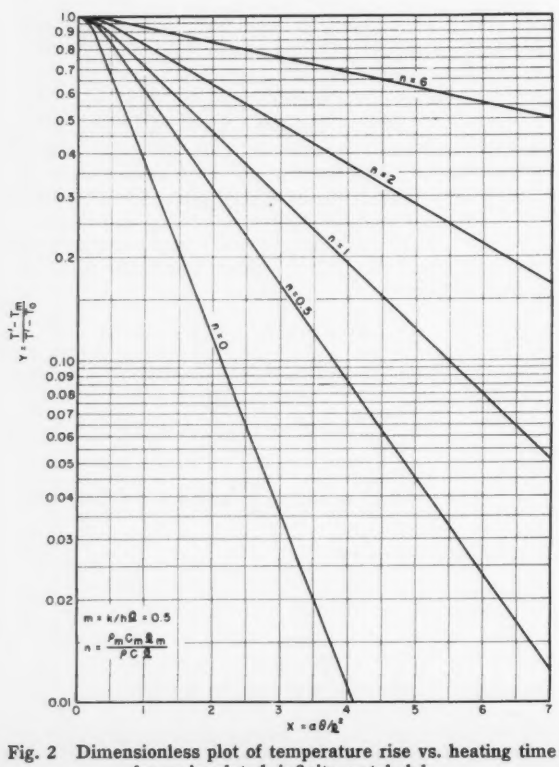

Fig. 2 Dimensionless plot of temperature rise vs. heating time for an insulated, infinite metal slab

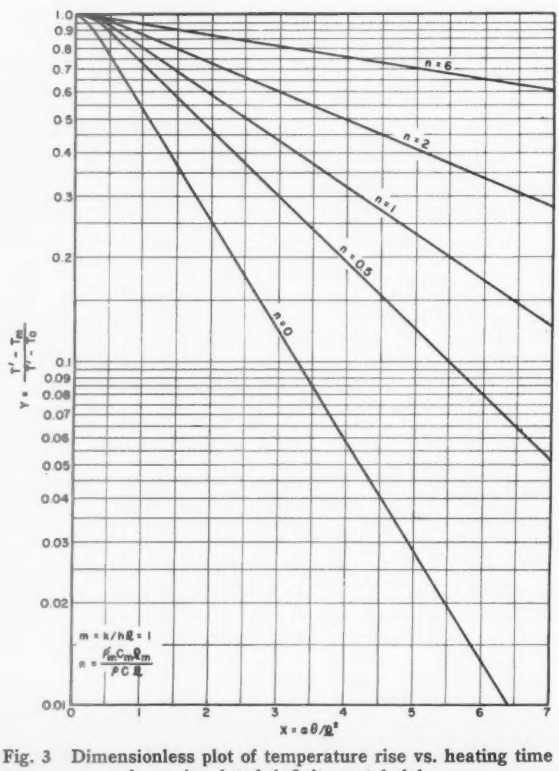

Fig. 3 Dimensionless plot of temperature rise vs. heating time for an insulated, infinite metal slab

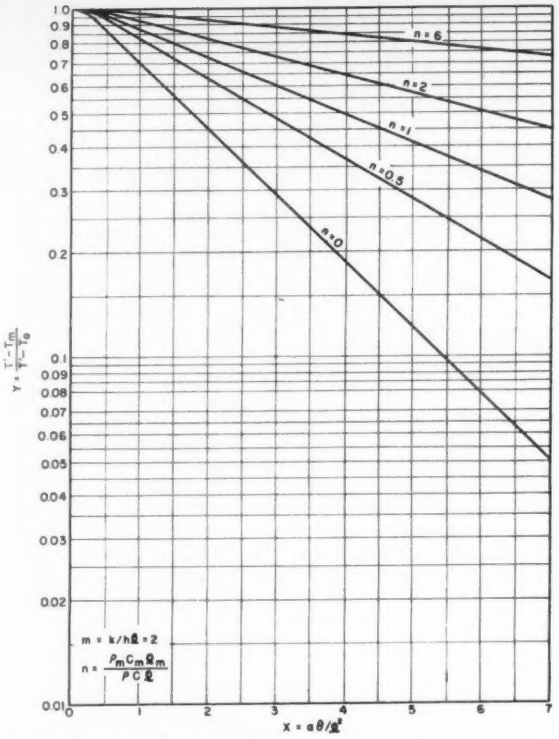

Fig. 4 Dimensionless plot of temperature rise vs. heating time for an insulated, infinite metal slab

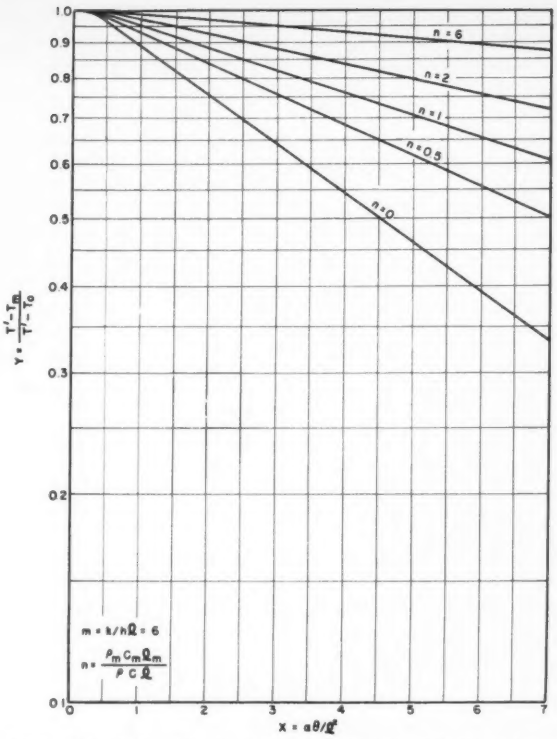

Fig. 5 Dimensionless plot of temperature rise vs. heating time for an insulated, infinite metal slab

$\beta_i = a_i l$, the positive roots of

$$\tan \beta_i = \frac{1 - mn\beta_i^2}{(m + n)\beta_i} \quad \ldots\ldots\ldots\ldots\ldots\ldots [17]$$

Equation [12] is symmetrical with respect to m and n; i.e., the values of the two parameters may be interchanged without affecting the equation. Thus m, the surface-resistance ratio, and n, the ratio of heat capacity per unit area of the metal to that of the insulation, are mathematically identical.

Graphical Representation of Solution

Equation [12] was solved numerically to give Y as a function of X for values of m and n of 0, 0.5, 1, 2 and 6 in all combinations. These results are plotted in Figs. 1 through 5. Each figure contains curves for five values of n for a given value of m. By double interpolation of m and n, the temperature rise of the metal slab for a given set of conditions can be determined from these curves.

The family of curves for $m = 0$ corresponds to Equation [21] of Carslaw and Jaeger (1), p. 107 for an infinite slab in contact with a well-stirred fluid of finite heat capacity on one surface, the other surface being at constant temperature. This is the solution to the case where there is no gas-film resistance. Greebler (2) has applied this specific solution to the transient heat-flow applications of aircraft insulation. Letting $n = 0$, the family of curves is obtained that corresponds to the mid-place lines on the charts for large slabs given by Gurney and Lurie (3). This is the solution when the thickness of the metal slab is zero.

Graphical Representation of Simplified, Approximate Solution

As was pointed out above, the use of the curves in Figs. 1

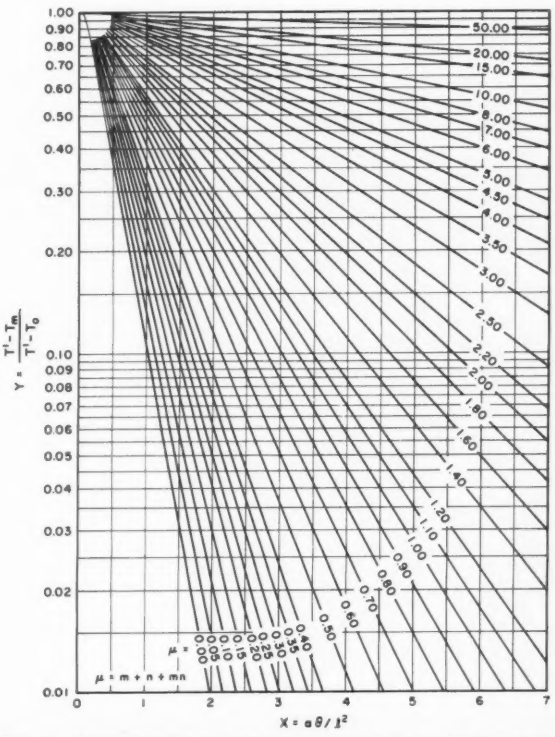

Fig. 6 Dimensionless plot of temperature rise vs. heating time for an insulated, infinite metal slab

through 5 may involve double interpolation. The necessity of double interpolation can be avoided with only a slight loss of accuracy by the adoption of a new empirical parameter

$$\mu = m + n + mn \quad [18]$$

Although Y is not an exact function of μ only, a maximum variation in Y of only about 4 per cent occurs when μ is held constant and m and n are allowed to vary over their full range of values. Values of Y given by Equation [12] are closely approximated by

$$Y = \sum_{i=1}^{\infty} \frac{2\mu e^{-X\beta_i^2} \sec \beta_i}{1 + \mu + \mu^2\beta_i^2} \quad [19]$$

where β_i are the positive roots of

$$\beta_i \tan \beta_i = \frac{1}{\mu} \quad [20]$$

Curves of Y vs. X for values of μ from 0 to 50 are shown in Fig. 6. The use of μ instead of m and n is adequate for engineering applications, and it is recommended that Fig. 6 be used rather than Figs. 1 through 5, since only a single interpolation is necessary.

Notice that Equation [19] may be obtained from Equation [12] by setting $m = 0$, and $n = \mu$ in the latter equation. Thus, Fig. 6 corresponds exactly to Fig. 1 where n is now replaced by μ.

Use of Fig. 6

Problem

The following example illustrates the use of Fig. 6.

The temperature of a flat sheet of steel, 0.15 in. thick, initially at 80 F, and insulated with a sheet of asbestos from hot gases which are at 3500 F, is to be kept below 800 F for 60 sec. The steel has a heat capacity of 0.15 Btu/lb°F, and a density of 0.28 lb/in.³. The asbestos has a heat capacity of 0.25 Btu/lb°F, a density of 0.0208 lb/in.³ and a thermal conductivity of 0.13 Btu/hr ft °F. The coefficient of heat transfer between the hot gases and asbestos is determined empirically to be approximately 125 Btu/hr ft² °F. (a) What thickness of asbestos is required? (b) What is the temperature of the steel after 45 sec of exposure to the gases assuming insulation with the required thickness of asbestos?

Data

C_m	= 0.15 Btu/lb °F	ρ	= 35.94 lb/ft³
C	= 0.25 Btu/lb °F	T'	= 3500 F
h	= 125 Btu/hr ft² °F	T_m	= 800 F
k	= 0.13 Btu/hr ft °F	T_0	= 80 F
l_m	= 0.0125 ft	θ_a	= 0.01667 hr
ρ_m	= 483.8 lb/ft³	θ_b	= 0.0125 hr

$$\alpha = 0.01447 \text{ ft}^2/\text{hr}$$

Solution

Since both X and μ are functions of the insulation thickness, part (a) must be solved by a trial-and-error process.

1) Assume $l = 0.0075$ ft

2) Calculate

$$m = \frac{k}{hl} = 0.1387 \qquad n = \frac{\rho_m C_m l_m}{\rho C l} = 13.47$$

$$\mu = m + n + mn = 15.48 \qquad Y = \frac{T' - T_m}{T' - T_0} = 0.7895$$

3) Obtain $X = 3.8$ from Fig. 6 corresponding to the above values of μ and Y. (The curve for $\mu = 15.48$ is determined by interpolation.)

4) Calculate $l = \sqrt{\frac{\alpha\theta_a}{X}} = 0.0080$ ft

5) Repeat steps 1) through 4) assuming $l = 0.0080$ ft.

The calculated value of l is now found to be 0.0081 ft. This is sufficiently close to the assumed value, and 0.0081 ft of asbestos is concluded to be adequate insulation.

The assumed and calculated values of l converge quit, rapidly. An initial assumption of $l = 0.075$ ft, for example requires only four repetitions of steps 1) through 4) to obtain the correct solution.

The solution to part (b) is obtained directly from the chart. For $l = 0.0081$ ft

$$m = 0.1283 \qquad n = 12.46$$
$$\mu = 14.19 \qquad X = \alpha\theta_b/l^2 = 2.774$$

$Y = 0.84$ is obtained from the chart for the above values of X and μ from which

$$T_m = T' - (T' - T_0)Y = 630 \text{ °F}$$

References

1 Carslaw, H. S., and Jaeger, J. C., "Conduction of Heat in Solids," Oxford University Press, London, 1947.

2 Greebler, P., "Thermal Properties and Applications of High-Temperature Aircraft Insulation," JET PROPULSION, vol. 24, 1954, pp. 374–378.

3 Gurney, H. P., and Lurie, J., "Charts for Estimating Temperature Distributions in Heating or Cooling Solid Shapes," *Industrial and Engineering Chemistry*, vol. 15, 1923, pp. 1170–1172.

4 Jaeger, J. G., "Radial Heat Flow in Circular Cylinders with a General Boundary Condition," *J. Proc. Roy. Soc. N.S.W.*, vol. 74, 1940, pp. 342–352.

5 Mayer, E., "Heat Flow in Composite Slabs," *Journal of the American Rocket Society*, vol. 22, 1952, pp. 150–158.

6 Schmidt, E., "Foppls Festschrift," Springer, Berlin, 1925, p. 179.

7 Williamson, E. D., and Adams, L. H., "Temperature Distribution in Solids During Heating and Cooling," *Physical Review*, vol. 14, 1919, pp. 99–114.

Technical Notes

Hypersonic Conical Shocks for Dissociated Air in Thermodynamic Equilibrium[1]

SAUL FELDMAN[2]

AVCO Research Laboratory, Everett, Mass.

The Taylor-Maccoll differential equation is shown to be integrable in closed form if the assumption is made that the flow in the shock layer (defined as the gas enclosed between the shock and the body) is incompressible, i.e., the density changes are assumed to be negligible.[3] This assumption yields results that, for dissociated air, agree to a high order of accuracy with the numerical integration of the complete Taylor-Maccoll equation. The calculated cone surface pressure coefficients for a wide range of cone angles and flight velocities between 10,000 and 26,000 fps, are shown to be 3 to 6 per cent larger than the Newtonian values at a flight altitude of 100,000 ft.

Nomenclature

a = speed of sound
C_p = $2(p - p_\infty)/\rho_\infty V^2{}_\infty$: pressure coefficient
h = enthalpy
p = pressure
u = velocity along a ray
v = velocity normal to a ray
V = $(u^2 + v^2)^{1/2}$: velocity
V_w = velocity of the flow immediately downstream of the conical shock
γ = ratio of specific heats
δ = angle streamline makes with the free stream flow direction when it emerges from the conical shock
η = variable defined by Equation [12]
θ = angle streamline makes with the free stream flow direction
ξ = variable defined by Equation [11]
ρ = density
ω = ray angle

Subscripts

c = cone
N = Newtonian
s = shock; also denotes an isentropic process
t = stagnation
∞ = free stream

Introduction

IN ORDER to predict with reliability the heating of a body flying through the atmosphere at hypersonic speeds, an accurate estimate of the surface pressure is of importance. Blunt bodies are being advocated for this flight regime, and the Newtonian "theory" for predicting pressures seems to be very popular in this regime.

[1] This work was sponsored by the Western Development Division, Air Research and Development Command, U. S. Air Force, under Contract AF 04(645)-18.

[2] Principal Research Scientist. Mem. ARS.

[3] Hayes, in Reference 1, has already demonstrated the usefulness of the constant density assumption in connection with a variety of hypersonic flow problems, including the cone problem, although his treatment is different from the one presented here.

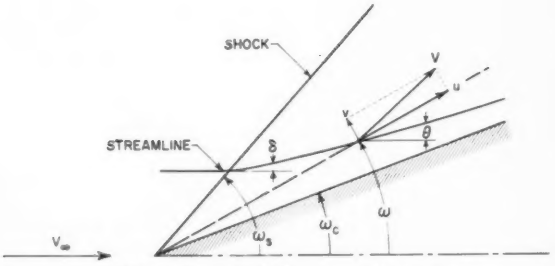

Fig. 1 Supersonic flow around a cone

No information is available in the literature, for flow Mach numbers larger than 5.8 in air (2),[4] as to the agreement of this theory with direct pressure measurements. At Mach numbers higher than 6 the dissociation of the gas behind the shock becomes of importance. Since for pointed bodies the pressure distributions can be obtained theoretically, it becomes of interest to compare the Newtonian values with these exact theoretical results. This comparison may also throw some light on the accuracy of the Newtonian approximation for other body shapes.

Wedges and cones are the simplest bodies to investigate, and in dissociated air, they can become quite "blunt" (included angles up to 135 deg for a cone) before the shock detaches.

For wedge angles of 100 to 120 deg included angle, and flight velocities between 10,000 and 26,000 fps, the results of (3) indicate that the Newtonian pressure coefficient underestimates the actual value by 10 to 20 per cent. The task here will be, therefore, to solve the cone problem.

The Taylor-Maccoll Equation for a Dissociating Gas in Thermodynamic Equilibrium

The coordinate system used here is given in Fig. 1. The conservation equations are

continuity $$\frac{d}{d\omega}(\rho v \sin\omega) + 2\rho u \sin\omega = 0 \quad [1]$$

irrotationality $$v = du/d\omega \quad [2]$$

momentum $$u\,du + v\,dv + dp/\rho = 0 \quad [3]$$

energy $$h + \frac{u^2 + v^2}{2} = h_t \quad [4]$$

The elimination of v between [1] and [2] gives

$$\rho(u'' + u'\cot\omega + 2u) + u'\rho' = 0 \quad [5]$$

where the accent denotes derivatives with respect to ω. The speed of sound is given by

$$a^2 = \left(\frac{\partial p}{\partial \rho}\right)_s \quad [6]$$

evaluated at constant entropy. This may be done by using a Mollier diagram for the gas under consideration, or calculated directly by statistical mechanical methods. The Mollier

[4] Numbers in parentheses indicate References at end of paper.

EDITOR'S NOTE: This section of JET PROPULSION is open to short manuscripts describing new developments or offering comments on papers previously published. Such manuscripts are published without editorial review, usually within two months of the date of receipt. Requirements as to style are the same as for regular contributions (see masthead page of this issue).

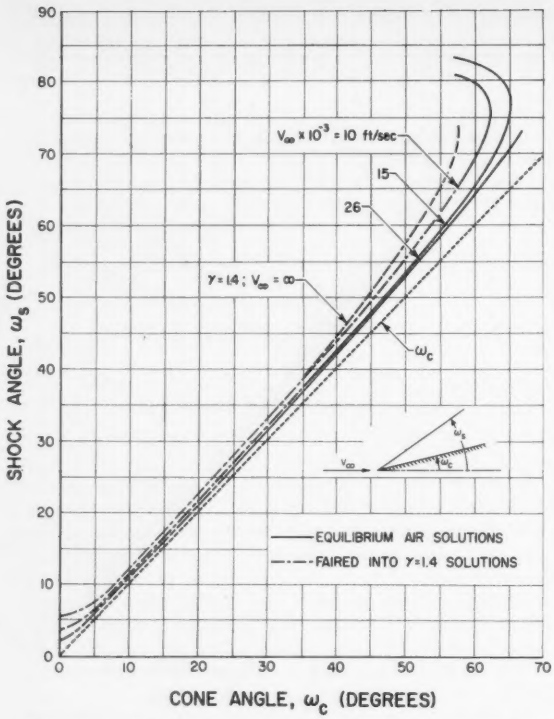

Fig. 2 Conical shock angles in dissociated equilibrium air

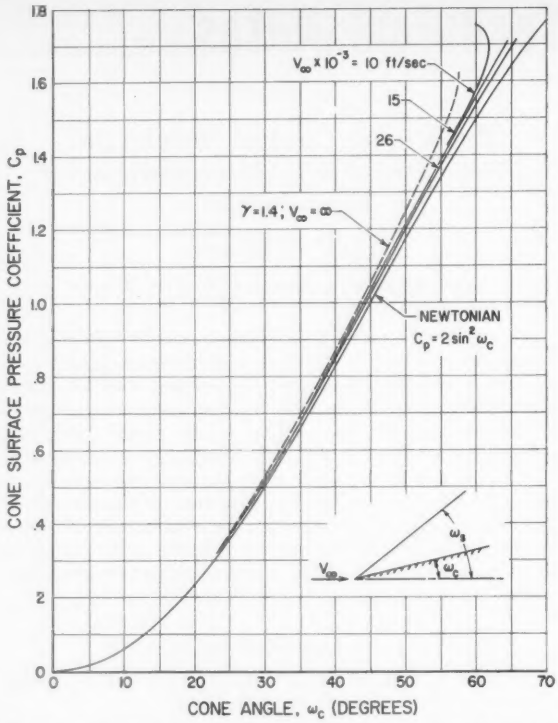

Fig. 3 Cone surface pressure coefficients. A comparison with the Newtonian value

diagram replaces here the usual equation of state. After use is made of [2] and [6], Equation [3] may be rewritten as

$$\rho u'(u'' + u) + a^2\rho' = 0 \quad \ldots\ldots [7]$$

ρ' can now be eliminated between [5] and [7] to yield the Taylor-Maccoll equation

$$(a^2 - u'^2)u'' = -a^2(2u + u' \cot \omega) + uu'^2 \quad \ldots\ldots [8]$$

The boundary conditions are

$$\left.\begin{array}{ll} \text{at } \omega = \omega_c & u_c' = 0 \\ \text{and at } \omega = \omega_s, & u_s = V_\infty \cos \omega_s \\ & u' = -V_w \sin(\omega_s - \delta) \end{array}\right\} \quad \ldots\ldots [9]$$

where δ is the wedge angle whose shock angle coincides with the conical shock angle ω_s, at the same free stream velocity V_∞. V_w is the velocity over the wedge.

For dissociated air behind the shock, V_w, ω_s and δ are known from (3). If the shock angle ω_s is assumed to be known, the only quantity that remains to be determined is the cone angle ω_c. Once ω_c is found, all other quantities in the flow field can be determined.

Note that in deriving [8] the energy equation has not been used. In order to integrate [8] numerically, a relationship between the speed of sound a, and the velocity u, has to be found. This relationship can be obtained by using a Mollier diagram that has constant speed of sound lines, thus relating speed of sound and enthalpy at constant entropy. The energy equation [4], then relates the enthalpy to the velocity. The results of calculations for cones flying through the atmosphere at speeds between 10,000 and 26,000 fps at 100,000 ft altitude are given in Figs. 2 and 3.

For a given cone angle in Fig. 2 the difference in ordinates, between any constant flight velocity curve and the one labeled ω_c, gives the shock layer angular thickness. Note that in dissociated air the thickness is about half the value it would be if no dissociation occurred.

Fig. 3 presents the cone surface pressure coefficients and compares them with the Newtonian and the undissociated $\gamma = 1.4$, $V_\infty = \infty$ values. Here again Newtonian theory underestimates the pressure coefficient by 3 to 6 per cent for the weak solutions, which are the ones of physical interest. Note that the pressure coefficient for a chemically frozen diatomic gas $\gamma = 1.4$ does not represent the behavior of air at hypersonic speeds.

Solution of the Conical Shock Equation for an Incompressible Fluid Downstream of the Shock[5]

Since the conical shock layer thickness in dissociated air at hypersonic speeds is fairly small and the flow in the shock layer is homentropic, one would expect the air density to have only small gradients in the ω direction. It is reasonable, therefore, to solve the conical shock equation assuming that the gas downstream of the shock is incompressible. Equation [8] then reduces to

$$u'' + u' \cot \omega + 2u = 0 \quad \ldots\ldots [10]$$

with the boundary conditions given by [9].

By letting

$$u(\omega) = \xi(\eta) \quad \ldots\ldots [11]$$

where

$$\eta = \cos \omega \quad \ldots\ldots [12]$$

and

$$0 < \eta < 1$$

Equation [10] reduces to Legendre's differential equation of the first degree

$$(1 - \eta^2)\xi'' - 2\eta\xi' + 2\xi = 0 \quad \ldots\ldots [13]$$

[5] After the manuscript was completed, the author was informed that Hayes has used, recently, an approach similar to the one presented in this section.

where the accents denote derivatives with respect to η. The boundary conditions for [13] are

$$\xi'(\eta_c) = 0 \quad \ldots\ldots [14]$$

$$\left.\begin{aligned} \xi(\eta_s) &= V_\infty \eta_s \\ \xi'(\eta_s) &= V_s \sin(\omega_s - \delta)/(1 - \eta_s^2)^{1/2} \end{aligned}\right\} \quad \ldots\ldots [15]$$

The general solution of [13] is

$$\xi = A\eta + B\left(\frac{1}{2}\eta \ln\frac{1+\eta}{1-\eta} - 1\right) \quad \ldots\ldots [16]$$

where A and B are constants of integration determined by [15]. They are

$$A = V_\infty\left[1 + k\left(\frac{1}{2}\ln\frac{1+\eta_s}{1-\eta_s} - \frac{1}{\eta_s}\right)\right] \quad \ldots\ldots [17]$$

and

$$B = -V_\infty k \quad \ldots\ldots [18]$$

where

$$k = \left[1 - \frac{V_w}{V_\infty}\frac{\sin(\omega_s - \delta)}{\sin\omega_s}\right]\eta_s(1 - \eta_s^2) \quad \ldots\ldots [19]$$

Equation [14] together with [16, 17, 18] give the following implicit expression for the cone angle

$$\frac{1}{2}\ln\frac{1+\eta_c}{1-\eta_c} + \frac{\eta_c}{1-\eta_c^2} = \left\{\eta_s(1-\eta_s^2)\left[1 - \frac{V_w}{V_\infty}\frac{\sin(\omega_s-\delta)}{\sin\omega_s}\right]\right\}^{-1} + \left(\frac{1}{2}\ln\frac{1+\eta_s}{1-\eta_s} - \frac{1}{\eta_s}\right) \quad \ldots\ldots [20]$$

A comparison is made in Table 1 of the cone angles obtained from the above expression, with the angles found by numerical integration of [8] the approximate method seems very satisfactory, at least for velocities larger than 10,000 fps.

The present scheme does not give accurate results for a gas with a specific heat ratio of 1.4, regardless of the flight Mach number.

The pressure in the flow field can be determined by integrating [3] with respect to η. This leads to a lengthy expression in η which will not be quoted here. However, a simple expression for the cone pressure coefficient will be derived in terms of the known pressure coefficient for the wedge that under the same flight conditions will have the same shock angle (3). The integration of the momentum equation [3], between the shock and the cone angle, gives

$$p_c - p_s = \frac{\rho_s}{2}(V_w^2 - V_c^2)$$

or

$$Cp_c = Cp_w + \frac{\rho_w}{\rho_\infty}[(V_w/V_\infty)^2 - (V_c/V_\infty)^2] \quad \ldots\ldots [21]$$

where

$$Cp_w = \frac{p_s - p_\infty}{(1/2)\rho_\infty V_\infty^2} \quad \ldots\ldots [22]$$

Cp_w, ρ_w/ρ_∞ and V_w/V_∞ are given in (3), while V_c/V_∞ is given by

$$V_c/V_\infty = \eta_c\left\{1 + k\left[\frac{1}{2}\ln\frac{(1+\eta_s)(1-\eta_c)}{(1+\eta_c)(1-\eta_s)} + \frac{1}{\eta_c} - \frac{1}{\eta_s}\right]\right\} \quad \ldots\ldots [23]$$

k being given by [19].

Again, a comparison of the pressure coefficients calculated from the exact solution and the approximate incompressible one, Table 1, shows very good agreement.

For a given flight velocity, it is interesting to note, from the last column of Table 1, that the Newtonian pressure coefficient is nearest the correct value at a cone angle intermediate between $\theta_c = 0$ and the detachment value.

Table 1 Comparison of approximate (analytical) and exact (numerical) solutions of the conical shock equations. (Altitude = 100,000 ft)

Flight velocity, $V_\infty \times 10^{-3}$ (ft/sec)	Shock angle, ω_s (degrees)	Cone angle, ω_c (degrees)		Cone pressure coefficient, Cp_c		$\frac{Cp_N}{Cp_c}$
		Exact	Approx.	Exact	Approx.	
10	66.76	58.10	58.03	1.5245	1.5239	0.9456
10	78.87	60.83	61.58	1.7437	1.7480	0.8745
15	37.78	34.96	34.84	0.6784	0.6774	0.9679
15	48.07	44.62	44.54	1.0173	1.0164	0.9699
15	59.73	54.88	54.81	1.3816	1.3808	0.9685
15	63.43	57.81	57.76	1.4826	1.4820	0.9659
15	67.14	60.50	60.45	1.5739	1.5735	0.9626
15	71.14	62.92	62.92	1.6596	1.6596	0.9553
26	25.42	23.99	23.91	0.3390	0.3383	0.9754
26	40.03	37.86	37.78	0.7708	0.7701	0.9774
26	58.89	55.29	55.26	1.3833	1.3828	0.9770
26	69.96	64.28	64.29	1.6703	1.6700	0.9719

References

1 Hayes, W. D., "Some Aspects of Hypersonic Flows," Ramo-Wooldridge Rept. MR6, Jan. 4, 1955.

2 Oliver, Robert E., "An Experimental Investigation of Flow About Simple Blunt Bodies at a Nominal Mach Number of 5.8," *Journal of the Aeronautical Sciences*, vol. 23, Feb. 1956, pp. 177–179.

3 Feldman, Saul, "Hypersonic Gas Dynamic Charts for Equilibrium Air," AVCO Research Laboratory, Everett, Mass., Jan. 1957.

Addendum to 'Stagnation Point Heat Transfer for Hypersonic Flow'[1]

MARY F. ROMIG[2]

Convair, a Division of General Dynamics Corp., San Diego, Calif.

A RATHER unusual oversight on the part of the author has apparently caused some confusion in the use of an empirical formula for stagnation point heat transfer presented in the title paper.[1]

This oversight was the complete omission of any physical units in the empirical formula. To permit correct use of the formula

$$q = 0.0145\, M_\infty^{3.1}\sqrt{\frac{p_\infty}{R_N}} \quad \ldots\ldots [12]$$

the units are as follows

q is in (Btu/ft^2 sec)
p_∞ is in (lb/ft^2)
R_N is in (ft)

The correct units were unfortunately not apparent from the analysis presented in the paper.

[1] JET PROPULSION, Dec. 1956, pp. 1098–1101.

[2] Staff Scientist, Scientific Research Laboratory. Mem. ARS.

Impact Points of Ballistic Rockets

R. E. ROBERSON[1]

Autonetics Div., North American Aviation, Inc., Downey, Calif.

A method of Singer and Wentworth for calculating the impact points of ballistic rockets is generalized to the case where the terminal point is at a different altitude than the initial point.

SINGER and Wentworth recently described a method for calculating impact points of ballistic rockets.[2] The condition they use in determining range angle is that the radial distance from the center of the earth at impact be equal to the radial distance R_L at burnout. An important generalization is when the former has a value $R_I \neq R_L$, particularly if the formulas are to be adapted to other applications.

The notation here follows that of Singer and Wentworth except for the introduction of R_I above, and of v_I for the velocity at "impact" (i.e., any chosen terminal condition which is specified by an assigned R_I) and θ_I for the inclination (generally negative) of v_I to the horizontal. Also $\Delta\phi^*$ is used rather than $\Delta\phi$, and t^* rather than t, for total range angle and total flight time, respectively, to distinguish this case.

From the Singer-Wentworth paper, the elliptical path is described by $r^{-1} = GM_E(R_L v_L \cos\theta)^{-2}[1 + \epsilon\cos\phi]$, with ϕ measured from perigee. The value of ϕ at the initial instant, $\phi(R_L)$, is obtained by setting $r = R_L$. The value of ϕ_I at impact is obtained by setting $r = R_I$ and properly interpreting the resulting inverse trigonometric function. It is convenient to write $\Delta\phi^* = \Delta\phi_1 + \Delta\phi_2$, where $\Delta\phi_1 = \pi - \phi(R_L)$, and recognize that $\phi_I = \phi(R_L) + \Delta\phi^* = \Delta\phi_2 + \pi$. Then it is easy to see that $\epsilon\cos\Delta\phi_2 = 1 - (R_L v_L^2\cos^2\theta)(GM_E)^{-1}(R_L/R_I)$. It follows that

$$\Delta\phi^* = \arccos\frac{1}{\epsilon}\left[1 - \frac{R_L v_L^2\cos^2\theta}{GE_E}\right] + \arccos\frac{1}{\epsilon}\left[1 - \frac{R_L}{R_I}\frac{R_L v_L^2\cos^2\theta}{GM_E}\right] \quad [1]$$

By differentiating r with respect to ϕ it is easy to show that

$$\tan\theta_I = \frac{-R_I}{R_L}\left[\frac{GM_E}{R_L v_L^2\cos^2\theta}\right]\epsilon\sin\Delta\theta_2 \quad [2]$$

and by using conservation of angular momentum one obtains

$$v_I = (R_L v_L\cos\theta)/(R_I\cos\theta_I) \quad [3]$$

These last two quantities, θ_I and v_I, may be of considerable interest if the trajectory actually continues beyond the nominal "impact" point.

One further quantity to be determined is the time of flight t^*. Now, rather than $t = [1 - 2A_f\{\phi(R_L)\}]T_e$, we have

$$t^* = [1 - A_f\{\phi(R_L)\} - A_f\{\pi - \Delta\phi_2\}]T_e \quad [4]$$

A case of particular interest is that in which R_I differs somewhat, but not much, from R_L. Let $R_I = (1 - \nu)R_L$ with $\nu \ll 1$. Then Equations [1–3] take the form, correct to first order in ν

$$\Delta\phi^* = \Delta\phi - \nu \quad [5]$$

$$\theta_I = -\theta + \nu\cos^2\theta[1 + \tan\theta - GM_E(R_L v_L^2\cos^2\theta)^{-1}] \quad [6]$$

$$v_I = v_L - \nu v_L \times [1 + \sin\theta\cos\theta + \sin^2\theta - \sin\theta\cos\theta\, GM_E(R_L v_L^2\cos^2\theta)^{-1}] \quad [7]$$

Also, using the expression for A_f from the reference and $\pi - \Delta\phi_2 = \pi - \Delta\phi_1 + \nu = \phi(R_L) + \nu$ we find

$$A_f[\pi - \Delta\phi_2] = A_f[\phi(R_L)] + \nu\frac{\sqrt{1-\epsilon^2}}{2\pi}\left\{\frac{1}{1+\epsilon}\sec^2\left[\frac{\phi(R_L)}{2}\right] - \frac{\epsilon[\epsilon + \cos\phi(R_L)]}{[1 + \epsilon\cos\phi(R_L)]^2}\right\}$$

whence

$$t^* = t + \frac{\nu T_e\sqrt{1-\epsilon^2}}{2\pi} \times \left\{\frac{\epsilon[\epsilon + \cos\phi(R_L)]}{[1 + \epsilon\cos\phi(R_L)]^2} - \frac{1}{1+\epsilon}\sec^2\left[\frac{\phi(R_L)}{2}\right]\right\} \quad [8]$$

One final point worth noting is that the change in latitude and longitude between burnout and impact is given incorrectly in the reference, as can be seen easily from the case $\gamma = 0$ with $\lambda_L \neq 0$. Correct expressions are

$$\lambda_{impact} - \lambda_{launch} = \arcsin(\sin\Delta\phi\sin\gamma\cos\lambda_L + \cos\Delta\phi\sin\lambda_L) - \lambda_L \quad [9]$$

$$\Delta\text{ longitude} = \arcsin\left(\frac{\sin\Delta\phi\cos\gamma}{\cos\lambda_I}\right) - \Delta\phi_E \quad [10]$$

The difference between these expressions and those actually used is not apparent in the example of the reference, in which $\lambda_L = 0$ and λ_I is close to zero.

Received June 20, 1957.

[1] Staff Specialist, Guidance Engineering Department. Mem. ARS.

[2] Singer, S. F., and Wentworth, R. C., "A Method of Calculating Impact Points of Ballistic Rockets," JET PROPULSION, vol. 27, April 1957, pp. 407–409.

Addendum to 'Heat Transfer to Satellite Vehicles Re-entering the Atmosphere"[1]

R. W. DETRA[2], N. H. KEMP[3] and F. R. RIDDELL[2]

Avco Research Laboratory, Everett, Mass.

IN (1)[4] a correlation formula for the stagnation point heat transfer rate to a blunt body of revolution in hypersonic flow was given as

$$q_s = \frac{20{,}800}{\sqrt{R}}\sqrt{\frac{\rho}{\rho_0}}\left(\frac{u}{u_c}\right)^{3.25}\left(1 - \frac{h_{ws}}{h_{s1}}\right)\text{ Btu/ft}^2\text{-sec} \quad [1]$$

Here R is the body nose radius, ρ and ρ_0 the ambient and sea-level density respectively, u the flight velocity, u_c the satellite velocity taken as 26,000 fps, and h_{ws} and h_{s1} the wall and stagnation enthalpies, respectively. While expressions of the form of Equation [1] are not exact results of the heat transfer theory on which they are based, they are convenient approximate formulas.

Since (1) was written, further refined heat transfer calculations have been made (2) and rates have also been measured in shock tubes under simulated hypersonic flight conditions (3). It is the purpose of this note to give a somewhat refined version of Equation [1] and show how it compares with experiment.

The new correlation expression which replaces Equation [1] is

$$q_s = \frac{17{,}600}{\sqrt{R}}\sqrt{\frac{\rho}{\rho_0}}\left(\frac{u}{u_c}\right)^{3.15}\left[\frac{h_{s1} - h_{ws}}{h_{s1} - (h_{ws})_{300}}\right]\text{Btu/ft}^2\text{-sec} \quad [2]$$

Received May 10, 1957.

[1] The heat transfer investigation of References (2, 3) on which this work is based was sponsored by the Western Development Division, Air Research and Development Command, U. S. Air Force, under Contract Af 04(645)-18.

[2] Principal Research Scientist.

[3] Senior Scientist.

[4] Numbers in parentheses indicate References at end of paper.

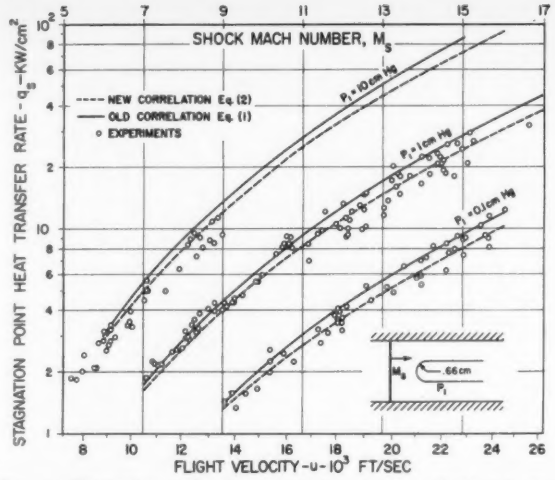
SHOCK MACH NUMBER, M_s
NEW CORRELATION Eq. (2)
OLD CORRELATION Eq. (1)
EXPERIMENTS
p_1 = 10 cm Hg
p_1 = 1 cm Hg
p_1 = 0.1 cm Hg
.66 cm
STAGNATION POINT HEAT TRANSFER RATE - q_s - KW/cm^2
FLIGHT VELOCITY - u - 10^3 FT/SEC

Fig. 1 Stagnation point heat transfer rate vs. flight velocity

The subscript 300 means evaluated at 300 K. Equation [2] agrees with the calculated heat transfer results in the range sea level to 250,000 ft and 7000 to 25,000 fps with an accuracy of ±10 per cent. It differs from [1] in the numerical coefficient, the power of u/u_c, and the enthalpy factor. The maximum change from Equation [1] for a 300 K wall temperature and satellite velocity is a reduction of 15 per cent, and the reduction decreases with decreasing velocity.

Shock tube experiments have been performed in air at the Avco Research Laboratory (2) to measure q_s. Both the flight stagnation enthalpy and fiight stagnation pressure are reproduced in these tests. The results are plotted in Fig. 1 as q_s against flight velocity, with an auxiliary scale of the Mach number of the moving incident shock in the shock tube (referred to a sound speed of 1129 fps). Three groups of points are shown for three different initial shock tube pressures p_1. They represent simulation of flight in three altitude ranges: p_1 = 0.1 cm Hg is 111,000–127,000 ft; p_1 = 1.0 is 64,000–80,000 ft; and p_1 = 10 is 11,000–31,000 ft. The expressions of Equations [1, 2] can be converted to the shock tube coordinates of Fig. 1 by means of normal shock relations and the properties of equilibrium air (4, 5). The curves of Equations [1, 2] are also shown. It can be seen that particularly at high Mach numbers, corresponding to high flight velocities, the new correlation is significantly nearer the mean of the data than the old one.

The effect on the results and conclusions of (1) of using the new correlation rather than the old one is negligible except at surface temperature parameters of over 5000 R-ft$^{1/8}$. The reason for this is that the surface temperature parameter varies as the fourth root of q_s, so the new correlation causes a change of at most a factor of 1.042 in that parameter, a factor which would hardly show on the figures of (1). Of course, some of the algebraic formulas of (1) relating to constant heat transfer trajectories will change slightly. In problems other than those considered in (1), where the heat transfer rate itself is important, the new correlation can make a significant difference.

References

1 Kemp, N. H., and Riddell, F. R., "Heat Transfer to Satellite Vehicles Re-entering the Atmosphere," JET PROPULSION, vol. 27, Feb. 1957, pp. 132–137.

2 Fay, J. A., and Riddell, F. R., "Theory of Stagnation Point Heat Transfer in Dissociated Air," RR 1, Avco Research Laboratory, Everett, Mass. Revised April, 1957. To be submitted to the *Journal of the Aeronautical Sciences.*

3 Rose, P. H., and Stark, W. I., "Stagnation Point Heat Transfer Measurements in Dissociated Air," RR 3, Avco Research Laboratory, Everett Mass.; revised April 1957. To be submitted to the *Journal of the Aeronautical Sciences.*

4 Hilsenrath, J., and Beckett, C., "Tables of Thermodynamic Properties of Argon-Free Air to 15,000°K," AEDC-TN-56-12, Arnold Engineering Development Center, USAF, Sept. 1956.

5 Feldman, S., "Hypersonic Gas Dynamic Charts of Equilibrium Air," Avco Research Laboratory, Everett, Mass., Jan. 1957.

Studies in a New Type of Flat Flame Burner[1]

WILLIAM T. BIEDLER III[2] and H. E. HOELSCHER[3]

The John Hopkins University, Baltimore, Md.

A new type of device for measuring flame velocities has been developed. This device is a burner utilizing a stable planar flame front which permits the study of stable flat flames, free from contact with any surface. Flame velocity as a function of concentration of combustible in the unburnt mixture has been determined for an air-propane system. The effect of the geometry of the system on flame properties is observed and discussed. Temperature and concentration measurements were made in the vicinity of the flame and are reported.

Introduction

THE process of controlled combustion and an understanding of this process is one of the challenging problems of many current research projects. To study this problem, the simplest possible physical system is most amenable to subsequent mathematic analysis of the results. Hence, it is desirable to avoid complex geometries similar to those of the conelike bunsen flame. This led to consideration of a flat-flame burner, representing a geometrically simple one-dimensional system.

Methods for measuring flame velocities have been surveyed by Fiock (2),[4] Linnett (4), and others. The general tenor of their remarks is that there is no one method capable of use over the entire range of flame velocities likely to be encountered (from 3 cm/sec to 1175 cm/sec) and that reported flame velocities vary widely according to the method of measuring them. One method of determining flame velocities with accuracy and precision is that used by Powling (5). A disk shaped planar flame front perpendicular to the axis of the burner was produced above and not in contact with the lip of the burner. This burner was modified by Egerton and Thabet (1) who measured flame velocities for various mixtures of hydrocarbons. The general features of their burner are presented in Fig. 1. This type of burner is excellent for the determination of flame velocities of very lean combustible mixtures. No other technique exists for examining flame velocities below 15 cm/sec.

A Powling-type burner basically met the requirements of the particular investigation contemplated, i.e., for the production of a homogeneous, laminar, premixed, stationary, geometrically-simple flame front. However, closer control of flame position and greater simplicity of construction seemed

Received June 4, 1957.

[1] This research was supported by the U. S. Air Force through the Air Force Office of Scientific Research and the Air Research and Development Command under Contract AF18(600)-1176.

[2] Research Assistant, Johns Hopkins University, Institute for Cooperative Research.

[3] Professor and Chairman, Department of Chemical Engineering.

[4] Numbers in parentheses indicate references at end of paper.

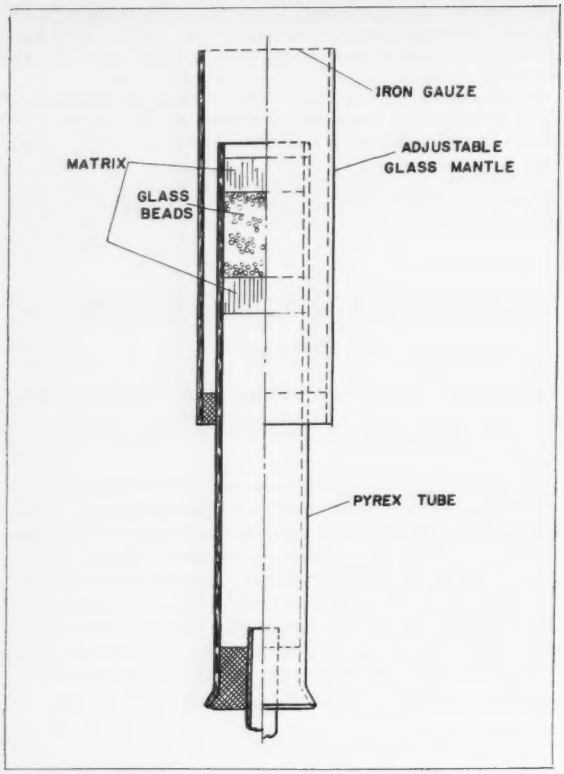

Fig. 1 Flat flame burner of reference 1

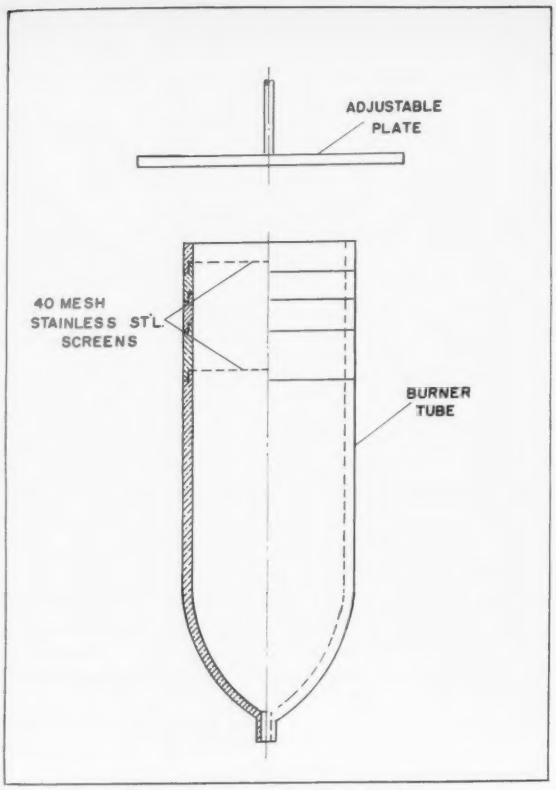

Fig. 2 Present flat flame burner

desirable. A succession of further modifications led to that burner shown in Fig. 2. The flat flames produced by this burner met all the previously established criteria of simplicity with the added advantages that the flame was free of surface contacts and could be probed more easily than in previous designs.

Apparatus and Experimental Procedure

The apparatus used in this study is quite standard. The air supply system consisted of two air compressors, a steel calming tank to remove pulsations, reducing and flow control valves, and a flowmeter with stainless steel float. The apparatus was interconnected using $\frac{1}{8}$ in. ID copper tubing. Instrument grade propane 99.9 per cent, a two-stage propane reducing valve and a series of needle valves for flow control, completed the assembly.

The burner system included a stainless steel mixing chamber, the burner itself, shown as Fig. 2, and the burner enclosure. The burner was constructed of cylindrical copper tubing and was 27 cm tall, 10 cm internal diam, and 0.63 cm wall thickness. The movable plate was a circular copper plate 0.63 cm thick and 17.8 cm in diam. The burner enclosure was a box 12 in. $\times$ 12 in. $\times$ 24 in. high made of aluminum with a 10 in. $\times$ 12 in. pyrex glass window for observation and photographic studies of the flame. A camera with a telephoto lens was used to photograph the flame.

Experimental Procedure

To initiate a run, the air compressors were turned on and, when a steady reading was observed on the air flowmeter, the burner was lighted using a lean mixture to prevent flashback onto the top internal screen. The gas flow was increased until a stable planar flame resulted above the burner.

Air flow rate, gas flow rate, atmospheric pressure, room tem-

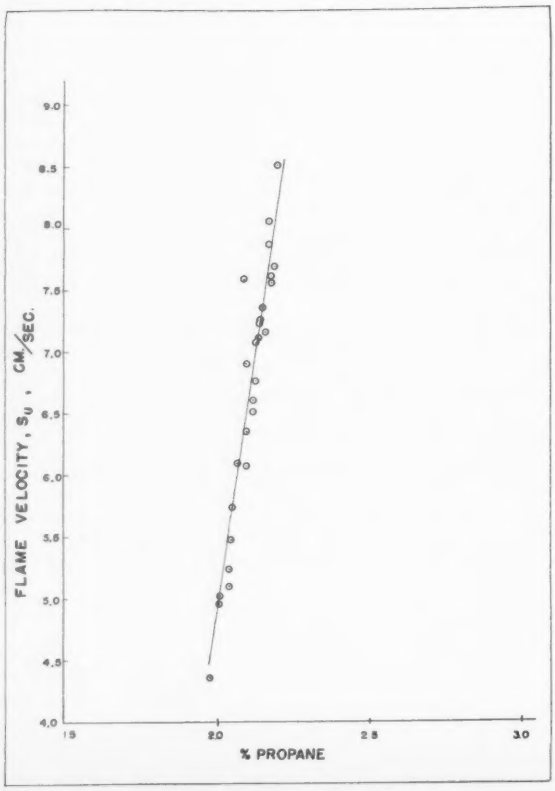

Fig. 3 Flame velocity vs. per cent propane

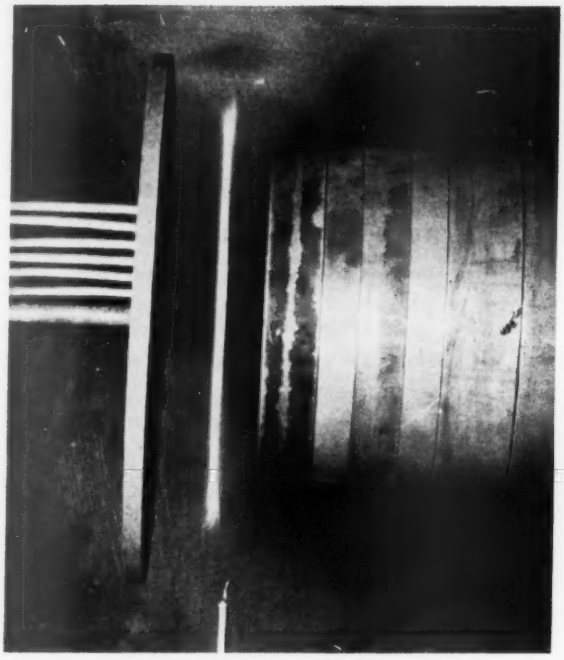

Fig. 4 Sample flame photograph

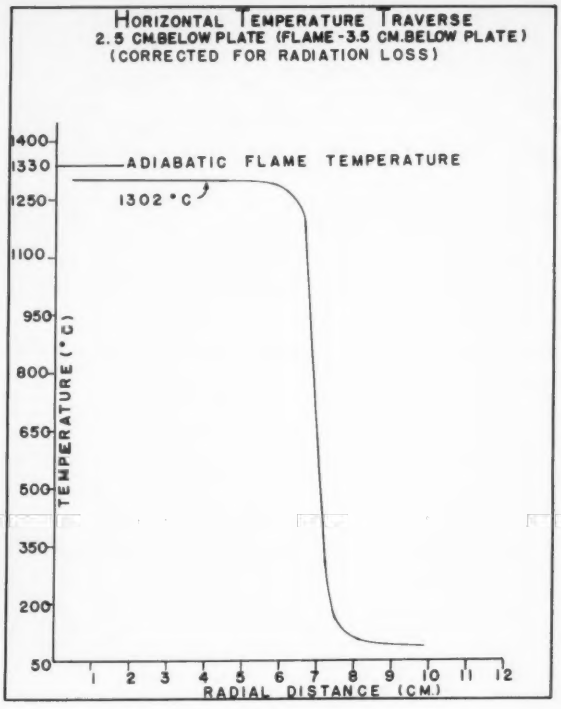

Fig. 5 Horizontal temperature traverse

perature, and plate position (i.e., distance above burner lip) were measured for each composition yielding a flame. A photograph was then taken of the flame.

In addition to the above measurements, attention was devoted to three special series of measurements. The velocity head was measured above the flame through six equidistant pressure taps in the plate. Temperature traverses were made both vertically and horizontally in the region between the flame and the plate through a slot milled in the plate. Finally, samples of the gases issuing from the flame region were taken and these were analyzed.

Results

In the burner shown in Fig. 2, a flat circular disk of flame was caused to float between the burner top and the movable plate. The flame is stable, thin, and has well-defined edges. The flame may be adjusted to a desired vertical position by changing the height of the plate above the burner lip. The plate may be moved vertically from a position approximately 3 cm above the burner lip to a position approximately 6 cm above the burner lip while maintaining a stable flame. The flame velocity apparently remains constant regardless of plate position.

Flame velocities of propane-air mixtures were measured to test the performance of this apparatus. The result is shown in Fig. 3. The data were obtained by photographing the flame under different flow rate and composition conditions. The flame area was then computed from the measured diameter. All volumetric flow rates were reduced to standard conditions of 760 mm of mercury and 18 C to compare the calculated flame velocities with those presented in (1). The solid line in Fig. 3 is a representation of the data from the work reported in this reference whereas the points represent measurements from this study. A sample photograph of the flame is reproduced in Fig. 4. It should be noted that the lower limits of stability was found at a concentration of 1.98 per cent propane. Below this a stable flame could not be maintained in the free space.

The plate was tapped for pressure measurements at six equidistant points outward from the center. Absolute and differential pressure measurements were made with a micromanometer (sensitivity ± 0.0001 in. of water). There was no detectible difference in velocity head or impact pressure at these six points.

A radial slot 0.63 cm wide and 8.3 cm long was milled from the edge of the plate toward the center. Visual and photographic studies indicated that this slot did not effect the flame. It was possible to investigate the temperature and concentration of the gas in the region between the plate and the flame by downstream probing through this slot. In order not to disturb the flame, upstream probing was done by inserting a probe through the enclosure wall.

Radial temperature traverses were made at various distances below the plate in the region between the plate and the flame. These data were corrected for radiation error using the method described by Friedman (3). Fig. 5 shows a typical horizontal traverse, 2.5 cm below the plate and 1 cm above the flame. Fig. 6 shows two typical vertical traverses, the first at 2 cm from the burner centerline and the second at 5 cm from the burner centerline. In both of the latter cases the flame was again at 3.5 cm below the plate. The theoretical adiabatic flame temperature for 2.16 per cent propane-air mixture is 1332 C (this is the gas composition used for all of the data shown in the figures and photograph accompanying this paper). It is observed that the corrected measured temperature at the flame front is very close to this theoretical value.

The concentration measurements of the burner exit gases, made on a gross averaged sample as well as on point samples taken between the flame and the plate, indicate that there is no unburned propane and no carbon monoxide in the off gases. This conclusion is believed to be accurate to within ± 0.03 per cent and is in agreement with reports of previous investigators.

It was suggested that the plate temperature may be exerting significant influence on the flame properties. As indicated in Fig. 6, the plate temperature was undoubtedly well above

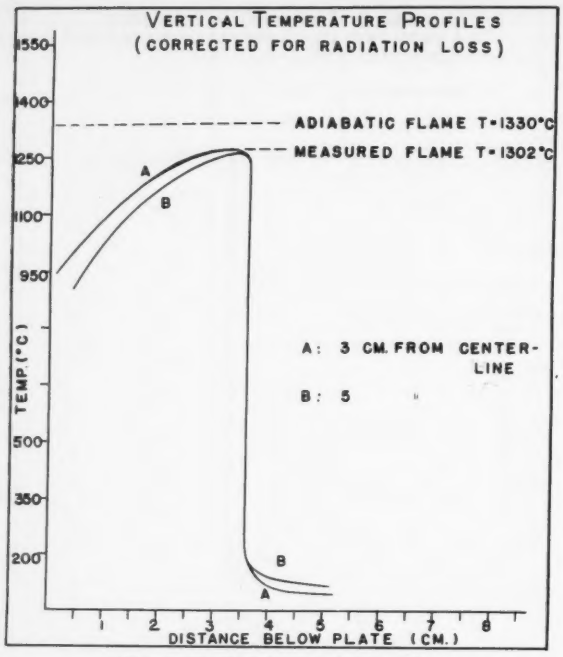

Fig. 6 Vertical temperature profiles

500 C. A new plate was constructed with provision for water cooling. The plate was hollow and a water stream was injected into the cavity tangentially and removed axially. The flow rate was high enough that the temperature increase between inlet and exit stream was less than 2 C. Using this water cooled plate, the data taken with the solid plate were rechecked. In all cases the data were reproduced exactly. The effect of a heated plate remains to be considered.

Conclusions

The flat flame burner described is suitable for the measurement of flame velocities in lean mixtures with a high degree of accuracy and sensitivity. These measurements may be made in this device under conditions where surface effects are known to be absent. This device is limited to the study of slow burning flames.

At the present time, relationships between the following parameters have been studied:

(a) Plate height above the burner lip.
(b) Flame height above the burner lip.
(c) Concentration of combustible in the inlet gas mixture.
(d) Flame velocity.

Thus far, only flame velocity and the concentration of combustible in the unburnt mixture seem to be directly related. Egerton and Thabet (1) state that for a given gauze height, Fig. 1, the product of the flame height above the burner and flame velocity is approximately constant. No satisfactory correlation of this type has been found in the present study. Over a wide range of condition, the flame height was observed to be solely a function of the plate height, all other variables being constant, since it permits the flame to be moved (for example, relative to a stationary thermocouple) without introducing extraneous effects on flame velocity.

References

1 Egerton, A., and Thabet, S. K., *Proceedings of the Royal Society* (London). *A211*, 445 (1952).

2 Fiock, E. F., "Physical Measurements in Gas Dynamics and Combustion," Princeton University, Princeton University Press, 1949, p. 409.

3 Friedman, R., "Fourth Symposium (International) on Combustion," Baltimore, Williams and Wilkins, 1953.

4 Linnett, J. W., "Fourth Symposium (International) on Combustion," Baltimore, Williams and Wilkins, 1953.

5 Powling, J., *Fuel*, vol. 28, 1949, p. 25.

Comments on the Powered Flight Trajectory of a Satellite

THEODORE N. EDELBAUM[1]

United Aircraft Corporation, E. Hartford, Conn.

Nomenclature

g	=	acceleration of gravity at the earth's surface
R_e	=	radius of the earth
u_x	=	horizontal component of velocity
u_y	=	vertical component of velocity
t	=	time
T	=	burnout time
y	=	altitude
D	=	distance of closest approach of satellite orbit
N	=	ratio of thrust to mass
ψ	=	angle between thrust vector and horizontal
$\lambda_1, \lambda_2, \lambda_3$	=	Lagrange multipliers

Discussion

TWO analyses of the optimum thrust angle variation of a satellite launching vehicle have appeared in JET PROPULSION (1, 2).[2] Both of these analyses have shown that the tangent of the angle between the thrust vector and the horizontal should vary linearly with time. However, neither of these analyses includes the effect of centrifugal force, which is significant for satellite launching vehicles.[3]

The significance of centrifugal force can be demonstrated by starting with the equations of motion for a round earth and noting what assumptions are necessary to reduce these equations to the flat-earth equations assumed in (1, 2). Assuming the vehicle to be a point mass moving in a vacuum around a spherical, nonrotating earth, the equations of motion may be written, in the notation of (1), as follows

$$\left.\begin{aligned} \frac{du_y}{dt} - \frac{u_x^2}{R_e + y} &= N \sin \psi - g \frac{R_e^2}{(R_e + y)^2} \\ \frac{du_x}{dt} + \frac{u_x u_y}{R_e + y} &= N \cos \psi \\ \frac{dy}{dt} &= u_y \end{aligned}\right\} \quad \ldots [1]$$

These equations may be simplified by assuming that the altitude during powered flight is small compared to the earth's radius. This assumption allows $R_e + y$ to be replaced by R_e in Equations [1] and also allows the second term in the second of Equations [1] to be dropped. This latter simplification may be seen by rearranging the second of Equations [1] with the aid of the third of Equations [1]

$$\frac{du_x}{u_x} + \frac{dy}{R_e} = \frac{N \cos \psi}{u_x} dt \quad \ldots [2]$$

Received July 31, 1957.

[1] Research Engineer, Research Department. Mem. ARS.

[2] Numbers in parentheses indicate References at end of note.

[3] The significance of centrifugal force has been recognized by F. M. Perkins in Reference 2. He eliminates it from consideration by the artifice of assuming a constant mean direction for gravity during the powered flight. This assumption allows him to obtain an approximate closed form solution to the optimum path.

As the altitude is always small compared to R_e, dy/R_e may be considered infinitesimal and can be eliminated. With these considerations, Equations [1] reduce to Equations [3]

$$\left.\begin{aligned} \frac{du_y}{dt} - \frac{u_x^2}{R_e} &= N \sin \psi - g \\ \frac{du_x}{dt} &= N \cos \psi \\ \frac{d_y}{dt} &= u_y \end{aligned}\right\} \quad \ldots [3]$$

The equations of motion [3] are equivalent to those used in (1, 2) except for the centrifugal acceleration term in the first equation. The centrifugal acceleration u_x^2/R_e may be eliminated only if it is small compared to the gravitational acceleration g or to the vertical component of the thrust to mass ratio $N \sin \psi$. As these assumptions are not usually satisfied for satellite launching vehicles, centrifugal acceleration must be retained in the equations of motion. The following is the derivation of the optimum path including this term.

The optimum launching trajectory of a satellite, for the equations of motion [3], can be found by use of the Calculus of Variations. For convenience, the problem is formulated as minimizing the time required to reach an orbit with a given distance of closest approach. This is equivalent to the problem of maximizing the distance of closest approach for a given burning time. The variational integral for minimizing time for a given functional relationship between altitude, horizontal velocity, and vertical velocity at burnout takes the form

$$I = \int dt + \left\{\lambda_1 \left(\frac{du_y}{dt} - \frac{u_x^2}{R_e} - N \sin \psi + g\right) + \lambda_2 \left(\frac{du_x}{dt} - N \cos \psi\right) + \lambda_3 \left(\frac{dy}{dt} - u_y\right)\right\} dt \quad \ldots [4]$$

The Euler equations for this integral take the following form

$$\left.\begin{aligned} E_{u_y} = 0 &= -\frac{d\lambda_1}{dt} - \lambda_3 \\ E_{u_x} = 0 &= -\frac{d\lambda_2}{dt} - \frac{2\lambda_1 u_x}{R_e} \\ E_y = 0 &= -\frac{d\lambda_3}{dt} \\ E\psi = 0 &= -\lambda_1 N \cos \psi + \lambda_2 N \sin \psi \end{aligned}\right\} \quad \ldots [5]$$

These equations may be operated upon to yield

$$\left.\begin{aligned} \tan \psi &= \frac{\lambda_1}{\lambda_2} \\ \lambda_1 &= \lambda_{1T} + \lambda_{3T}(T - t) \\ \lambda_2 &= \lambda_{2T} + \int \frac{2\lambda_1 u_x}{R_e} d(T - t) \end{aligned}\right\} \quad \ldots [6]$$

The values of y_T, V_{xT}, and V_{yT} must be such that the resulting orbit has the required distance of closest approach. This can be insured by imposing a transversality condition for the distance of closest approach on the ratios of the burnout value of the Lagrange multipliers of Equations [6]. For the present problem, the transversality conditions are conditions [7], where $D_y := \partial D/\partial y$ etc.[4]

$$\left.\begin{aligned} \frac{\lambda_{1T}}{\lambda_{2T}} &= \frac{D_{u_y}}{D_{u_x}} \\ \frac{\lambda_{3T}}{\lambda_{2T}} &= \frac{D_y}{D_{u_x}} \end{aligned}\right\} \quad \ldots [7]$$

[4] The expression for distance of closest approach may be found in Reference 1.

The solution of Equations [3] and [6] with the initial boundary conditions and the terminal conditions [7] is the solution of the problem for any given variation of thrust and mass with time. Unfortunately, the necessary inclusion of centrifugal force does not allow any simple closed form solution for the optimum path.

References

1 Fried, B. D., "On the Powered Flight Trajectory of an Earth Satellite," JET PROPULSION, vol. 27, June 1957, pp. 641–643.

2 Perkins, F. M., "Flight Mechanics of Ascending Satellite Vehicles," JET PROPULSION, vol. 26, May 1956, pp. 352–358.

Some Decomposition Products of Normal Propyl Nitrate

S. A. GREENE[1] and L. J. GORDON[2]

Aerojet-General Corp., Azusa, Calif.

PERFORMANCE calculations based on equilibrium constants were made for normal propyl nitrate as a monopropellant. Table 1 shows a calculated composition and resultant flame temperature.

When the material is decomposed in a motor, the flame temperature as measured with an unshielded thermocouple is found to be 2100 ± 100 F, considerably higher than the calculated temperatures. Gas samples, removed from the motor by a water-cooled probe just upstream of the nozzle, were analyzed by the technique of gas chromatography. The results are shown in Table 2. Not recorded, but qualitatively identified, were HCN, NH_3, H_2O, CO_2, and $C_{(s)}$. No attempt was made to measure these quantitatively since it was thought that reaction between all components except the last would take place in the sample bombs, and representative gas samples would not be obtained.

It can be shown for this system that a mass balance cannot

Table 1 Equilibrium Calculation for Decomposition of Normal Propyl Nitrate with Flame Temperature of 1880 F at 300 psia

Component	Per cent volume
H_2	43.7
CO	39.3
N_2	7.6
CH_4	3.2
$C_{(s)}$	1.5
CO_2	1.5
H_2O	3.2
NH_3	Trace

Table 2 Analyses of Some Decomposition Products of Normal Propyl Nitrate

	Per cent volume				
Gas	1	2	3	4	Average
H_2	19.1	21.0	21.4	21.5	20.8
CO	49.2	48.2	50.7	48.9	49.2
N_2	9.6	7.8	7.5	7.1	8.0
CH_4	13.6	16.7	16.7	15.7	15.7
C_2H_6	2.5	0.7	1.0	1.7	1.5
C_2H_4	6.0	5.6	2.7	5.1	4.8

Received June 18, 1957.

[1] Chemist, Project 107A Research Department.

[2] Chemical Engineer, Solid Engine and Chemical Department. Mem. ARS.

be made when using the analyses of Table 2 or any combination of the qualitatively identified products. Such products as NO, N_2O, or (C_2N_2) would permit a mass balance, but the NO was looked for and not found; qualitative analyses for the latter two products were not attempted. Some flame-temperature calculations were made on the basis of a postulated analysis composed of the experimentally analyzed products and (C_2N_2). The calculated flame temperature was found to be 400 F higher than the observed flame temperatures.

Although this work does not permit quantitative conclusions, indications are that even at 2200 F, performance calculations based on equilibrium constants must be considered suspect.

Thermal Conductivity and Prandtl Numbers for Nonpolar Polyatomic Gases at High Temperatures

ELDON L. KNUTH[1]

University of California, Los Angeles, Calif.

Nomenclature

A^* = ratio of Schmidt number for elastic-sphere model to Schmidt number for given intermolecular-force model
c_p = specific heat at constant pressure
D = coefficient of self-diffusion
Pr = $c_p\mu/\lambda$ = Prandtl number
Sc = $\mu/\rho D$ = Schmidt number
λ = coefficient of thermal conductivity
μ = coefficient of viscosity
ρ = density

Superscript

$'$ = refers to the property of a monatomic gas having the same molecular weight and the same intermolecular force constants as the polyatomic gas

THE purpose of this note is to present, in a form convenient for use by aerodynamic and propulsion engineers, expressions which permit the calculating of the coefficient of thermal conductivity and the Prandtl number for nonpolar polyatomic gases at high temperatures, starting only with the specific heat of the polyatomic gas and expressions for properties of a monatomic gas.

Molecular transfer of heat in a polyatomic gas is considered to take place by transfer (through collisions) of the molecular energy associated with translation and by transfer (through self-diffusion and inelastic collisions) of the molecular energies associated with rotation and vibration (1)[2] p. 238. If one assumes that the transfer of translational energy and the self-diffusion of molecules are not affected by the presence of internal degrees of freedom, and that the transfer of energy from molecule to molecule is so rapid that an equilibrium (Maxwellian) distribution of molecules corresponding to the local temperature is realized even though a temperature gradient exists, then the following expression for the coefficient of thermal conductivity of a polyatomic gas may be derived, see (1) p. 238 or (4) p. 501:

$$\lambda = \lambda' + \rho D(c_p - c_p')$$

The first term in the right-hand side corresponds to transfer of energy associated with the translational degrees of freedom whereas the second term corresponds to transfer of energy associated with the internal degrees of freedom.[3] Since it is assumed that the presence of internal degrees of freedom has a negligible effect on the coefficients of viscosity and diffusion, this equation may be written in the following form also

$$\frac{\lambda}{\lambda'} = 1 + \frac{\mathrm{Pr}'}{\mathrm{Sc}'}\frac{c_p - c_p'}{c_p'}$$

The value of the Prandtl number for the polyatomic gas may be obtained directly now from the relation

$$\mathrm{Pr} = \mathrm{Pr}'\frac{c_p}{c_p'}\frac{\lambda'}{\lambda}$$

Using results of molecular theory of gases, several suggestions for bringing these equations into agreement with experimental results have been made. The various suggestions may be considered equivalent to assuming a value of $\frac{2}{3}$ for Pr′ and various values for Sc′. Eucken (2), without the benefit of much of our present knowledge, assumes the equivalent of $\mathrm{Sc}' = 1$; Chapman and Cowling (1) p. 238, mention that $\mathrm{Sc}' = 0.83$ (result for Bernoulli elastic-sphere model) and $\mathrm{Sc}' = 0.64$ (result for Maxwell repulsion model) would give conductivity values of the correct order of magnitude; Vines and Bennett (7) subscribe to $\mathrm{Sc}' = 0.83/A^*$, where A^*, a measure of the deviation from results for the elastic-sphere model, is equal to 1.10 for a wide range of temperatures (result for Lennard-Jones attraction-repulsion model), so that $\mathrm{Sc}' = 0.76$, whereas Hirschfelder (5) p. 25, speculates that one should use perhaps $\mathrm{Pr}'/\mathrm{Sc}' = 1$, implying that $\mathrm{Sc}' = 0.67$. The resulting equations for Prandtl number as a function of specific heat, as well as data for 15 nonpolar gases, compiled by Keyes (6), Hilsenrath and Touloukian (3), and Vines and Bennett (7), are presented in Fig. 1 and the table. For each gas, the Prandtl

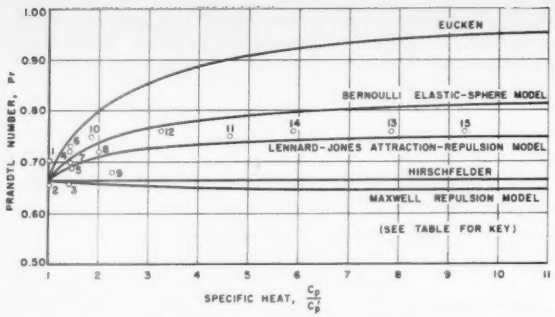

Fig. 1. Prandtl number vs. specific heat for nonpolar gases

Values of Prandtl number and specific heat for 15 Nonpolar gases

	Gas	Temp., (F)	c_p/c_p'	Pr	Ref.	A^*
1	He	260	1.00	0.70	3	1.13
2	A	572	1.00	0.65	6	1.10
3	H_2	800	1.42	0.66	3	1.12
4	CO	260	1.41	0.72	3	1.10
5	N_2	752	1.47	0.69	6	1.11
6	NO	260	1.44	0.73	3	1.10
7	O_2	260	1.45	0.70	3	1.10
8	N_2O	212	2.01	0.72	6	1.10
9	CO_2	620	2.28	0.68	3	1.09
10	CH_4	212	1.88	0.75	6	1.09
11	C_3H_8	284	4.62	0.75	7	1.10
12	C_2H_6	284	3.24	0.76	7	1.09
13	C_6H_{12}	320	7.86	0.76	7	1.10
14	C_6H_6	320	5.90	0.76	7	1.10
15	C_6H_{14}	320	9.31	0.76	7	1.10

Note: Values of A^* are determined from Table I-N of Reference 4 using values for the maximum energy of attraction tabulated in Table I-A of same book.

Received July 19, 1957.

[1] Associate Research Engineer. Mem. ARS.

[2] Numbers in parentheses indicate References at end of note.

[3] See Reference 4, p. 534, for an equation relating the coefficient of thermal conductivity for a monatomic gas with the pertinent parameters. The specific heat for a monotomic gas is simply the Boltzmann constant multiplied by $\frac{5}{2}$.

number used corresponds to the highest temperature for which data are given. Examining the table, it is seen that the calculated values of A^* substantiate the use of $A^* = 1.10$ for the Lennard-Jones attraction-repulsion model. Examining the figure, it is seen that the presented data agree best with the curve for the Lennard-Jones attraction-repulsion model, especially for the gases having many internal degrees of freedom.

Since interactions of polar molecules are not described adequately by the simple interaction potentials, such as the Lennard-Jones potential, one would not expect data for polar molecules to agree with the presented theoretical curves. Water vapor is the polar gas encountered most frequently perhaps by aerodynamic and propulsion engineers. Also, since the assumption of large average distances between molecules, in comparison with molecular diameters, is fundamental to the molecular theory of transport phenomena in gases, one would expect experimental and theoretical results to agree better, for a given pressure, at high temperatures than at low temperatures. These expectations are substantiated by available experimental data, not presented in the accompanying figure, see (7).

It is concluded that the equations

$$\frac{\lambda}{\lambda'} = 1 + 0.88\,\frac{c_p - c_p'}{c_p'}$$

$$\mathrm{Pr} = \frac{2}{3}\,\frac{c_p}{c_p'}\,\frac{\lambda'}{\lambda}$$

provide the best available analytical approximations for the coefficient of thermal conductivity and the Prandtl number for nonpolar polyatomic gases at high temperatures. It is believed that these relations are in a form convenient for use by aerodynamic and propulsion engineers.

Addendum

Subsequent to the submission of the manuscript for this technical note, the author discovered that Hirschfelder has superseded his speculation with a detailed study (*Journal of Chemical Physics*, Feb., 1957). He concludes, as is done in the present note, that the best analytical expression for the thermal conductivity of a nonpolar polyatomic gas is obtained using results for the Lennard-Jones model (or for the similar Buckingham model). The author believes that the present publication will hasten acceptance of the modified Eucken equation by aerodynamic and propulsion engineers.

References

1 Chapman, S., and Cowling, T. G., "The Mathematical Theory of Non-Uniform Gases," Cambridge: University Press, 1952.

2 Eucken, A., "Uber das Wärmeleitvermögen, die spezifische Wärme und die innere Reibung der Gase," *Physikalische Zeitschrift*, vol. 14, April 1913, pp. 324–332.

3 Hilsenrath, J., and Touloukian, Y. S., "The Viscosity, Thermal Conductivity, and Prandtl Number for Air, O_2, N_2, NO, H_2, CO, Co_2, H_2O, He, and A," *Trans. ASME*, vol. 76, Aug., 1954, pp. 967–985.

4 Hirschfelder, J. O., Curtiss, C. F., and Bird, R. B., "Molecular Theory of Gases and Liquids." New York: John Wiley and Sons, Inc., 1954.

5 Hirschfelder, J. O., "Heat Transfer in Chemically Reacting Gas Mixtures," WIS-ONR-18. Madison: University of Wisconsin, Feb. 6, 1956.

6 Keyes, F. G., "The Heat Conductivity, Viscosity, Specific Heat, and Prandtl Numbers for Thirteen Gases," Project Squid TR 37. Cambridge, Mass: MIT, April 1, 1952.

7 Vines, R. G., and Bennett, L. A., "The Thermal Conductivity of Organic Vapors. The Relationship between Thermal Conductivity and Viscosity, and the Significance of the Eucken Factor," *The Journal of Chemical Physics*, vol. 22, March, 1954, pp. 360–366.

Optimal Rocket Trajectories

D. F. LAWDEN[1]

Canterbury University College, Christchurch, New Zealand

FRIED, B. D., has proved (1)[2] that, if air resistance and variations in the magnitude and direction of gravity during the thrust period of a satellite vehicle can be neglected, then, for optimum performance, the tangent of the thrust attitude angle must be a linear function of the time.

This result may be generalized as follows: Taking horizontal and vertical axes Ox, Oy, respectively, through the launcher and assuming the trajectory to lie in the plane Oxy, let (q_1,q_2) be the rocket coordinates at "all-burnt" and let $(\dot{q}_1,\dot{q}_2)$ be its velocity components. Then, if R is any function of the variables $(q_1,q_2,\dot{q}_1,\dot{q}_2)$, (e.g., rocket range, maximum altitude or eccentricity of subsequent orbit), R will take a stationary value (usually a maximum) for a thrust direction program determined by the equation

$$\tan\psi = \frac{\dfrac{\partial R}{\partial q_2}(T-t) + \dfrac{\partial R}{\partial \dot{q}_2}}{\dfrac{\partial R}{\partial q_1}(T-t) + \dfrac{\partial R}{\partial \dot{q}_1}}$$

where ψ is the angle made by the direction of thrust with Ox at time t after launching and T is the total period of thrust. Thus $\tan\psi$ is always a bilinear function of the time, viz.

$$\tan\psi = \frac{at+b}{ct+d}$$

The proof will be found in (2).

Clearly, $\tan\psi$ is a linear function of t if, and only if, R is independent of q_1.

References

1 Fried, B. D., "On the Powered Flight Trajectory of an Earth Satellite," JET PROPULSION, vol. 27, June 1957, pp. 641–643.

2 Lawden, D. F., "Dynamic Problems of Interplanetary Flight," *Aeronautical Quarterly*, vol. 6, 1955, pp. 165–180.

Received August 15, 1957.

[1] Professor of Mathematics.

[2] Numbers in parentheses indicate References at end of note.

Note on 'Take-off from Satellite Orbit'

J. B. PETERSON[1]

The Ramo-Wooldridge Corp., Los Angeles, Calif.

Nomenclature

c = effective exhaust velocity of the rocket
r_0 = radius of initial satellite orbit
g = magnitude of gravitational attraction at $r = r_0$
M_0 = total mass
M_1 = burnout mass
ν = ratio of circumferential thrust to gravitational force at $r = r_0$

THIS note concerns the result arrived at by Tsien[2] that the mass ratio factor for escape from a satellite orbit $c/\sqrt{gr_0}$

Received July 26, 1957.

[1] Rocket Propulsion Systems, Mem. ARS.

[2] "Take-off from Satellite Orbit," by H. S. Tsien, *Journal of The American Rocket Society*, vol. 23, July-Aug. 1953, pp. 233–236.

$\log_e (M_0/M_1)$ is a monotonically decreasing function of ν, the thrust factor for circumferential thrust. This penalty in mass ratio for low acceleration is caused by leaving the working medium at a higher orbital energy than corresponds to the altitude of the original orbit. There seems to be a way to reduce this penalty in mass ratio to an arbitrarily small value if one is willing to accept a penalty in time instead.

It appears advantageous to make the escape trajectory a succession of short periods of acceleration near the perigee and long periods of coasting. If there is no acceleration except tangential acceleration near the perigee of an elliptical orbit, the altitude of the perigee will not change greatly. In the limit as the period of thrust approaches zero, i.e., a pulse at the perigee, the trajectory will approach a succession of ellipses with the same perigee. This result comes from the consideration that the orbit of the vehicle must be elliptical, both before and after the pulse. Since both before and after the impulse the velocity is normal to the earth radius, the vehicle must be at the perigee of both orbits. In this case the working fluid will be given off with the same distribution of orbital energies as in the impulsive case and the mass ratio corresponding to impulsive accelerations to escape velocity can be achieved.

The Performance of a Rocket with Tapered Exhaust Velocity

HOWARD S. SEIFERT[1]

The Ramo-Wooldridge, Los Angeles, Calif.

The effect of varying the exhaust gas velocity of a rocket so that the exhaust gases possess little or no kinetic energy in an earth observer's frame of reference is examined. Under certain boundary conditions an improvement in terminal velocity of 10 to 20 per cent is obtained relative to a rocket with fixed exhaust velocity. Given a fixed budget of energy per unit payload mass, the optimum mass of working fluid into which to distribute this energy (for maximum burnout speed) is calculated as a function of gravitational field strength.

Introduction

A CONSIDERABLE fraction of the propellant energy of a rocket is dissipated in the exhaust which, even if expanded with 100 per cent thermodynamic efficiency, trails along after or away from the rocket at high speed, carrying energy which would preferably have been retained in the payload. The conventional chemical propellant must be ejected at constant speed with respect to the rocket, a relatively inefficient process. Recent general interest in the use of nuclear energy for rocket propulsion suggests the possibility that the exhaust velocity of a rocket may become a controlled variable rather than a constant as it has been so far. This paper will calculate the relative performance of rockets with tapered-velocity exhaust and fixed-velocity exhaust under certain boundary constraints, and show that improvement in payload velocity can be obtained. An additional calculation will be made to show certain optimum circumstances under which a constant but arbitrarily adjustable exhaust velocity may be used.

Statement of the Problems

Two problems will be examined:

a. Given two rockets with identical mass ratios, mass flow rates, and propellant masses, what will be the ratio of their burnout velocities if they consume amounts of energy which are equal, but distributed in the first one in such a way as to cause the exhaust trail to have zero (or small) velocity relative to ground, and in the second in the usual manner with a fixed velocity relative to the rocket? Presumably the first distribution should be more efficient, since more of the propellant energy goes into the payload.

b. Suppose we are given a fixed amount of energy per unit payload which may be distributed uniformly into any desired fraction ζ of the mass of a rocket in order to propel the remaining payload fraction $1 - \zeta$. What is the value of ζ which will result in the highest terminal velocity of the residue? The possibility of optimum ζ is intuitively evident, since with fixed energy, if ζ is too low not much momentum will result per unit energy expended while if ζ is too high the consequent low exhaust velocity will reduce performance.

In both the above problems it has been assumed that any arbitrary amount of energy may be associated with a unit mass; in other words, temperature is not a limiting factor. This is not true at present, but there is no a priori reason to believe that the containment of high temperature matter is an unsolvable problem.

The Tapered Exhaust Velocity Program

The equation of motion of a rocket moving vertically, and possessing at $t = 0$ an initial exhaust velocity c_0 which increases by the same amount that the vehicle speed increases, is

$$(M_0 - \dot{m}t)(a + g) = \dot{m}\left[\int_0^t a\,dt + c_0\right] \quad [1]$$

where

M_0 = initial total mass
$\dot{m}$ = mass flow rate (constant)
a = upward acceleration relative to ground
g = constant gravitational field acceleration
c_0 = initial (constant) exhaust velocity

This may be reduced by differentiation to

$$\frac{da}{2a + g} = \frac{dt}{t_0 - t} \quad [2]$$

where $t_0 = M_0/\dot{m}$. If the initial acceleration is $a_0[= (c_0\dot{m}/M_0) - g]$, then Equation [2] may be integrated twice to give

$$v' = \left(c_0 - \frac{gt_0}{2}\right)\left(\frac{t}{t_0 - t}\right) - \frac{gt}{2} \quad [3]$$

where v' is the vehicle velocity upward. At burnout

$$t = t_b = \zeta M_0/\dot{m} = \zeta t_0$$

where

$$\zeta = \frac{R - 1}{R} = \frac{M_p}{M_0 + M_p} = \text{loading fraction}$$

$$R = \frac{1}{1 - \zeta} = \frac{M_0 + M_p}{M_0} = \text{mass ratio}$$

The velocity at burnout ($t = t_b$) follows from Equation [3]

$$v_b' = c_0(R - 1) - \frac{gt_b}{2}(R + 1) \quad [4]$$

Let us define a gravity loss parameter $\gamma_b = gt_b/c$, which is essentially the decrease in missile speed at burnout caused by the gravitational deceleration measured in multiples of an exhaust velocity c. This exhaust velocity c is that of an equal-energy rocket of constant-exhaust velocity. It will presently be related to c_0. Using γ_b in Equation [4], we arrive at

$$v_b' = c_0(R - 1)\left(1 - \frac{\gamma_b}{2}\cdot\frac{R + 1}{R - 1}\cdot\frac{c}{c_0}\right) \quad [5]$$

Received May 15, 1957.

[1] Senior Staff Member, Guided Missile Research Div. Mem. ARS.

The velocity reached by a *conventional* rocket with the same R and burning time t_b is

$$v_b = c\ln R - gt_b = c(\ln R - \gamma_b) \quad \ldots\ldots [6]$$

We may then express the ratio of the burnout velocities of the tapered-c vs. constant-c vehicles as

$$\frac{v_b'}{v_b} = \frac{c_0(R-1)\left(1 - \frac{\gamma_b}{2}\cdot\frac{R+1}{R-1}\cdot\frac{c}{c_0}\right)}{c(\ln R - \gamma_b)}$$

$$\frac{v_b'}{v_b} = \left[\frac{(R-1)}{\ln R - \gamma_b}\right]\left[\frac{c_0}{c} - \frac{\gamma_b}{2}\cdot\frac{R+1}{R-1}\right] \quad \ldots\ldots [7]$$

The two rockets must expend equal energies, as well as have the same values of M_0, $\dot{m}$, R, and t_b; c_0 and c are therefore related. The energy equivalence may be expressed as

$$\frac{1}{2}m_p c^2 = \frac{1}{2}\int_0^{t_b}[v' + c_0]^2\dot{m}\,dt \quad \ldots\ldots [8]$$

where

c = exhaust velocity of constant-c rocket
m_p = total propellant mass of either rocket
$\dot{m}$ = constant mass flow rate of either rocket
v' = instantaneous velocity of tapered-c rocket

Substituting Equation [3] in [8] and simplifying, after extensive algebra, results in

$$\frac{c_0}{c} = \frac{\gamma_b}{2} + \sqrt{\frac{1 - \gamma_b^2/12}{R}} \quad \ldots\ldots [9]$$

We may now eliminate c_0/c from [7] by the use of [9] and have the comparison v_b'/v_b in terms of the two fundamental parameters R and γ_b

$$\frac{v_b'}{v_b} = \frac{1}{\ln R - \gamma_b}\left(\frac{R-1}{R^{0.5}}\cdot\sqrt{1 - \gamma_b^2/12} - \gamma_b\right) \quad \ldots [10]$$

A typical value of $\gamma_b = gt_b/c$ is 0.25. In efficient rockets, it is seldom that $\gamma_b > 1$. Therefore we may neglect $\gamma_b^2/12$ relative to unity and simplify [10] to

$$\frac{v_b'}{v_b} \cong \frac{(R-1)R^{-0.5} - \gamma_b}{\ln R - \gamma_b} \quad \ldots\ldots [11]$$

Values of v_b'/v_b are shown in Table 1, and plotted in Fig. 1, indicating the effect of the tapered-exhaust velocity on v_b'/v_b. It can be seen that in field-free space ($\gamma_0 = 0$) at $R = 5$, an 11 per cent improvement in relative terminal velocity can be obtained. In the presence of gravitational fields, the *ratio* is increased, although both *velocities* decrease, of course, in absolute magnitude.

Maximum Temperature of Tapered Exhaust

If the exhaust stream is produced by thermal expansion, the temperature of the gas reservoir will be proportional to the square of the exhaust velocity relative to the rocket. The maximum temperature will be reached at burnout in the tapered-c case. The ratio of maximum temperatures T_m'/T_m, tapered to constant operation, will be

$$\frac{T_m'}{T_m} = \frac{(v_b' + c_0)^2}{c^2} \quad \ldots\ldots [12]$$

Let us use relations [5] and [9] to evaluate the field-free case ($\gamma_b = 0$)

$$\frac{T_m'}{T_m} = \frac{[c_0(R-1) + c_0]^2}{c^2} = \frac{c_0^2}{c^2}\cdot R^2 = R \quad \ldots\ldots [13]$$

For example, we see from Table 1 that an 11 per cent improvement in $v_b(R = 5)$ results in a fivefold rise in maximum temperature. If Equation [12] is evaluated for $R = 5$ and $\gamma_b = 0.25$, the ratio T_m'/T_m becomes 4.4.

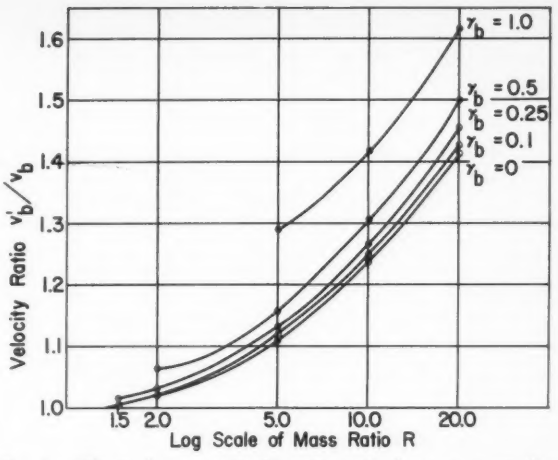

Fig. 1. Effect of mass ratio R and gravity loss γ_b on velocity ratio v_b'/v_b

Maximum Velocity of Tapered Exhaust

The maximum exhaust velocity c_m' of the tapered-c rocket relative to the fixed exhaust c is given by

$$\frac{c'_{max}}{c} = \frac{v_b' + c_0}{c_0}$$

Table 1 Effect of R and γ_b on burnout velocity ratio (v_b'/v_b)

R \ γ_b	0	0.1	0.25	0.5	1.0
			(v_b'/v_b)		
1.5	1.005	1.008	1.015	*	*
2.0	1.020	1.023	1.032	1.072	*
5.0	1.11	1.12	1.13	1.16	1.29
10.0	1.24	1.25	1.27	1.31	1.42
20.0	1.42	1.43	1.46	1.50	1.62

* For these large values of γ_b, both v_b' and v_b are negative; i.e., the rocket is sinking rather than rising at burnout, and the ratio, v_b'/v_b is not significant.

Using Equations [4] and [9] and the fact that $gt_b = c\gamma_b$ leads to

$$\frac{c_m'}{c} = R^{0.5}\cdot\sqrt{1 - \gamma_b^2/12} - \gamma_b/2 \quad \ldots\ldots [14]$$

Thus for $R = 5$ and $\gamma_b = 0.25$, $c_m'/c = 2.11$. If $\gamma_b = 0$, $c_m'/c = \sqrt{R} = 2.24$. The total span of exhaust velocities $c_m'/c_0 = 3.7$; whereas if $\gamma_b = 0$ $c_m'/c_0 = R = 5$. This indicates that c_0 is substantially lower in field-free space than on the earth's surface.

Comments on Tapered Exhaust Rocket

The initial exhaust velocity c_0 must be determined by equating total energy in the propellant in the uniform and tapered programs. If it is desired that the tapered exhaust be absolutely motionless with respect to an earth observer, it is necessary to start off the rocket with a boost velocity equal to c_0. This will modify Equation [4] and all subsequent equations involving [4].

The preceding calculations are of interest primarily in situations where energy is limited in quantity and there is no penalty associated with high rate of release of energy (i.e., power or temperature not limiting). This is, in fact, the re-

verse of conditions governing present chemical rockets. However, there are propulsion techniques, such as accelerated particle beams, in which the controlling factors may differ from those of present conventional engines.

Optimum Mass Ratio With Fixed Energy Per Unit Payload

Let us assume that a fixed amount of energy E/m_0 per unit payload m_0 can be distributed over a propellant mass m_p and that a constant mass flow rate m and exhaust velocity c will be used. What mass ratio $R = (m_p + m_0)/m_0$ will provide maximum terminal velocity for m_0?

If the energy E is distributed uniformly over the working fluid mass m_p, then the ideal exhaust velocity c is given by

$$E = (0.5)m_p c^2 \quad [15]$$

Inserting this c into the conventional velocity Equation [6] gives

$$v_b = \left(\frac{2E}{m_p}\right)^{0.5} \ln\left(\frac{m_p + m_0}{m_0}\right) - gt_b \quad [16]$$

We may express this v_b in terms of the fundamental quantities mass ratio R and initial acceleration ratio $\alpha = a_0/g$ by means of the following relations:

$$R = \frac{m_p + m_0}{m_0} \quad [17]$$

Table 2 Take-off acceleration vs. optimum mass ratio

$\alpha = \frac{a_0}{g}$	$R_m = \left(\frac{m_p + m_0}{m_0}\right)_{opt}$
0.0*	12.5
0.5	9.7
1.0	8.0
2.0	7.0
4.0	6.0
9.0	5.4
∞	5.0**

* $\alpha = 0$ means no initial acceleration (rocket momentarily balanced against g).
** Field-free case.

$$\left(\frac{1}{m_p}\right)^{0.5} = \left(\frac{1}{m_0}\right)^{0.5}\left(\frac{m_0}{m_p}\right)^{0.5} = \left(\frac{1}{m_0}\right)^{0.5}\left(\frac{1}{R-1}\right)^{0.5} \quad [18]$$

$$gt_b = g\frac{m_p}{\dot{m}} = g\left(\frac{R-1}{R}\right)\frac{m_0 + m_p}{\dot{m}}$$

$$gt_b = g\left(\frac{R-1}{R}\right)\frac{(m_p + m_0)}{F}c$$

$$gt_b = \left(\frac{R-1}{R}\right)\frac{gc}{a_0 + g}$$

$$gt_b = \left(\frac{R-1}{R}\right)\frac{c}{1+\alpha} \quad [19]$$

where F = constant thrust, and a_0 is the initial acceleration in a direction opposite to the gravitational field, with $\alpha = a_0/g$. Substituting [19] and [18] into [16]

$$v_b = \left(\frac{2E}{m_0}\right)^{0.5}\left(\frac{1}{R-1}\right)^{0.5}\left[\ln R - \frac{R-1}{R(1+\alpha)}\right] \quad [20]$$

We shall now examine Equation [20] to see if v_b has a maximum with respect to R. The available energy per unit payload E/m_0 is presumed to be specified.

Calculation of Maximum v_b With Respect to R

Taking the derivative of [20] with respect to R, and setting it equal to zero results in

$$\ln R_m = \frac{R_m - 1}{R_m}\left[2 + \frac{1}{1+\alpha}\left(1 - \frac{2}{R_m}\right)\right] \quad [21]$$

where R_m is the mass ratio for maximum v_b. We note that in field-free space, $\alpha = a_0/g$ approaches infinity, and that for takeoff from earth with 1 g upward acceleration $\alpha = 1.0$. Solving the transcendental Equations [21] numerically yields the results shown in Table 2 for the relation between α and R_m.

Conclusion

We see from Table 2 that in field-free space a rocket with mass ratio 5 will give greatest terminal velocity to m_0 per unit of energy available. To cite an extreme example, (Reference 1), if $m_0 = 1$ ton, and E is the energy available from the fission of 3.75 lb of uranium, then the v_b available by distributing this E into the fission fragments only, could be multiplied more than fortyfold by distributing this same E instead into 4 tons of inert working fluid.

Reference

1 Seifert, H. S., and Mills, M. M., *Physical Review*, vol. 71, 1947, p. 279; Cit., *Jet Propulsion Lab Memo* 3–4, Jan. 23, 1947.

A Flow Reactor for High Temperature Reaction Kinetics[1]

L. CROCCO,[2] I. GLASSMAN[3] and I. E. SMITH[4]

Department of Aeronautical Engineering, Princeton University, Princeton, N. J.

THE purpose of this note is to describe a new type of flow reactor designed for the study of the reaction kinetics of propellants at high temperatures. In principle the apparatus consists of a tubular duct in which a high temperature stream of inert gas flows. A secondary cold stream of monopropellant or fuel-oxidizer mixture is introduced into and mixed rapidly with the inert gas, thus conditions within a rocket motor combustion chamber are simulated without the complication of recirculation. Downstream of the injection point reaction commences and continues until all the reactants have been consumed. By varying the velocity of the inert carrier gas the reaction zone may be extended over any desired length.

By introducing only a small quantity of the reactants compared with the mass flow of carrier the decrease in temperature resulting from the mixing of the two streams is small, and likewise the increase in temperature due to the exothermic reaction will also be relatively small. Endothermic decomposition reactions which give a subsequent decrease in temperature may be studied by this scheme, as well.

Because the zone in which the reaction takes place is large and the temperature gradient small, such factors as the heat transfer to the unreacted gas and the back diffusion of active species, which are dominant effects in self-propagating flames, are rendered negligible. In this way an unambiguous determination of the reaction kinetics in the presence of inerts is possible.

This scheme has been used to determine the rate of decomposition of ethylene oxide with either nitrogen or helium as

[1] This research was supported by the U. S. Air Force through the Air Force Office of Scientific Research of the Air Research and Development Command under Contract AF 18(600) 1527. Reproduction in whole or part is permitted for any purpose of the U. S. Government.

[2] Robert Goddard Professor of Jet Propulsion. Mem. ARS.

[3] Assistant Professor. Mem. ARS.

[4] AGARD Exchange Fellow and Research Associate.

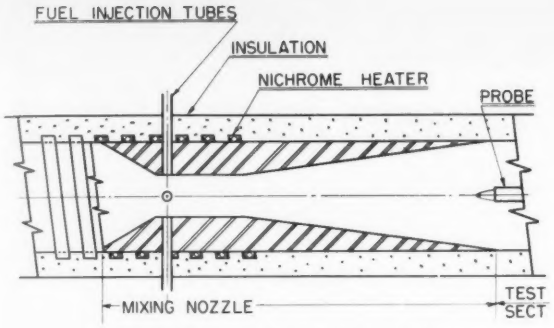

Fig. 1 Cross section of mixing nozzle

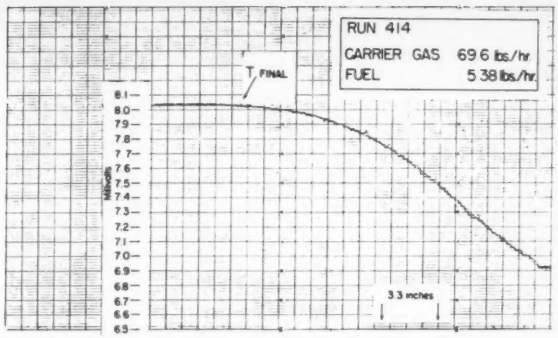

Fig. 2 Typical temperature-distance record for ethylene oxide decomposition reaction-range 1020 K to 1100 K

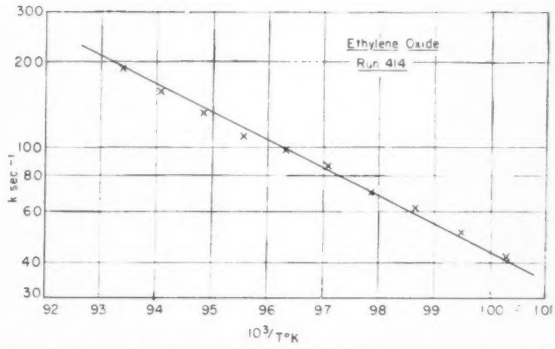

Fig. 3 Plot of ethylene oxide decomposition reaction rate data

the carrier gas. Comparable results have been obtained demonstrating the independence of the reaction on the physical nature of the inert gas.

The duct employed is a stainless steel tube 2 in. in diam and approximately 6 ft long. In order to maintain a constant temperature along its length the duct is heated electrically, and the wall temperature may be determined from the power input. The inert gas is heated to the same temperature by passage through a packed ceramic bed which has previously been heated by a fuel oil burner. A fine control over this temperature is obtained by metering a certain amount of cold carrier gas into the heated stream.

The test fuel injection section of the duct is shown in Fig. 1, and consists of a sharply convergent section followed by a parallel throat $\frac{3}{4}$ in. in diam and about $1\frac{1}{2}$ in. long. Four small bore injection tubes branching from a common manifold carry the fuel and are arranged so that the streams issuing from them impinge on one another, thus a region of high turbulence is created. The gas mixture is then brought back to the duct section by means of the 15 deg diffuser.

The course of the reaction is followed by means of an axially-traversing probe carrying at its tip a platinum-platinum/rhodium thermocouple which is 0.001 in. in diam. The output from this thermocouple is balanced by a potentiometer for zero injection of fuel and during an experiment the out of balance EMF due to the change in temperature as the fuel reacts is recorded on a sensitive recording potentiometer. A single longitudinal transverse of the probe provides a record of the temperature change through the reaction zone, from which the reaction rate at any specific temperature covered may be determined. The determination of the reaction rate over a wider temperature range is made by carrying out a series of such determinations at different initial temperatures.

Evidence for the complete mixing of the injected and carrier streams within the nozzle has been obtained by injecting cold nitrogen into the hot carrier stream. By employing a special probe to enter the throat temperature records of the mixing of the streams have been made and these demonstrate that a practically homogeneous mixture is obtained in between 0.5 and 3 millisecs according to the flow rate of carrier gas.

A temperature record which covers a range from 1020 K to 1100 K obtained for a typical experiment is given in Fig. 2. The mean velocity of the gas stream was 1520 cm/sec corresponding to a time scale of 66 millisecs per meter of duct.

The rate constant for the ethylene oxide reaction has been calculated assuming first order kinetics (1)[5] from the following relationships

$$-\frac{dc}{dt} = kc$$

$$cQ = C_p(T_f - T)$$

$$\frac{1}{(T_f - T)}\frac{dT}{dt} = k = Ae^{-E/RT}$$

where c is the concentration at any point, T the corresponding temperature, T_f the final temperature, Q the heat of reaction for the fuel-inert gas mixture, $\bar{C}_p$ a mean specific heat, t the time, k the reaction rate constant, R the gas constant, A the collision frequency, and E the activation energy.

A plot of log k against $1/T$ is shown in Fig. 3 for a typical experiment. The points are best represented by a straight line indicating the correct assumption of an over-all-first-order reaction mechanism, and the slope corresponds to an activation energy of 42–44 kcal/mole. This value is significantly lower than that obtained by Mueller and Walters (1), who found 52.7 kcal/mole over a temperature range of 623–713 K, though Lossing, Ingold, and Tickner (2) also found 42 kcal/mole at 1123 K.

The complete results of this investigation, including information on rates of other gaseous systems and on the induction or ignition lags of both gaseous and liquid fuels as a function of temperature, will be published at a later data.

References

1 Mueller, K. H., and Walters, W. D., "The Thermal Decomposition of Ethylene Oxide," *Journal of the American Chemical Society*, vol. 73, 1951, p. 1458.

2 Lossing, F. P., Ingold, K. U., and Tickner, A. W., "Free Radicals by Mass Spectrography," *Discussions of the Faraday Society*, vol. 14, 1953, p. 34.

[5] Numbers in parentheses indicate References at end of note.

Index of Papers Published in JET PROPULSION

A Publication of the American Rocket Society

Volume 27—January through December 1957

Issue	Pages
January	1–104
February	105–240
March	241–364
April	365–488
May	489–620
June	621–750
July	751–846
August	847–966
September	967–1062
October	1063–1134
November	1135–1218
December	1219–1290

ALLEN, H. JULIAN
Hypersonic Flight Problems (Introductory Remarks) 1145
ANKENEY, D. P., *see* EGBERT, B. R.
ARTHUR, P. D. and MCJONES, R. W.
Effective Lift Drag Ratio With Jet Lift.. 676
BARR, G. M. and MORRISON, S. C.
Measurements of Vibration Environment in a Supersonic Liquid Propellant Rocket Sled 1017
BARR, K., and STEEGER, E. J.
Supersonic Rain Erosion Testing of Missile Radomes 1034
BARTAS, J. G.
Wall Temperatures in Ribbed Combustion Chambers 784
BARTZ, D. R.
A Simple Equation for Rapid Estimation of Rocket Nozzle Convective Heat Transfer Coefficients 49
BATCHELDER, G. W. and ELDER, J. K.
A More Explicit Notation for the Temperature Sensitivity Coefficients of Solid Rocket Propellants 546
BATDORF, SAMUEL B.
Structural Problems in Hypersonic Flight 1157
BERMAN, K. and CARNAVOS, T. C.
Experiments With Cavitating Venturis.. 148
BERNING, WARREN W., *see* JONES, LESLIE M.
BERTOTTI, B., *see* CASCI, C.
BEUTLER, F. J. and RAUCH, L. L.
Precision Measurement of Supersonic Rocket Sled Velocity—Part I 1021
BIEDLER, III, WILLIAM T. and HOELSCHER H. E.
Studies in a New Type of Flat Flame Burner 1257
BLACK, H. D., *see* STRUBLE, R. A.
BLITZER, L.
Effect of Earth's Oblateness on Satellite Period 405
BLOOM, JR., RALPH
On the Hazards of Concentrated Hydrogen Peroxide 666
BONNETT, M. E.
Aberdeen Proving Ground Ballistic Track 992
BREWINGTON, W. H., *see* TIGER, B.
BRIGGS, J. Z., *see* FREEMAN, R. R.
CAMACK, W. G. and FORSTER, H. K.
Test of a Heat Transfer Correlation for Boiling Liquid Metals 1104
CAMBEL, ALI BULENT, *see* HUELLMANTEL, L. W.
CANTRELL, T. D., *see* TSCHINKEL, J. G.
CARNAVOS, T. C., *see* BERMAN, K.
CARROLL, JOHN J., *see* GORE, MARVIN R.
CARROLL, K. L. and NORTHROP, C. L.
Redstone Arsenal Ballistic Ramp 1011
CASCI, C. and BERTOTTI, B.
On the Slowing Down of Time 665
CHARWAT, A. F.
The Stability of Bodies of Revolution at Very High Mach Numbers 866
CHUBB, T. A., FRIEDMAN, H., KUPPERIAN, JR., J. E. and LINDSAY, J. C.
Flare Measurements From Rockets 1094
COLE, DANDRIDGE M.
The Earth-Mars Constant Thrust Brachistochrone 176
Times Required for Continuous Thrust Earth-Moon Trips 416
COPLEN, JR., H. L.
Reliability Concepts in Rocket Controls Design 637
CROCCO, L., GLASSMAN, I. and SMITH, I. E.
A Flow Reactor for High Temperature Reaction Kinetics 1266
DASKIN, WALTER, *see* FERRI, ANTONIO
DAVIES, H. and SMITH, D. S.
Design Considerations of Two Large Liquid Rocket Sled Pusher Vehicles... 999
DEMPSTER, J. R. H. and SODHA, M. S.
On Secondary Atomization of Droplets.. 896
DEMUTH, O. J., *see* HOUSE, W. C.
DETRA, R. W., KEMP, N. H. and RIDDELL, F. R.
Addendum to "Heat Transfer to Satellite Vehicles Re-entering the Atmosphere" 1256
DILLAWAY, ROBERT B.
A Philosophy for Improved Rocket Nozzle Design 1088
DODGE, C. H., *see* HOUSE, W. C.
DORLING, E. B.
British High Altitude Rocket Research Program 289
DUWEZ, P., *see* HIESTER, N. K.
EBER, G. R.
The Capabilities of the Holloman Track 1013
EDELBAUM, THEODORE N.
Comments on the Powered Trajectory of a Satellite 1260
EGBERT, B. R. and ANKENEY, D. P.
Supersonic Track Facilities at the Naval Ordnance Test Station 985
EGGERS, JR., A. J.
Performance of Long Range Hypervelocity Vehicles 1147
ELDER, J. K., *see* BATCHELDER, G. W.
FAY, J. A., RIDDELL, F. R. and KEMP, N. H.
Stagnation Point Heat Transfer in Dissociated Air Flow 672
FELDMAN, LEWIS, *see* FERRI, ANTONIO
FELDMAN, SAUL
Hypersonic Conical Shocks for Dissociated Air in Thermodynamic Equilibrium 1253
FERRI, ANTONIO, FELDMAN, LEWIS and DASKIN, WALTER
The Use of Lift for Re-entry from Satellite Trajectories 1184
FORSTER, H. K., *see* CAMACK, W. G.
FREELAND, J. L., *see* STEHLING, K. R.
FREEMAN, R. R. and BRIGGS, J. Z.
Molybdenum for High Temperature Strength 138
FRIED, B. D.
Powered Flight Trajectory of a Satellite 641
FRIEDMAN, H., *see* CHUBB, T. A.
FUHS, A. E., *see* WILLIAMS, F.
FULLER, J. L., *see* HOUSE, W. C.
GLASSMAN, IRVIN
Impulse Expressions for Rocket Systems Containing a Solid Phase 542
See WILLIS, D. ROGER
See also CROCCO, L.
GLAWE, GEORGE E.
A High Temperature Combination Sonic Aspirated Thermocouple and Total Pressure Probe 543
GLUCKSTEIN, MARTIN E.
Note on "Study of Premixed Flames Using Radioactive Tracers" 1102
GOLDSMITH, M.
On the Optimization of Two-Stage Rockets 415
GORDON, JOHN S.
Estimation of Optimum Mixture Ratio for Fuming Nitric Acid Propellants... 799
GORDON, L. J., *see* GREENE, S. A.
GORE, MARVIN R. and CARROLL, JOHN J.
Dynamics of a Variable Thrust, Pump Fed, Bipropellant, Liquid Rocket Engine System 35
GRAHAM, A. R., *see* ZUCROW, M. J.
GRAVES, A. E., *see* TSCHINKEL, J. G.
GREENE, S. A. and GORDON, L. J.
An Effect of Carbon in an Adiabatically Expanded Gas Stream 667
Ethylene Oxide as a Monopropellant 798
Some Decomposition Products of Normal Propyl Nitrate 1261
GROVER, JOHN H., KESLER, M. G. and SCURLOCK, A. C.
Rotating Flame Stabilizer 386
GROVER, JOHN H. and HOLTER, WILLIAM H.
Solution of the Transient Heat-Conduction Equation for an Insulated, Infinite Metal Slab 1249
GUSTAVSON, JOHN
The Possibility of Interstellar Flight 69
HAEUSSERMANN, W.
Stability Areas of Missile Control Systems 787
HALEY, ANDREW G.
Seventh IAF Congress Stresses Cooperation 60
HANAWALT, ARNOLD J., *see* SCHMIDT, CRAIG M.
HANSEN, C. FREDERICK
Some Characteristics of the Upper Atmosphere Pertaining to Hypervelocity Flight 1151
HANSEN, WILLIAM H., *see* JONES, LESLIE M.
HARSHMAN, R. C.
Properties of the Alkyl Hydrazines 398
HARVEY, T. J.
Bending Dynamics of a Spinning Missile 669
HEGENWALD, JR., J. F. and MURPHY, JR., E. A.
Sled Testing the Emergency Escape System: The Human Factor 1025
HENDRICKS, R. K.
Track Testing at the Air Force Armament Center 997
HENRY, IRVIN G.
Lifetimes of Artificial Satellites of the Earth 21
HERTZBERG, A., *see* RUSSO, A.
HIESTER, N. K., TIETZ, T. E., LOH, E., and DUWEZ, P.
Solar Furnace Performance 507
HOELSCHER, H. E., *see* BIEDLER, III, WILLIAM T.
HOLTER, WILLIAM H., *see* GROVER, JOHN H.
HOTTEL, HOYT C., TOONG, TAU-YI and MARTIN, JOHN J.
Flame Stabilization in a Boundary Layer 28
HOUSE, W. C., DODGE, C. H., WALDO, R. D., SCHAFF, JR., A., FULLER, J. L. and DEMUTH, O. J.
Future Sounding Rockets 269
HUELLMANTEL, L. W., ZIEMER, R. W. and CAMBEL, ALI BULENT
Stabilization of Premixed Propane-Air Flames in Recessed Ducts 31
HURD, CHARLES O., *see* SIMKIN, DONALD J.
ITOKAWA, HIDEO
The Japanese Sounding Rockets 286
JOB, F. R.
Use of the Rocket Jet in Mining and Quarrying 392
JOHN, R. R. and SUMMERFIELD, MARTIN
Effect of Turbulence on Flame Radiation 169
See also WILSON, E. S.
JONES, LESLIE M., HANSEN, WILLIAM H., SPENCER, NELSON W., STROUD, WILLIAM G. and BERNING, WARREN W.
The Nike-Cajun Sounding Rocket 266
KAEPPELER, H. J.
On Thermonuclear Power Plants 1098
KATTUS, J. R.
High Temperature Structural Materials for Missiles 644
KEEFE, J. H. and RALEIGH, C. W.
Transportation of Hydrogen Peroxide... 663
KEMP, N. H.
See also DETRA, R. W.
See also FAY, J. A.
KEMP, N. H. and RIDDELL, F. R.
Re-entry Heat Transfer to Satellite Vehicles 132
KESLER, M. G., *see* GROVER, J. H.
KNUTH, ELDON L.
Thermal Conductivity and Prandtl Numbers for Nonpolar Polyatomic Gases at High Temperatures 1262
KUPPERIAN, JR., J. E., *see* CHUBB, T. A.
KRUCICANIN, SLOBODAN P.
Comment on "Thermonuclear Power Plants" 1102
LAITONE, E. V.
Spin-Stabilized Unsymmetrical Bodies.. 417
LARISCH, E., *see* SHECHTMAN, I.
LAROCCA, E. W.
Time-Temperature Relationships for Rupture of Metals in Combustion Atmospheres 674
LAWDEN, D. F.
Optimal Rocket Trajectories 1263
LAWRENCE, A. L., *see* SINGER, S. F.

(*Continued on page 1270*)

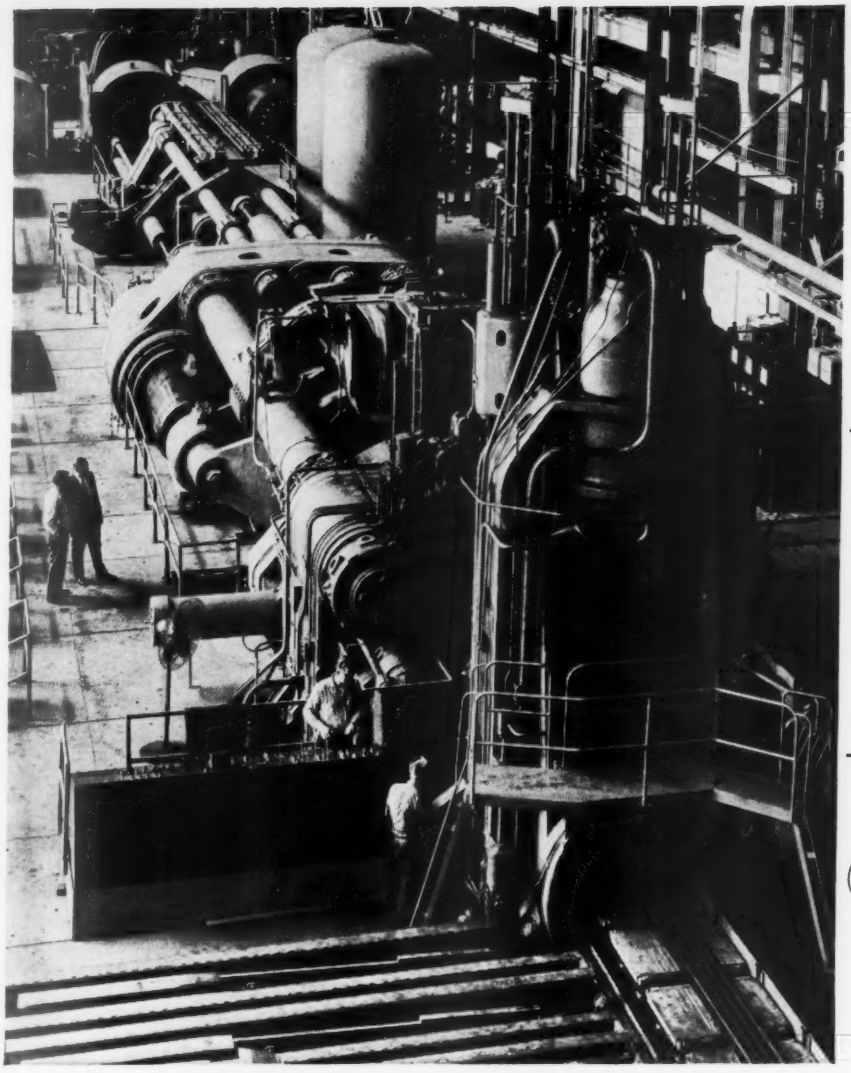

HOW THE 13,200-TON PRESS BOOSTS EXTRUSION CAPACITY

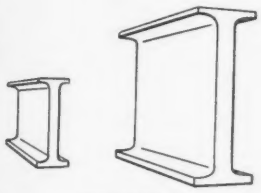

FROM 11" TO 28"

STRUCTURAL SHAPES

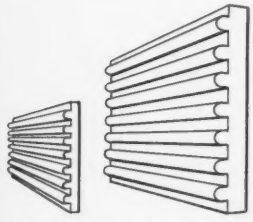

FROM 9" TO 20"

STIFFENED SECTIONS

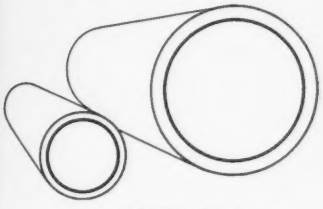

FROM 10" TO 24" O. D.

TUBING

DOW'S NEW EXTRUSION PRESS PACKS 13,200-TON PUNCH

Here's a whole new range of large magnesium extrusions:
24-inch O. D. Tubing 28-inch I-Beams 80-foot-long sections

This mammoth press, newest addition to The Dow Chemical Company's rolling and extrusion mill at Madison, Illinois, is the world's largest magnesium extrusion facility. Its vastly increased capacities afford new opportunities for designers working with light metals. A wide variety of new magnesium applications for aircraft, missile, military and general industrial use are now possible and practical. In addition to extruding magnesium, the press is also available for large aluminum extrusions.

Here's how the big press will increase maximum dimensions of representative magnesium extrusions: Integrally stiffened sections, from 9 to 20 inches wide; I-Beams from 11 to 28 inches high; round tubing from 10 to 24 inches outside diameter; and maximum lengths of 80 feet. A large number of shapes and forms can be produced, limited only by the design of the die through which the metal is extruded. Many complex shapes that formerly required separate operations can now be formed in one operation.

If your design calls for large magnesium or aluminum extrusions, contact the nearest Dow Sales Office or write to THE DOW CHEMICAL COMPANY, Midland, Michigan, Department MA 1406F-1.

YOU CAN DEPEND ON DOW

The might of VOODOO was proved with Statham Transducers

IN THE F-101

Statham transducers gathered pressure and acceleration data in McDonnell Aircraft Corporation's program to prove out the aerodynamic design and structural design.

WHEN THE NEED IS TO KNOW...FOR SURE SPECIFY STATHAM

Accelerometers • Load Cells
Pressure Transducers

Catalog, complete with prices, available upon request.

Statham

LOS ANGELES 64, CALIFORNIA

Annual Index

(*Continued from page 1268*)

LEDUC, RENÉ
Early Work and Latest Realizations With Ramjet Engines 64

LEES, LESTER
Recent Developments in Hypersonic Flow 1162

LEHMAN, J. H., *see* WOLF, H.

LINDSAY, J. C., *see* CHUBB, T. A.

LOH, E., *see* HIESTER, N. K.

LOOS, H. G.
Time Dilatation in Space Flight 665

MAGER, ARTUR
Leading Edge Cooling 293

Marshak, R. E.
Scientific Research in the Soviet Union .. 200

MARTIN, JOHN J., *see* HOTTEL, HOYT C.

MASTERSON, J. E., *see* ROSS, M. D.

McJONES, R. W., *see* ARTHUR, P. D.

MICHELSON, IRVING
Ultimate Design of High Altitude Sounding Rockets 1107

MIELE, ANGELO
Optimum Burning Program as Related to Aerodynamic Heating for a Missile Traversing the Earth's Atmosphere ... 1231

MIESSE, C. C.
The Free Vibration of a Variable Mass .. 1103

MOHRLOCK, JR., H. F.
The Development of RESCU Mark I ... 1028

MORRISON, R. B., *see* NICHOLLS, J. A.

MORRISON, S. C., *see* BARR, G. M.

MURPHY, JR., E. A., *see* HEGENWALD, JR., J. F.

NEWELL, JR., H. E.
The High Altitude Sounding Rocket 261

NICHOLLS, J. A., WILKINSON, H. R. and MORRISON, R. B.
Thrust by Repeated Detonation 534

NORTHROP, C. L., *see* CARROLL, K. L.

OMAN, R. A., *see* WADLEIGH, K. R.

ORDAHL, D. D. and WILLIAMS, M. L.
Photoelastic Stress Data for Rocket Grains 657

PENNER, S. S.
Rational Scaling Procedures for Liquid-Fuel Rocket Engines 156

PENNER, S. S. and WILLIAMS, F.
On Excess Enthalpy, Flame Extinction and Minimum Ignition Energies 544

PETERSON, J. B.
Note on "Take-Off" From Satellite Orbit" 1263

POLAND, H. M., *see* ROTH, JR., C. E.

POWELL, W. B.
Heat Transfer to Fluids Near Critical Temperature 776

PRIEM, RICHARD J.
Breakup of Water Drops and Sprays With a Shock Wave 1084

PROVART, R.
Recovery of Rocket Powered Vehicles and/or Their Components 125

PUNTE, CHARLES L.
Note on "Hazards Associated With 90 Per Cent Hydrogen Peroxide Aerosols" 51

PUTNAM, ABBOTT A.
Comparison of Reverse Jet and Obstacle Type Flameholders 177

RALEIGH, C. W., *see* KEEFE, J. H.

RAPP, L. R. and STRIER, M. P.
Chemical Aspects of Hypergolic Ignition 401

RAUCH, L. L., *see* BEUTLER, F. J.

REESE, B. A., *see* WARNER, C. F.

RIDDLE, F. R., *see* KEMP, N. H.
See also DETRA, R. W.
See also FAY, J. A.

ROBERSON, R. E.
Impact Points of Ballistic Rockets 1256

Romig, Mary F.
Addendum to "Stagnation Point Heat Transfer for Hypersonic Flow" 1255

ROSS, M. D. and MASTERSON, J. E.
Rockair 276

ROTH, JR., C. E. and POLAND, H. M.
Liquid Rockets for Supersonic Sleds 1006

RUSSO, A., and HERTZBERG, A.
A Method for Improving the Performance of Shock Tubes 1191

SANDERS, JOHN C.
Comments on "Dynamics of a Liquid Rocket System" 421

SCALA, S. M. and SUTTON, G. W.
Vectored Injection Into a Hypersonic Laminar Boundary Layer 895

SCHAFF, JR., A., *see* HOUSE, W. C.

SCHMIDT, CRAIG M. and HANAWALT, ARNOLD J.
Skin Temperatures of a Satellite 1079

SCHNEIDER, P. J.
Temperatures and Thermal Stresses in Transpiration-Cooled Power-Producing Plates and Tubes 882

SCHURMANN, E. E. H.
Optimum Staging Technique for Multi-staged Rocket Vehicles 863

SCURLOCK, A. C., *see* GROVER, J. H.

SEGER, R. R.
Track Testing at the Air Force Flight Test Center 995

SEIFERT, HOWARD S.
The Performance of a Rocket With Tapered Exhaust Velocity 1264

SHECHTMAN, I., and LARISCH, E.
Comments on "Thermonuclear Power Plants" 176
Further Comments on "Thermonuclear Power Plants" 1102

SIMKIN, DONALD J. and HURD, CHARLES O.
Vapor Pressure and Heat Contents of Saturated Liquid and Vapor Hydrogen Peroxide 419

SIMMONS, ROBERT F. and WOLFHARD, HANS G.
The Structure of Chlorine Flames 44

SINGER, S. F. and LAWRENCE, A. L.
Terrapin 281

SINGER, S. F. and WENTWORTH, R. C.
Ballistic Rockets' Impact Points 407

SLAVIN, R. M.
The Air Force Rockaire Program 279
See also TOWNSEND, JR., J. W.

SMITH, D. S., *see* DAVIES, H.

SMITH, I. E., *see* CROCCO, L.

SODHA, M. S., *see* DEMPSTER, J. R. H.

SPENCER, NELSON W., *see* JONES, LESLIE M.

STALDER, JACKSON R.
A Survey of Heat Transfer Problems Encountered by Hypersonic Aircraft 1178

STEEGER, E. J., *see* BARR, K.

STEHLING, K. R. and FREELAND, J. L.
A Mechanical Igniter for Liquid Rocket Engines 896

STRIER, M. P., *see* RAPP, L. R.

STROUD, WILLIAM G., *see* JONES, LESLIE M.

STRUBLE, R. A. and BLACK, H. D.
A Generalized Closed Form for Burnt Velocity 151

STUHLINGER, E.
Flight Path of an Ion-Propelled Space Ship 410

SUMMERFIELD, MARTIN, *see* JOHN, R. R.
See also WILSON, E. S.

THOMAS, JR., A. N.
Some Fundamental Aspects of Ramjet Propulsion 381

TIETZ, T. E., *see* HIESTER, N. K.

TIGER, B., and BREWINGTON, W. H.
Demonstrating System Reliability by the Sequential Probability Ratio Test 890

TOONG, TAU-YI, *see* HOTTEL, HOYT C.

TOWNSEND, JR., J. W. and SLAVIN, R. M.
Aerobee-Hi Development Program 263

TSCHINKEL, J. G. and CANTRELL, T. D.
Hydrogen Peroxide Field Analyzer 290

TSCHINKEL, J. G. and GRAVES, A. E.
Peroxide Warm-up Equipment 796

UNTERBERG, W.
Heating Problems in Ramjet Tailpipes .. 514

USELLER, JAMES W.
Effect of Turbojet Compressor Coolants on Afterburner Combustion 25

VANDREY, J. F.
Aerodynamic Heating at Great Altitudes 522

VASSEY, E.
The French Missile Veronique 285

WADLEIGH, K. R. and OMAN, R. A.
Instrumentation for Two-Phase, Two-Component Flows 769

WALDO, R. D. *see* HOUSE, W. C.

WARNER, C. F., *and* REESE, B. A.
Investigation of the Factors Affecting the Attachment of a Liquid Film to a Solid Surface 877

WAY, S.
Similitude Considerations in Turbojet Engines 162

WENTWORTH, R. C., *see* SINGER, S. F.

WEST, C. D.
Boost Phase Trajectory Analysis Techniques 527

WILDE, KENNETH A.
An Approximate Specific Impulse Equation for Condensable Gas Mixtures ... 668

WILKINSON, H. R., *see* NICHOLLS, J. A.

WILLIAMS, F. and FUHS, A. E.
Apparent Emission Intensities From a Turbulent Flame Composed of Wrinkled Laminar Flames 1099
See also PENNER, S. S.

WILLIAMS, M. L., *see* ORDAHL, D. D.

WILLIS, D. ROGER and GLASSMAN, IRVIN
The Mixing of Unbounded Coaxial Compressible Streams 1241

WILSON, E. S., JOHN, R. R. and SUMMERFIELD, M.
Spectroscopic Studies of the Effect of Boundary Layer Flow on Flameholding 892

WOLF, H. and LEHMAN, J. H.
The Determination of Thermal Entrance Lengths for Gases in Turbulent Flow in Smooth Round Ducts 897

WOLFHARD, HANS G., *see* SIMMONS, ROBERT F.

ZAEHRINGER, A. J.
Solid Propellant Bibliography 900

ZIEMER, R. W., *see* HUELLMANTEL, L. W.

ZIMNEY, C. M.
The ASP Sounding Rocket 274

ZUCROW, M. J. and GRAHAM, A. R.
Film Cooling for Rocket Motors 650

ZWICK, S. A.
Thermal Stresses in an Infinite, Hollow Case-Bonded Cylinder 872

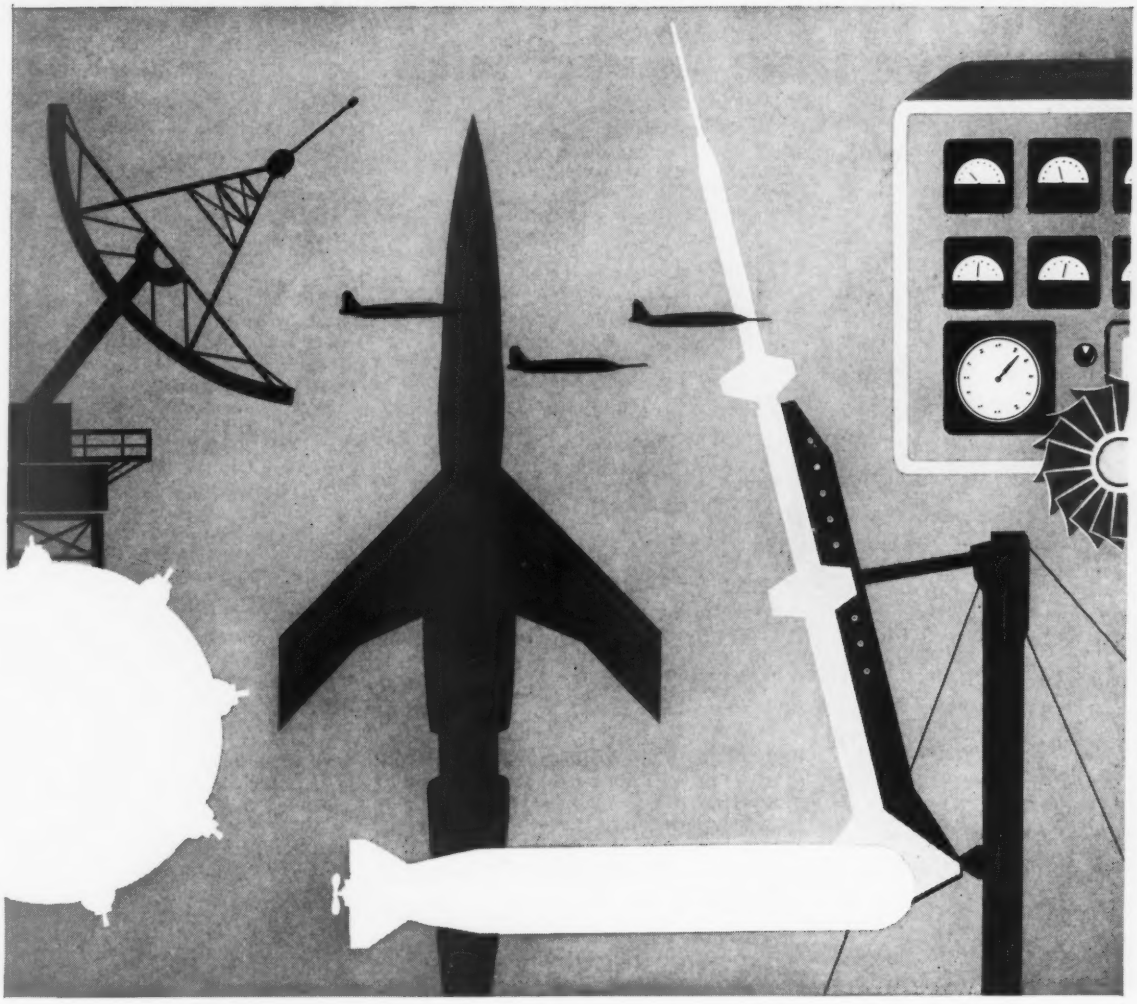

Throughout the Pattern of Modern Defense...

AMF has experience you can use

• Most defense problems fit into AMF's "big picture"... a picture drawn from AMF's tremendous backlog of experience in defense work. Wherever you are, there's probably an AMF defense component or integrated system... a product of AMF experience... operating near you. • Guided missiles ride on AMF equipment to AMF launching sites ... to be loaded, fueled and fired by AMF-built equipment. Under the sea, AMF-built weapons wait for unfriendly submarines on the prowl. Along our borders, AMF radarscopes search the sky for "stranger" aircraft. • There is little room for failure where the job is the nation's defense. And the nation looks to companies like AMF to design, test and produce a variety of defense products. With a wide range of experience in the most sensitive fields of defense work, AMF may well be the answer to your problems... in defense or industry.

- *Armament*
- *Ballistics*
- *Radar Antennas*
- *Guided Missile Support Equipment*
- *Auxiliary Power Supplies*
- *Control Systems*

AMF DEFENSE PRODUCTS

Defense Products Group
AMERICAN MACHINE & FOUNDRY COMPANY
1101 North Royal Street, Alexandria, Va.

Asbury Park • Atlanta • Boston • Brooklyn • Dallas • Dayton • Los Angeles • Seattle • Tucson • Washington, D. C.

computer time saved with

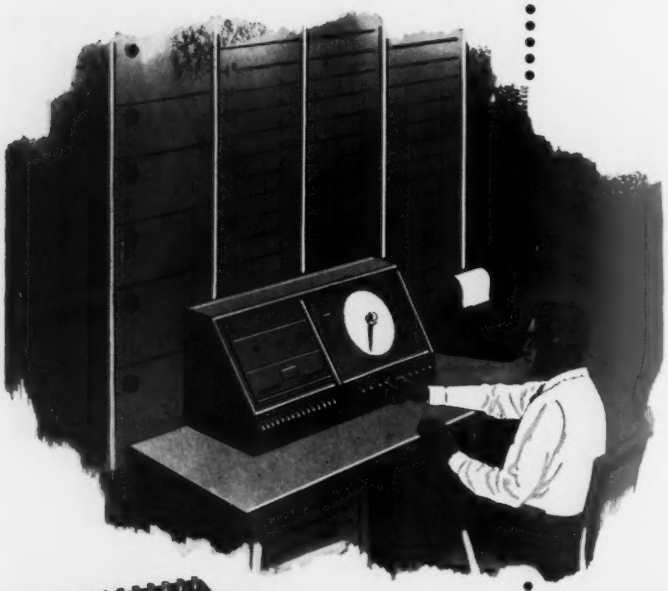

ELECTROGRAPH
MODEL 420

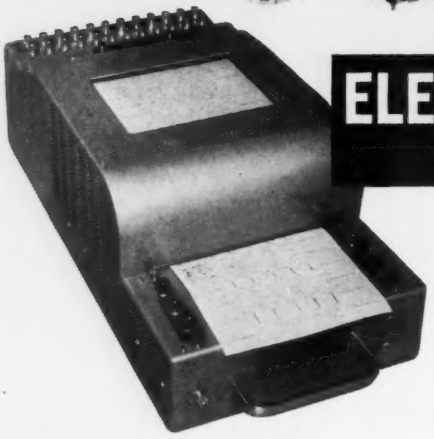

Visual editing of tape-recorded intelligence through use of Electrograph records saves many hours of valuable computer time.

24-channel Electrophotographic
Recording Oscillograph

Now you can edit telemetered tape-recorded information and select the data to be fed into the data reduction computer. As many as 24 channels of tape signals connected to the Electrograph galvanometers through appropriate discriminators may be recorded simultaneously. The analog record is instantly readable as it is discharged from the recorder. Proper keying of the permanent record to the tape permits visual selection of the data to be placed into the computer.

Records produced by the Electrograph are permanent, requiring no further processing, and may be stored indefinitely without loss of trace definition.

For further information regarding the Electrograph, you are invited to write, wire or call for bulletin CGC-311.

Century Electronics & Instruments, Inc.

1333 No. Utica, Tulsa, Oklahoma

Book Reviews

Ali Bulent Cambel,
Northwestern University,
Associate Editor

Elements of Gasdynamics, by H. W. Liepmann and A. Roshko, John Wiley and Sons, Inc., New York, 1957, xv + 439, $11.00

Reviewed by Ellsworth A. Brown Jr.
Northwestern University

The authors have presented a timely book on gasdynamics which will be welcome to both the student and the teacher. It presents an up-to-date coverage of gasdynamics fundamentals in one readily readable volume.

As indicated by the authors, this book was originally planned as a revision of the well-known "Introduction to Aerodynamics of a Compressible Fluid" by Liepmann and Puckett. However, one has only to look into the first chapter of the new volume on "Concepts from Thermodynamics" to realize that it is more than a revision. The vast field of gasdynamics and the great strides in aerodynamics have required considerable increase in scope. Whereas, in the earlier volume the discussion was generally limited to results based upon a perfect gas, the present volume includes such additional factors as real gas effects, condensation, dissociation and multicomponent systems. Many of the problems of present day gasdynamics require this more general approach.

Although most of the topics from the earlier volume are included in the present work, each topic has been rewritten to include not only the advances of the past 10 years, but also expanded to give a more complete treatment of the wider field of gasdynamics. For example, only optical methods of measurement were discussed in "Introduction to Aerodynamics of a Compressible Fluid" This has been expanded to give a survey of temperature, pressure, velocity and Mach number measuring techniques, as well as a discussion of special instruments such as the hot wire and X-ray absorption.

Several new topics have been included. Chapter 10 "Similarity Rules of High-Speed Flow," Chapter 11 "Transonic Flow," Chapter 13 "Effects of Viscosity and Conductivity" and Chapter 14 "Concepts from Gaskinetics" represent material not included or discussed very briefly in the earlier volume.

The job of covering such a large field as the fundamentals of gasdynamics in one manageable volume obviously requires some selectivity in the subject matter. One may regret the brief treatment of some topics such as rarefied gasdynamics which is limited to a few sections in the chapter on "Concepts from Gaskinetics." But there is no question that this book contains a wealth of material in a clear and understandable fashion.

The book is intended as a text at the senior or first year graduate level. The authors have done an admirable job of writing such a book. Without question the book will find wide acceptance as a text on gasdynamics.

Pneumatic controls

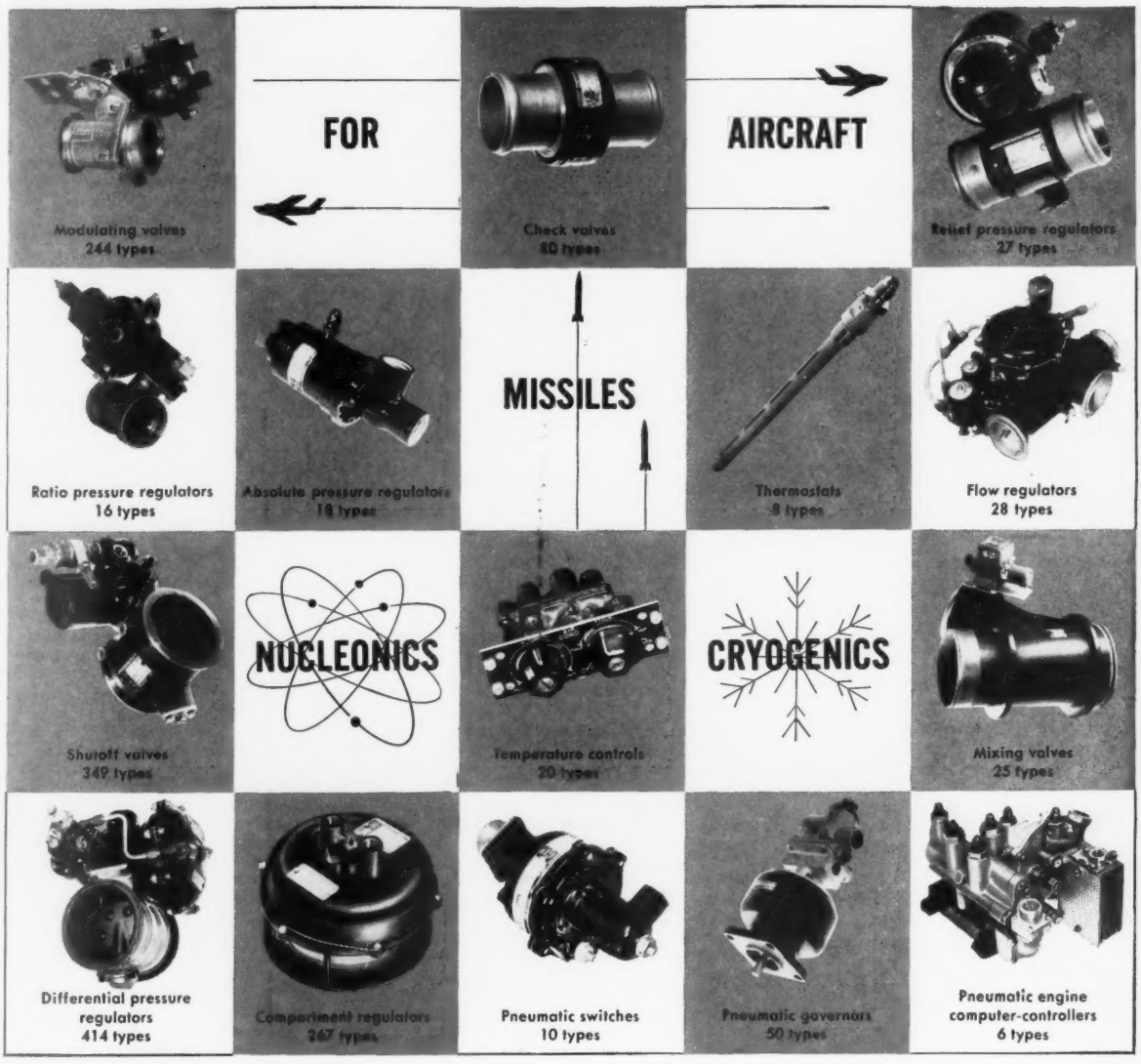

AiResearch is the largest designer and manufacturer of pneumatic controls for the aircraft and associated industries. During the past 10 years more than 300,000 units have been produced and are in service.

Temperatures of the fluids (including gas and liquids) range from −400°F to +2000°F at pressures to +6000 psig. The units operate at any ambient pressure at ambient temperatures from −300°F to over +1000°F. Line diameters range from ⅛ inch to 15 inches.

This equipment is developed and tested in the finest pneumatic facilities in the world. Your inquiries are invited.

• *Outstanding opportunities for qualified engineers*

THE GARRETT CORPORATION

AiResearch Manufacturing Divisions

Los Angeles 45, California . . . Phoenix, Arizona

Designers and manufacturers of aircraft and missile systems and components: REFRIGERATION SYSTEMS • PNEUMATIC VALVES AND CONTROLS • TEMPERATURE CONTROLS CABIN AIR COMPRESSORS • TURBINE MOTORS • GAS TURBINE ENGINES • CABIN PRESSURE CONTROLS • HEAT TRANSFER EQUIPMENT • ELECTRO-MECHANICAL EQUIPMENT • ELECTRONIC COMPUTERS AND CONTROLS

last minute data on

IMPREGNATED GLASS FABRICS

for applications 60°F-10,000°F

send coupon now for new data on high temperature materials

Send the coupon below for latest data on Trevarno impregnated glass fabrics for high temperature, high strength, missile and aircraft applications. Trevarno Silicone and Phenolic materials have been tested and proved to give optimum heat resistance and strength performance, and exceptional electrical and mechanical properties as well. Also available is data on new Trevarno chopped F-120 Phenolic material for molded parts for performance at 4,000°F.

Trevarno GLASS FABRICS

COAST MANUFACTURING AND SUPPLY COMPANY
P. O. Box 71, Livermore, California

Please send me data on materials for the temperature ranges I have checked below:

60°F to 160°F . . . . ☐
160°F to 750°F . . . ☐
800°F to 1500°F . . . ☐
1500°F to 5 to 10,000°F ☐
New chopped Phenolic . ☐

Name_____
Company_____
Address_____
City_____ State_____

New Patents

George F. McLaughlin, *Contributor*

Gas turbine with acoustic surge control (2,807,932). Albert G. Bodine Jr., Van Nuys, Calif.

Bladed compressor section in which a periodic surge flow phenomena occurs at a characteristic sound wave frequency. An acoustic wave attenuation means having a frequency response for the sound wave stall surge frequency, is acoustically coupled to the turbine air flow passage.

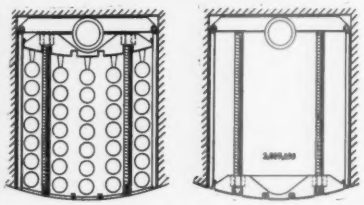

Magazine for releasable loads (2,807,193). R. A. Robert and P. P. Matge, Drancy, France.

Rocket magazine for mounting in an aircraft fuselage. The bottom wall of the magazine is made of a material breakable upon impact of the lowermost rocket during its downward advance. The undersurface of the suspending member is shaped to provide a continuous surface with adjacent parts of the fuselage when the suspending member reaches its lowermost position.

Propellant supply systems for jet reaction motors (2,808,700). Willi Kretschmer, Aylesbury, England, assignor to the Government of Great Britain.

A normally closed main valve in the propellant supply system arranged to open in response to a rise in outlet pressure to a predetermined value less than its inlet pressure.

Injector for rocket motor (2,808,701). Donald W. Lewis, Los Angeles, Calif.

Liquid fuel and oxidizer conveying tubes spaced from a supporting block through which passages supply propellant and oxidizer. The tubes, with multiple aperatures, are disposed to define an injector face spaced from the block.

Diffuser cone (2,809,491). Leon R. Wosika, San Diego, Calif., assignor to Solar Aircraft Co.

In the front part of the duct for diffusing exhaust gases, the cone angle increases to more than 13 deg, but less than the angle at which the gases stall. In the center part, the angle decreases to less than 13 deg, but not more than zero deg. In the rear part, the angle increases to 13 deg at its end.

Apparatus for measuring and/or controlling fuel/air ratio of gas turbines without direct gravimetric fuel metering (2,809,492). Seymour M. Arkawy, Peekskill, N. Y., assignor to Simmonds Aerocessories, Inc.

Control system for maintaining a predetermined gas temperature by controlling the ratio of mass fuel flow to air flow in terms of measured pressure drop and variable pressure coupled to fuel/air ratio adjusting means.

Guide load switch (2,809,558). Sidney Hersh, Silver Spring, Md., assignor to the U. S. Navy.

Guide button extending from a missile into a guide rail. A switch, closed when a missile is in loaded position, is rocked by the button when sliding the missile onto the track, latching the missile in place on the rail.

Rocket projector (2,809,559). Charles C. Lauritsen, Pasadena, Calif., assignor to the U. S. Navy.

Channel-shaped guides for supporting electrically ignitible rockets. Adaptor guides, mounted in spaced relationship within the first guides, support smaller rockets.

Missile firing device (2,809,624). Harold Becher and Martin Pepper, New York, assignors to Dellenbarger Machine Co.

A switch actuated by a missile positioned in the launching barrel controls a valve to permit air to escape. Gas under pressure ejects the missile from the barrel.

Pressure vessel (2,809,762). Carlos J. Cardona, North Hollywood, Calif., assignor to Fairchild Engine and Airplane Corp.

A thin-walled sphere containing a liner of rubbery material. A reinforced exterior layer of glass fibers is wound on the sphere and impregnated with a resin.

Connector ring for two-stage rockets (2,809,584). Bernard Smith, Inyorken, Calif., assignor to the U. S. Navy.

Pair of flanges, one fixed to the rear of the rocket and the other to the front of the booster motor. Grooved rings clamped around the flanges are held together by three explosive bolts. Actuation of the bolts releases the ring, disengaging the rocket from the booster.

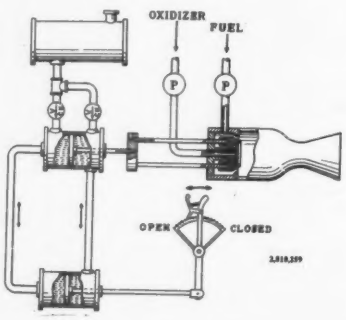

Injector for reaction motor (2,810,259). Harry W. Burdett Jr., Wycoff, N. J., assignor to Reaction Motors, Inc.

Ports in the combustion chamber wall are progressively uncovered and covered by a piston as it slides in a slot in a direction away from and toward the chamber. At least one propellant is supplied under pressure greater than that existing in the chamber.

EDITORS NOTE: Patents listed above were selected from the Official Gazette of the U. S. Patent Office. Printed copies of Patents may be obtained from the Commissioner of Patents, Washington 25, D. C., at a cost of 25 cents each; design patents, 10 cents.

Rocket propulsion method (2,810,257). Don R. Carmody, Evan A. Mayerle and Alex Zletz, Park Forest, Ill., assignors to Standard Oil Co. (Indiana).

Method consists of separately and simultaneously injecting into the combustion chamber a nitric acid oxidizer and a fuel consisting of triethyltrithiophosphite and a liquid hydrocarbon mixture which boils over the range of 200 to 400 F.

Aircraft auxiliary jet engine nacelle (2,810,534). Paul G. Fandeux, Courbevoie, France, assignor to SNCASO.

Streamlined nacelle fixed under the fuselage of an airplane. The leading edge of the intake mouth is located at a distance from the nose tip at least equal to half the diameter of the cross section of the nacelle.

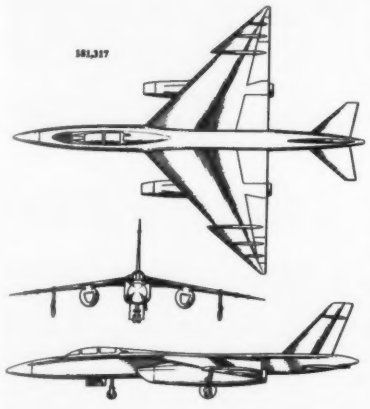

Aircraft design (181,317). Edgar Schmued and Welko E. Gasich, Los Angeles, Calif., assignors to Northrop Aircraft Corp.

Jet propelled airplane with two engine pods suspended below the delta wing.

Method for resizing internally threaded rocket motor tubing (2,811,730). Conrad R. Vegren, Washington, D. C.

Means for reducing the diameter of the end of a tube. Force is applied radially inward to the end portion of sufficient magnitude to permanently deform it to smaller diameter.

Balanced jet nozzle and cooling means therefore (2,811,827). Ralph Kress, La Mesa, Calif., assignor to Solar Aircraft Co.

An actuating mechanism imparts simultaneous opposite movements to a pair of coaxial members defining an exhaust orifice. Members can be rapidly moved with minimum effort to vary the area of the exhaust orifice for various operating conditions.

Bleed means for confined supersonic flow (2,811,828). George H. McLafferty, Manchester, Conn., assignor to United Aircraft Corp.

Ramjet with bleed means composed of apertures in the inlet diffuser wall. Appertures comprise upstream and downstream lips along the axis of flow. Downstream lips are recessed, forming a reentrant angle with the wall.

Ramjet employing carbon layer of insulation for solid carbon propellant (2,811,829). Alfred A. Topinka, Cleveland, Ohio.

Combustion chamber lined with solid carbon as a fuel and propellant. Carbon is protected from the shell by insulation of lamp black and powdered carbon. A complimentary burning section has an additional air inlet and a lining of refractory material.

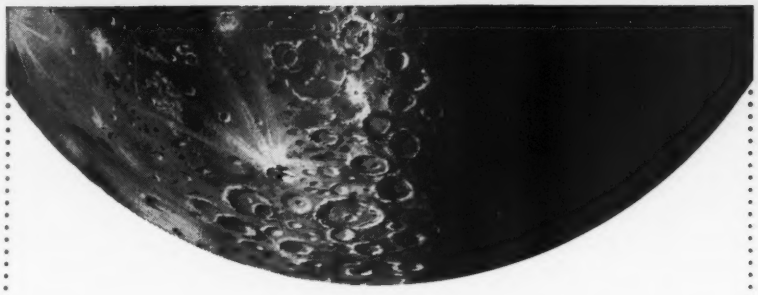

Men who know

TURBINES, PUMPS, COMPRESSORS

Get in on the development of the most advanced high-speed rotary equipment ever built

Here's your opportunity to step up to a new, higher level of turbo-machinery technology—the Large Rocket Engine.

Whatever type of rotating machinery you know best, your experience could be extremely valuable in the important developments now going on at Rocketdyne. The seasoned and ambitious man who has cut his teeth on jet engines, steam or gas turbines, or other elements of rotating machinery, is urgently needed to apply mechanical principles to meet the increasing demands of power plant performance.

The combination of high speed, light weight, heavy loadings and exceptional pressures required in rocket engine work is leading to an entirely new breed of high-performance rotating machinery... and a new breed of engineer. You can be one of this advance guard of the turbo-machinery field—if you have the desire to build your professional status by accepting new challenges.

Rocketdyne is building high-thrust rocket engines for the nation's major missiles. You'll work with the leading producer in the nation's fastest growing industry. You and your work will be recognized as a vital part of the overall achievements. Testing facilities are among the world's finest. The power produced is beyond anything ever before thought possible. If you would like to tackle new assignments working alongside some of the finest minds in turbo-engineering, write and tell us about your background: A. W. Jamieson, Rocketdyne Engineering Personnel Dept. **R-12,** 6633 Canoga Avenue, Canoga Park, California.

ROCKETDYNE

A DIVISION OF NORTH AMERICAN AVIATION, INC.

BUILDERS OF POWER FOR OUTER SPACE

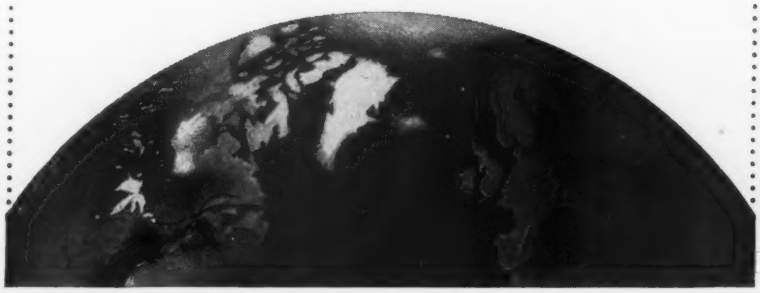

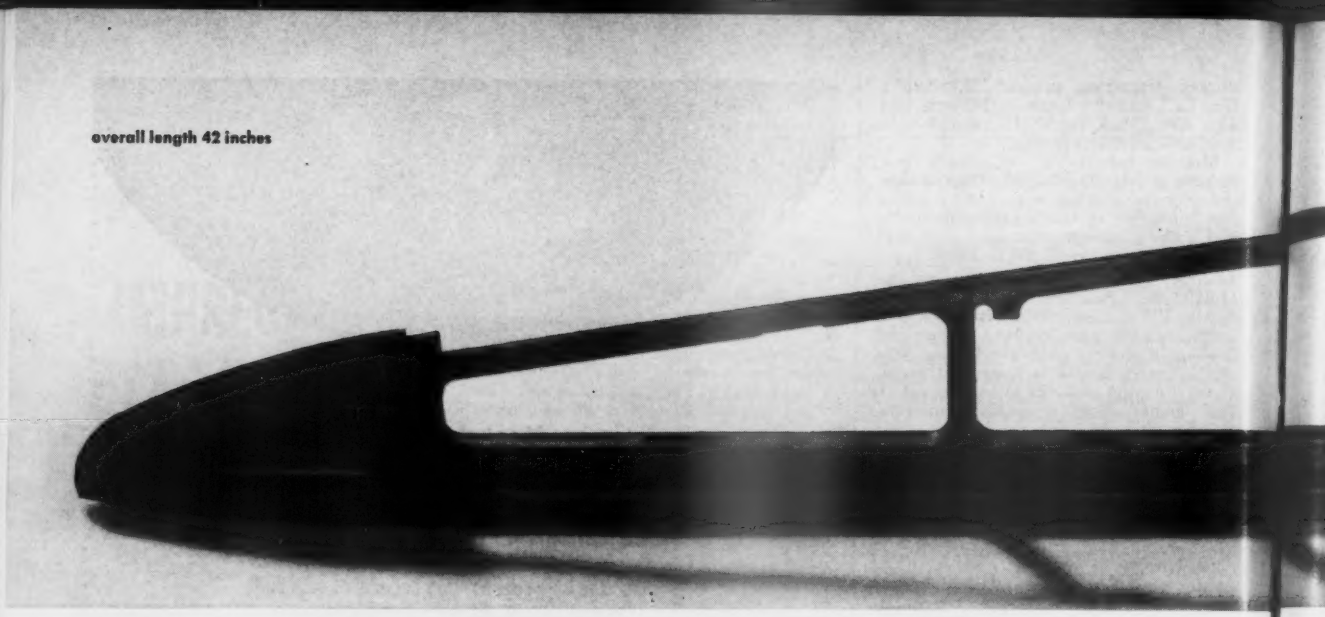

Now...from Doehler-Jarvis...die castings of

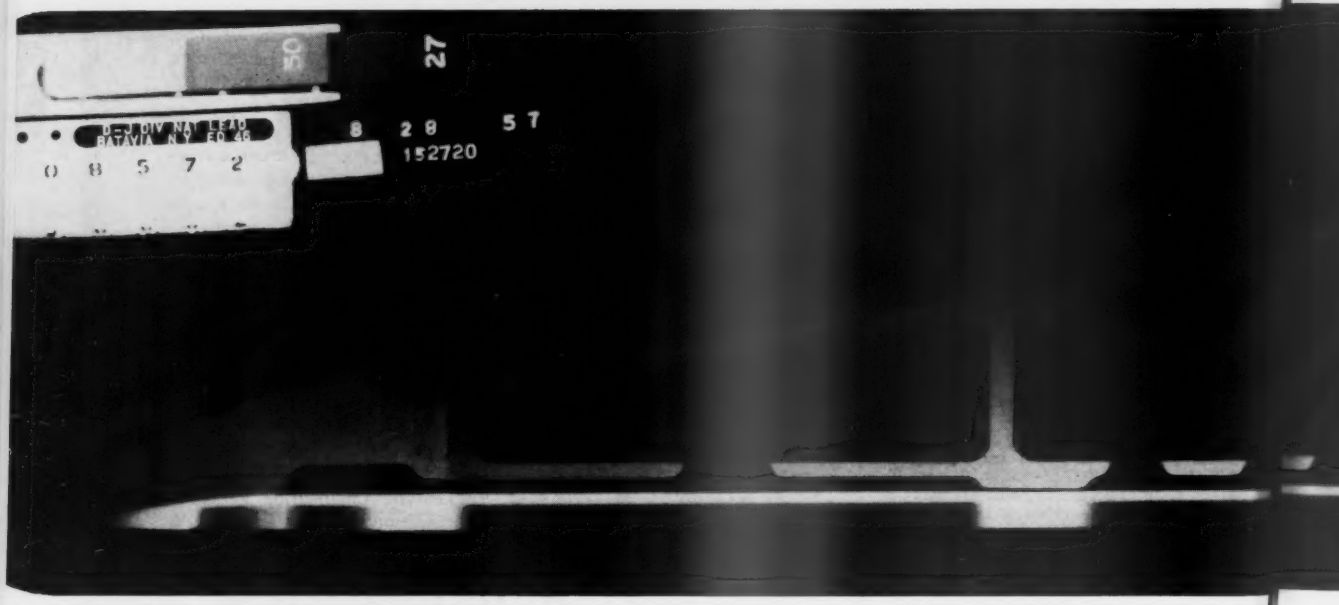

X-ray of the Falcon's fin proves the

The Falcon is an air-to-air missile built by Hughes Aircraft Company for the U. S. Air Force. Its light weight die cast stabilizer fins resist severe strain during course changes. It uses other Doehler-Jarvis die castings also.

Now *you* can have structurals die cast to standards as high as those for primary aircraft structurals*.

Die cast! With all the economy, precision, surface superiority ease of assembly that implies. Die cast of aluminum, or of high-purity magnesium alloy, like the 42" Falcon stabilizer fi

They said it couldn't be done!

But there you see such a structural! Along with X-ray proof of soundness, uniformity, primary-aircraft-structural* quality

Mind you! The Falcon fin is in commercial production Doehler-Jarvis has die cast thousands. Each has had to pass 73 inspections before acceptance . . . including 100% X-ray.

In *one* control, sections of castings are continuously tested for tensile strength. In this examination of physical properties the castings normally exceed tensile specifications by 15%

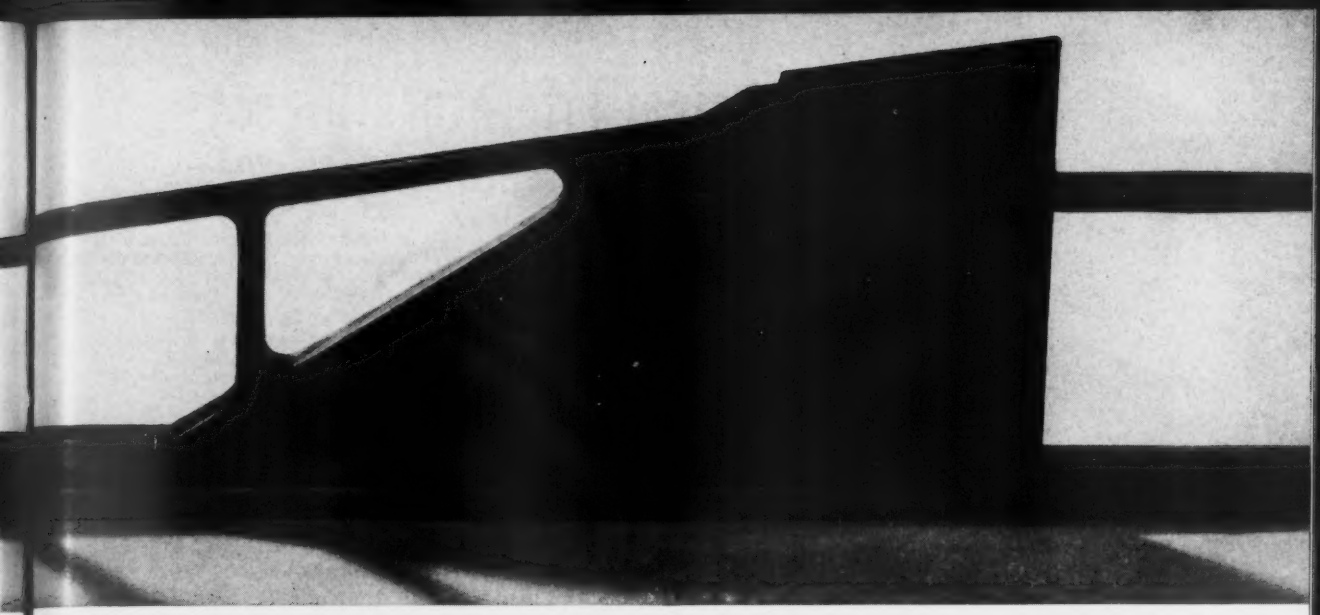

# of primary-aircraft-structural* quality

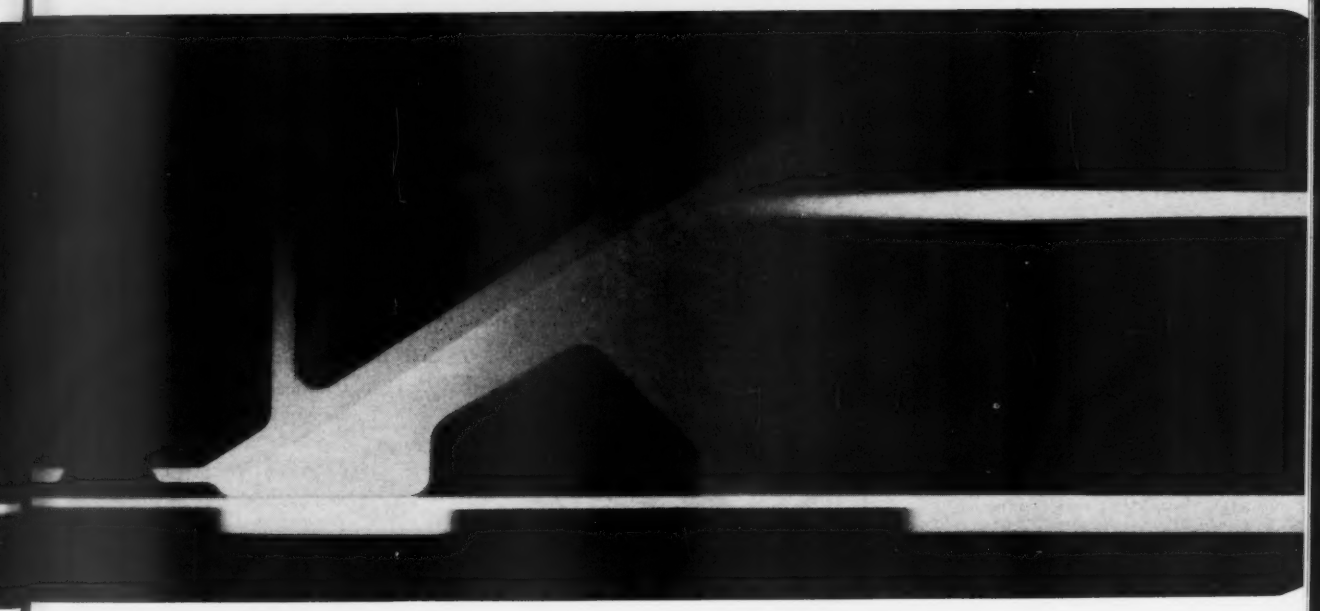

their uniformity and soundness

more. Quality is so high there has never been a single test below specification.

How did this come about?

Like many developments in die casting, this one started with a customer's need . . . Hughes Aircraft's.

They, and the Armed Services, needed such castings. The parts *might* be made other ways. But at what cost! What sacrifice in weight — and materials! If it *could* be die cast, if there *were* a magnesium alloy able to stand supersonic air stresses . . .

It took a while. But, with close cooperation from engineers of both Doehler-Jarvis and Hughes, the way was found.

Now you can list die castings of primary-aircraft-structural* quality among D and J availabilities. Get them from any Doehler-Jarvis plant.

*A primary aircraft structural is a major load-bearing component member any single failure of which would result in loss of the aircraft.

Doehler-Jarvis

DIVISION OF NATIONAL LEAD COMPANY

General Offices: Toledo 1, Ohio

In Canada:

Barber Die Casting Co. Limited

Hamilton, Ontario

LIBRASCOPE
SHAFT POSITION-TO-DIGITAL

CONVERTERS

Equipped with ANTI-AMBIGUITY
DOUBLE BRUSH PICKOFFS

Useful in a wide variety of applications, including digital aircraft and missile controls, machine tool controls, digital readout from strip chart recorders, and as the modulator and de-modulator in pulse-code modulated radio links.

GRAY CODE MODEL — Capacity of 8 binary digits (single brush pickoff).
BINARY MODEL — Capacity of 7 to 19 binary digits.
BINARY CODED DECIMAL MODEL Capacity range from 0-1999 to 0-35,999.

Units for special codes or capacities are built to meet specific requirements.

SHOCK ENDURANCE.....20g
TEMPERATURE RANGE..—50° to 83°C min.
CODE DISCS.....Rhodium plated phenolic
PICKOFFS.....Multiple wire brush. Two pickoffs/channel
ROTATION.....Continuous, either direction.

RUGGED—NON-MAGNETIC—LONG LIFE
MAY BE READ WHILE IN MOTION

SPECIAL CONVERTERS DESIGNED TO MEET YOUR INDIVIDUAL PROBLEMS

Send for illustrated brochure

LIBRASCOPE

A SUBSIDIARY OF GENERAL PRECISION EQUIPMENT CORPORATION

808 Western Avenue • Glendale, California

Technical Literature Digest

M. H. Smith, *Associate Editor,* **and M. H. Fisher,** *Contributor*
The James Forrestal Research Center, Princeton University

Nuclear Propulsion

The Lithium Hydride, Deuteride and Tritide Systems, by F. K. Heumann and O. N. Salmon, *Atomic Energy Comm.*, KAPL-1667, Dec. 1956, 54 pp.

Fast Fuel Rod Design and Analysis, by C. R. Stahl, R. J. Futz and R. G. Kennison, *Atomic Energy Comm.*, KAPL-423, Nov. 1950, 47 pp.

Neutron Energy Distributions Inside the Fast Reactor, by Norris Nereson, *Atomic Energy Comm.*, LA-1192, Dec. 1950, 49 pp.

Pressure Drop Tests on Twisted Ribbon Core Assemblies, by A. B. Schultz, *Atomic Energy Comm.*, ANL-5189, Aug. 1953, 42 pp.

Reactions Produced by the Electrical Explosion of a Metal Immersed in a Fluid, by Robert F. Plott, *Atomic Energy Comm.*, ANL-5040, Dec. 1950, 35 pp.

A Correlation of Fast Neutron Fission Cross Sections, by John R. Huizanga, *Atomic Energy Comm.*, ANL-5150, Nov. 1953, 7 pp.

Studies of Mixing in the Lower Plenum of a Quarter Scale Flow Model of the PWR Reactor, by Herbert R. Hazard and Abraham Rotkowitz, *Atomic Energy Comm.*, BMI-1172, Feb. 1957, 19 pp.

Study of a Liquid Metal Neutron Absorber for the Control of a Gas Cooled Power Reactor, by Banjamin B. Gordon, J. James Stone and Harold M. Epstein, *Atomic Energy Comm.*, BMI-1119, July 1956, 18 pp.

Enrico Fermi Fast Breeder Reactor Plant (Atomic Power Development Associates, Inc.,) *Atomic Energy Comm.*, APDA-115, Nov. 1956, 107 pp.

Nuclear Powered Gas Turbines for Light Weight Power Plants, by Frederick G. Hammitt and Harold A. Ohlgren, *ASME Pap.* 57-NESC-79, March 1957, 26 pp. (*Nuclear Engineering and Sci. Conf., 2nd.*, Philadelphia, March 11–14, 1957).

Fuel Cycles in Single Region Thermal Reactors, by Manson Benedict and Thomas H. Pigford, *ASME Pap.* 57-NESC-41, March 1957, 21 pp. (*Nuclear Engng. and Sci. Conf., 2nd.*, Philadelphia, March 11–14, 1957).

The Diffusion Theory of Fine Structure in Thermal Neutron Reactor Assemblies Consisting of Cylindrical Fuel Elements Set in a Square Lattice Array, by A. C. Clark and D. A. Newmarch, *Gt. Brit., Atomic Energy Res. Estab., Rep.* RP/R 1657, 1956, 18 pp.

Theory of the Ideal A.C. Conduction

EDITOR'S NOTE: Contributions from E. R. G Eckert, J. P Hartnett, T. F. Irvine Jr. and P. J. Schneider of the Heat Transfer Laboratory, University of Minnesota. are gratefully acknowledged.

"MONOBALL"®
Self-Aligning Bearings

CHARACTERISTICS

	ANALYSIS	RECOMMENDED USE
1	Stainless Steel Ball and Race	For types operating under high temperature (800-1200 degrees F.).
2	Chrome Alloy Steel Ball and Race	For types operating under high radial ultimate loads (3000-893,000 lbs.).
3	Bronze Race and Chrome Steel Ball	For types operating under normal loads with minimum friction requirements.

Thousands in use. Backed by years of service life. Wide variety of Plain Types in bore sizes 3/16" to 6" Dia. Rod end types in similar size range with externally or internally threaded shanks. Our Engineers welcome an opportunity of studying individual requirements and prescribing a type or types which will serve under your demanding conditions. Southwest can design special types to fit individual specifications. As a result of thorough study of different operating conditions, various steel alloys have been used to meet specific needs. Write for revised Engineering Manual describing complete line. Dept. JP-57.

SOUTHWEST PRODUCTS CO.
1705 SO. MOUNTAIN AVE., MONROVIA, CALIFORNIA

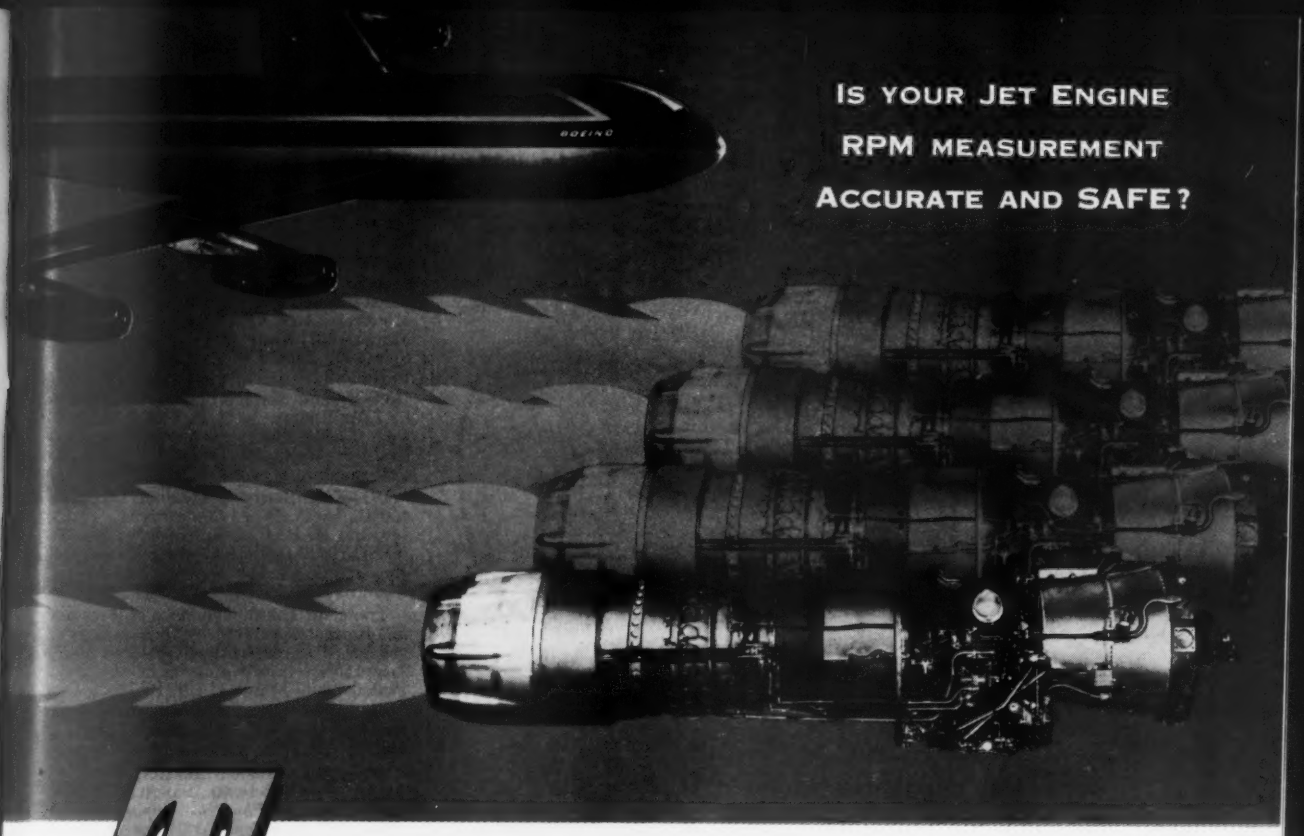

IS YOUR JET ENGINE
RPM MEASUREMENT
ACCURATE AND SAFE?

TAKCAL®

READS JET ENGINE SPEED to GUARANTEED ACCURACY of 10 RPM in 10,000 RPM (±0.1%)

The inter-relation of RPM to efficiency and thrust in jet engines is fundamental. Proper adjustments for maximum thrust, maximum engine life and maximum safety of operation can be made only upon accuracy of instrumentation. The TAKCAL tests to guarantee that accuracy.

The new B & H TAKCAL incorporates a refinement of the frequency meter principle. It operates in the low (0 to 1000 cps) range, reading the frequency of the tachometer generator on a scale calibrated in percent RPM corresponding to the engine's RPM. It reads engine speed while the engine is running with a guaranteed accuracy of ±0.1% in the range of 0 to 110% RPM. Additionally, the TAKCAL circuit can be used to trouble-shoot and isolate errors in the aircraft tachometer system, with the circuit and tachometer paralleled to obtain simultaneous reading.

The TAKCAL's component parts are identical with those used in the J-Model JETCAL Analyzer. They are here assembled as a separate unit tester and for use with all earlier models of the JETCAL Tester.

The TAKCAL operates accurately in all ambient temperatures from –40°F. to 140°F. Low in cost for an instrument of such extreme accuracy, it is adaptable to application in many other fields.

For full information write or wire . . .

B & H INSTRUMENT CO., INC.
3479 West Vickery Blvd. • Fort Worth 7, Texas

B & H makes the *JETCAL*® Analyzer and *TEMPCAL*® Tester

Sales-Engineering Offices:

VALLEY STREAM, L. I.: 108 So. Franklin, LO 1-9220 • DAYTON, OHIO: 209 Commercial Bldg., BA 4-4563 • COMPTON, CAL.: 105 N. Bradfield St., NE 6-8970
ENGLAND: Bryans Aeroquipment Ltd. (Licensee), 15, Willow Lane, Mitcham, Surrey

Insure Product Performance...
REVERE SPECIALTY WIRES

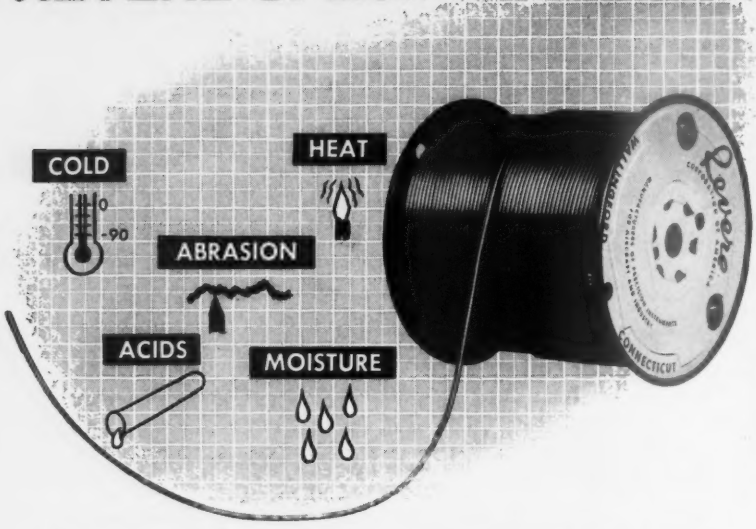

For those tough design jobs where ordinary hook-up and thermocouple wires die from the heat, get brittle in cold, abrade and corrode . . . Revere SPECIALTY wires stand up. Built to MIL and customer specifications. Range includes:

HOOK-UP WIRES

For High Temperatures

REVCOTHENE — (Extruded Monochlorotrifluoroethylene) —40°F to +275°F, AWG 28 to 10, silver-plated copper conductors, inert, excellent dielectric strength, no volatile plasticizers, non-flammable, thin wall, abrasion and moisture resistant.

PERMACODE — Teflon* — insulated wire with striping down to the conductor for permanent identification, single or multiple stripes, 15 colors, —130°F to +410°F, AWG 28 to 16, silver-plated copper conductors, excellent abrasion and dielectric characteristics.

MULTI-CONDUCTOR CABLES

A variety of telemetering and other multi-conductor cables constructed to customer specifications. Teflon, polyethylene, polyvinyl, nylon, glass, Revcothene, asbestos insulations for singles and jackets. Twisting, braiding, shielding, color coding to suit conditions.

THERMO-COUPLE WIRES

Iron-constantan, copper-constantan, Chromel-Alumel conductors, AWG 36 to 14, various insulation combinations and protective braids, temperature range from —100°F to +1500°F, constructed to rigid tolerances.

*E. I. du Pont trademark

Saturants for flame and abrasion resistance, metallic braids for severe service and electrical shielding. Color coding in 15 solid colors and stripes.

Prompt delivery of standard stock wires. Write for samples and literature on specialty hook-up or thermocouple wire.

20

REVERE CORPORATION OF AMERICA
Wallingford, Connecticut
A SUBSIDIARY OF NEPTUNE METER COMPANY

neptune

Pump, by W. Murgatroyd, *Gt. Brit., Atomic Energy Res. Estab., Rep.* ED/R 1566, 1956, 9 pp., 7 fig.

A Homopolar Generator for High Current Low Voltage D.C. Supply, by D.A. Watt, *Gt. Brit., Atomic Energy Res. Estab., Rep.* ED/R 1843. (Declassified edition of *AERE Rep.* CE/R821), 1956, 24 pp.

The Time and Temperature Dependence of Thermal Stresses in Cylindrical Reactor Fuel Elements, by Kenneth R. Merckx, *ASME, Pap.* 57-NESC-78, March 1957, 8 pp. (*Nuclear Engng. and Sci. Conf., 2nd.*, Philadelphia, March 11–14, 1957).

Decay and Storage of Irradiated Fuel, by J. W. Ullman and E. D. Arnold, *ASME Pap.* 57-NESC-93, March 1957, 6 pp. (*Nuclear Engng. and Sci. Conf., 2nd.*, Philadelphia, March 11–14, 1957).

UO_2-NaK Slurry Studies in Loops at 600°C., by B. M. Abraham, H. E. Flowtow and R. D. Carlson, *ASME Pap.* 57-NESC-104, March 1957, 12 pp. (*Nuclear Engng. and Sci. Conf., 2nd.*, Philadelphia, March 11–14, 1957).

Transient Thermodynamics of Reactors and Process Apparatus, by Dale H. Brown, *ASME, Pap.* 57-NESC-81, March 1957, 11 pp. (*Nuclear Engng. and Sci. Conf., 2nd.*, Philadelphia, March 11–14, 1957).

Open Cycle Takes Nuclear Engine Lead, by Robert Cushman, *Aviation Week*, vol. 66, May 27, 1957, p. 27.

A Possible Fusion Reactor, by Goro Miyamoto, Gliti Iwata, Sigeru Mori and Kenji Inoue, *J. Phys. Soc. Japan*, vol. 12. April 1957, p. 438.

Combustion, Fuels and Propellants

Interaction of a Free Flame Front with a Turbulence Field, by Maurice Tucker, *NACA Rep.* 1277, 1956, 19 pp. (supersedes *NACA TN* 3407).

Effect of Standing Transverse Acoustic Oscillations on Fuel-Oxidant Mixing in Cylindrical Combustion Chambers, by William R. Mickelsen, *NACA TN* 3983, May 1957, 49 pp.

Transverse Wave and Entropy Wave Combustion Instability in Liquid Propellant Rockets, by Sinclaire M. Scala, *Princeton Univ., Dept. Aeron. Engng., Rep.* 380, 1957, 138 pp. (PhD. thesis).

Longitudinal Combustion Instability in a Duct with Oblique Flame Front, by Marcel Vinokur, *Princeton Univ., Dept. Aeron. Engng.*, May 1957, 118 pp. (PhD. thesis).

Generalized Design Equations for an Internal Burning Star Configuration Solid propellant Charge and Method of Calculating Pressure Time and Thrust Time Relationships, by L. Piasecki and G. Robillard, *Calif. Inst. Tech., Jet Propulsion Lab.*, Mem. 20-135, Sept. 1956, 33 pp.

Combustion in Laminar Mixing Regions and Boundary Layers, by Donald Allen Dooley, Pasadena, *Calif. Inst. Tech.*, 1956, 244 pp. (Ph.D. thesis).

Rate of Recombination of Radicals, III: Rate of Recombination of Ethyl Radicals, by A. Shepp and K. O. Kutschke, *J. Chem. Physics.*, vol. 26, May 1957, pp. 1020–1028.

A Precision Calorimeter for the Measurement of Heats of Combustion, by Charles E. Holley Jr. and Elmer H. Huber Jr., *Atomic Energy Commission*, LA-2084, Jan. 1957, 18 pp.

Temperature Measurements During

Firing of Simulated Submarine Rocket Launcher, by Norman E. Jensen Jr. and James C. Coe, *Naval Air Missile Test Center, Tech. Rep.* 16, June 1947, 17 pp. (Declassified from Confidential by authority of NAMTC letter A9/Ser. 362, 7/20/56.)

Reactions of Gaseous Ions, II: Acetylene, by F. H. Field, J. L. Franklin and F. W. Lampe, *J. American Chem. Soc.*, vol. 79, June 5, 1957, p. 2665.

Some Factors Influencing Stability Limits of Bunsen Flames, by P. F. Kurz, *Combustion and Flame,* vol. 1, no. 2, June 1957, pp. 162–178.

Mixing and Combustion in Free and Enclosed Turbulent Jet Diffusion Flames, by P. D. Sunavala, C. Hulse and M. W. Thring, *Combustion and Flame,* vol. 1, no. 2, June 1957, pp. 179–193.

A Law of Similarity for Temperatures in Enclosed Turbulent Flames, by C. Codegone, *Combustion and Flame,* vol. 1, no. 2, June 1957, pp. 194–198.

On the Positive and Negative Ions in Diffusion Flames, by Tosiro Kinbara and Hideo Ikegami, *Combustion and Flame,* vol. 1, no. 2, June 1957, pp. 199–211.

Influence of Diborane on Blow-Off Limits of Hydrocarbon Flames, by P. F. Kurz, *Combustion and Flame,* vol. 1, no. 2, June 1957, pp. 212–216.

Flame Zone Studies IV—Microstructure and Material Transport in a Laminar Propane-Air Flame Front, by R. M. Fristom and A. A. Westenberg, *Combustion and Flame,* vol. 1, no. 2, June 1957, pp. 217–228.

Experimental Techniques for the Study of Flat Flames by Infra-red Spectroscopy, by D. J. Cole and G. J. Minkoff, *Combustion and Flame,* vol. 1, no. 2, June 1957, pp. 241–249.

Homogeneous Decomposition of Hydrogen Peroxide Vapor, by Charles N. Satterfield and Theodore W. Stein, *J. Physical Chem.*, vol. 61, May 1957, pp. 537–540.

Calculation of Experimental Isotope Effects for Pseudo-First Order Irreversible Reactions, by James Yang-peh Tong and Peter E. Yankwich, *J. Physical Chem.*, vol. 61, May 1957, pp. 540–543.

Studies of Diffusion Flames, III: The Diffusion Flames of the Butanols, by S. Ruven Smith, Alvin S. Gordon and Maynard H. Hunt, *J. Physical Chem.*, vol. 61, May 1957, pp. 553–558.

A Kinetic Approach of the Thermodynamics of Irreversible Processes, by O. K. Rice, *J. Physical Chem.*, vol. 61, May 1957, pp. 622–629.

Nitric Oxide Decomposition at 2200–2400° K., by C. P. Fenimore and G. W. Jones, *J. Physical Chem.*, vol. 61, May 1957, pp. 654–657.

Thermal Design of Large Storage Vessels for Liquid Hydrogen and Helium, by Russell B. Scott, *J. Res., Nat. Bur. Standards.*, vol. 58, June 1957, pp. 317–326.

Chemical Aspects of High Energy Solid Propellants, *Missiles and Rockets,* vol. 2, June 1957, pp. 110, 112.

Field Methods for Determination of Unsymmetrical Dimethylhydrazine and Water in NIKE Fuels, by R. F. Muraka, Stephen P. Bango, Lois L. Taylor and Julia S. Whitlick, *Calif. Inst. Tech., Jet Propulsion Lab., Prog. Rep.* 20-315, March 1957, 11 pp.

Propellant Stability Testing at Picatinny Arsenal; a Résume of Facilities, Methods and Programs, *Picatinny Arsenal, Samuel Feltman Ammunition Labs., TN* 8, June 1957, 28 pp.

The Thermodynamic Properties of 54

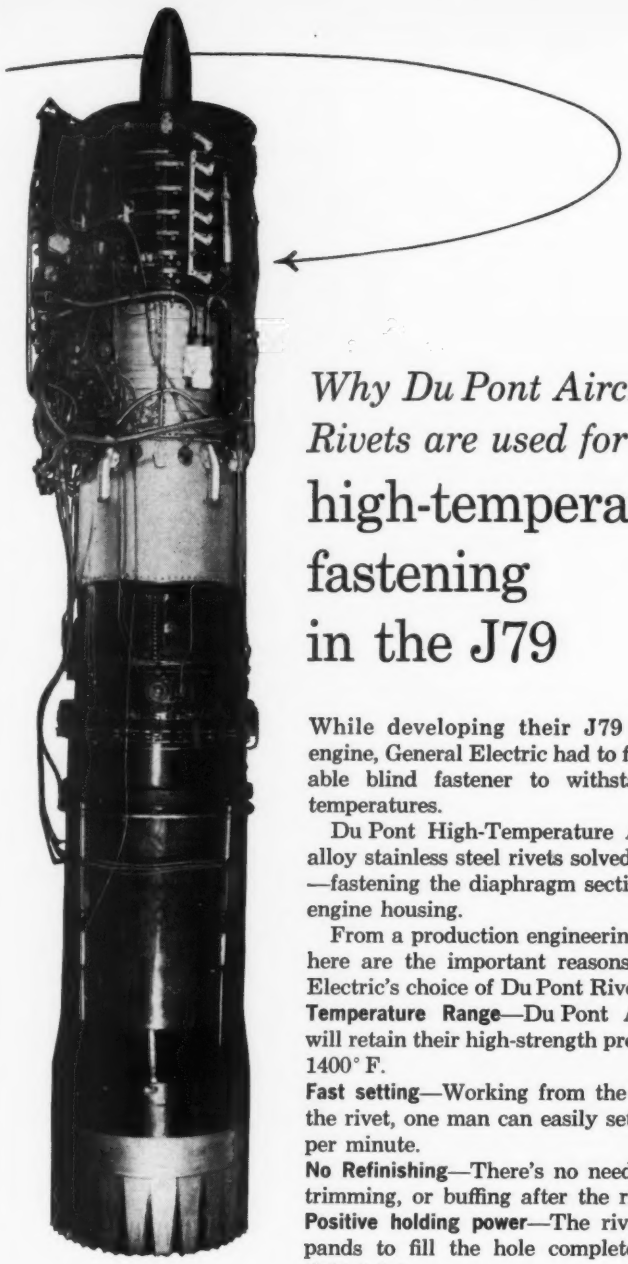

Watch CBS for the Du Pont "Show of the Month"

Why Du Pont Aircraft Rivets are used for

high-temperature fastening in the J79

While developing their J79 gas turbine engine, General Electric had to find a dependable blind fastener to withstand elevated temperatures.

Du Pont High-Temperature A-286 Superalloy stainless steel rivets solved the problem—fastening the diaphragm section inside the engine housing.

From a production engineering standpoint, here are the important reasons for General Electric's choice of Du Pont Rivets.

Temperature Range—Du Pont A-286 Rivets will retain their high-strength properties up to 1400° F.

Fast setting—Working from the head end of the rivet, one man can easily set 20-25 rivets per minute.

No Refinishing—There's no need for cutting, trimming, or buffing after the rivets are set.

Positive holding power—The rivet shank expands to fill the hole completely, insuring tight joints.

Find out how Du Pont Rivets can solve your high-temperature fastening problems. Call your Du Pont representative or write: E. I. du Pont de Nemours & Co. (Inc.), 2543 Nemours Building, Wilmington 98, Delaware.

DU PONT AIRCRAFT BLIND EXPANSION RIVETS

DU PONT REG. U.S. PAT. OFF.

A Product of Du Pont Research

BETTER THINGS FOR BETTER LIVING . . . THROUGH CHEMISTRY

this is a

This Visicorder Oscillograph record* is a symbol of the leadership that is typical of Honeywell engineering. In laboratories all over the world the Visicorder's instantly-readable direct records are showing the way to new advances in rocketry, control, computing, product design and component test and in nuclear research.

*reproduced actual size, unretouched

The Model 906 Visicorder is years ahead of the trend. It is the first oscillograph that combines the convenience of direct recording with the high frequencies and sensitivities of photographic-type instruments. The Visicorder alone among oscillographs lets you monitor high-speed variables as they go on the record.

is a record of leadership

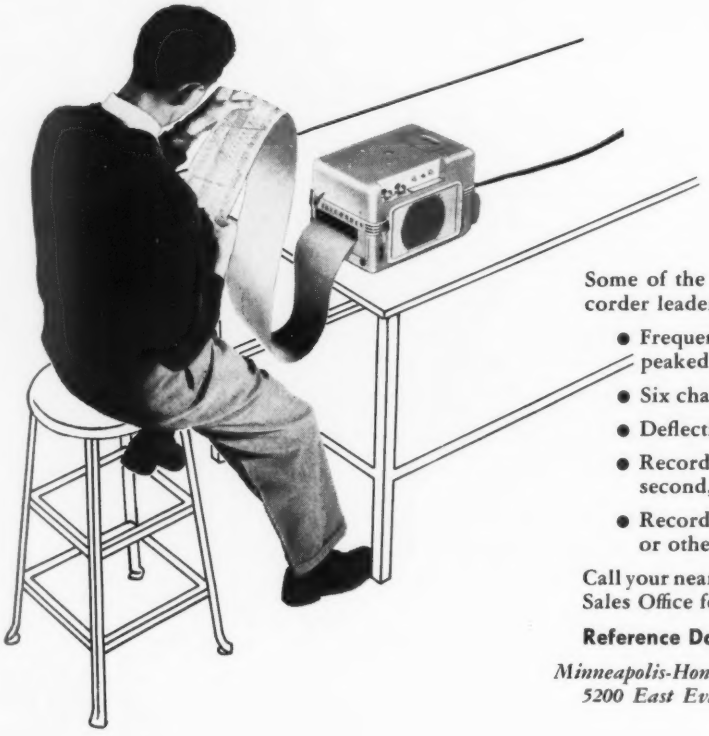

Some of the general features which give the Visicorder leadership in the direct-recording field are:

- Frequencies from DC to 2000 cps without peaked amplifiers or other compensation
- Six channels plus 2 timing traces on 6″ paper
- Deflection 6″ peak to peak; traces may overlap
- Record speeds 0.2, 1, 5, and 25 inches per second, minute, or hour
- Records require no liquids, powders, vapors, or other processing

Call your nearest Minneapolis-Honeywell Industrial Sales Office for a demonstration.

Reference Data: Write for Visicorder Bulletin

Minneapolis-Honeywell Regulator Co., Heiland Division, 5200 East Evans Avenue, Denver 22, Colorado.

MINNEAPOLIS
Honeywell

Heiland Division

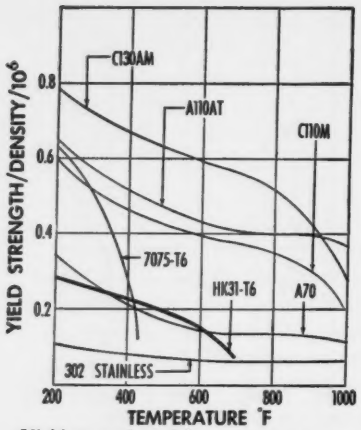

Yield strength, weight vs. temperature.

For High Strength-to-Weight Ratios at Elevated Temperatures— TITANIUM and MAGNESIUM

The experience, the specialists, the equipment-and-facilities to design and produce the *very difficult* fabrication and assembly work in these and other light metals—you'll find at B&P.

To make this titanium pressurized tank, B&P welds two cylinders. Each is drawn in one operation. Tank withstands 5000 psi pressure.

Magnesium turret enclosure for a bomber. Design, lofting, prototypes, production fabrication and assembly are all done by B&P.

ENGINEERING FACILITIES IN DETROIT AND LOS ANGELES . . Write for Titanium and Magnesium engineering data—also folder on B&P's facilities to handle tough jobs.

BROOKS & PERKINS, Inc.

1932 West Fort St.
Detroit 16, Mich.
Phone: TAshmoo 5-5900

IN LOS ANGELES:
11655 Vanowen St.
North Hollywood, Cal.
Phone STanley 7-9665

D-4

OFFICES IN NEW YORK, WASHINGTON, DALLAS

Elements Considered as Ideal Monatomic Gases, by Harwood G. Kolsky, *Atomic Energy Commission,* LA-2110, March 1957, 138 pp.

Basic Chemistry of High Temperature Inorganic Systems, Semi-Annual Progress Report, Jan.-June 1956, by S. J. Yosim and T. A. Milne, *Atomic Energy Commission,* NAA-SR-1797, March 1957, 23 pp. (North American Aviation, Inc.).

Heat Transfer and Fluid Flow

Nusselt Values for Estimating Turbulent Liquid Metal Heat Transfer in Non-Circular Ducts, by James P. Hartnett and Thomas F. Irvine Jr., *ASME, Pap.* 57-NESC-30, March 1957, 8 pp. (*Nuclear Engng. and Science Conference,* 2nd, Philadelphia, March 11–14, 1957).

Gas Coolant for Nuclear Reactors, by Michael Silverberg, *ASME, Pap.* 57-NESC-76, March 1957, 4 pp. (*Nuclear Engng. and Science Conference,* 2nd., Philadelphia, March 11–14, 1957).

A Method of Cascade Design for Two-Dimensional Incompressible Flow, by S. Rosenblat and L. C. Woods, *Australia, Aeron. Res. Comm., Rep.* ACA 58, March 1956, 30 pp.

Bibliography on Shock Waves, Shock Tubes and Allied Topics, by K. Dolder and R. Hide, *Gt. Brit., Atomic Energy Res. Estab. Rep.* G/R 2055, 1956, 97 pp.

Bibliography on the Origin of Turbulence and Related Subjects, by Maurice H. Smith, *Princeton Univ., James Forrestal Res. Center, Lit. Search* 13, April 1957, 126 pp.

Experiments on the Inhibition of Thermal Convection by a Magnetic Field, by Y. Nakagawa, *Proc. Royal Soc.,* vol. A240, April 24, 1957, pp. 108–113.

The Aerodynamic Variable Nozzle, by A. I. Martin, *J. Aeron. Sci.,* vol. 24, May 1957, pp. 357–362.

Fluctuations and Hot Wire Anemometry in Compressible Flows, by Mark V. Morkovin, *North Atlantic Treaty Organization, Advisory Group Aeron. Res. Dev., AGARDograph* 24, Nov. 1956, 102 pp.

Shock Waves in a Relaxing Medium, by S. P. D'yakov, *Russian Transl.* 3908, (translation of *Zhur. Eksp. Teor. Fiz.,* vol. 27, no. 6, 1954, pp. 728–734).

Shock Waves in Binary Mixtures, by S. P. D'yakov, *Russian Transl.* 3922 (translation of *Zhur. Eksp. Teor. Fiz.,* vol. 27, no. 3, 1957, pp. 283–287).

The Stability of Shock Waves, Investigation of the Problem of the Stability of Shock Waves in Arbitrary Media, by S. P. D'yakov, *Russian Transl.* 4295, (translation of *Zhur. Eksp. Teor. Fiz.,* vol. 27, no. 3, 1954, pp. 288–295).

Two-Dimensional Flow in the Vicinity of the Stagnation Point of an Incompressible Viscous, Electrically Conducting Field in the Presence of a Magnetic Field, by Joseph L. Neuringer, *Republic Aviation, Inc.,* June 1957, 19 pp.

Mass Transfer Cooling in High Speed Laminar Couette Flow, by E. R. G. Eckert and P. J. Schneider, *Minnesota Univ., Mech. Engng. Dept. TR* 12 (*AF Off. Sci. Res. TN* 57-186; *ASTIA AD-*126,481), April 1957, 44 pp.

Static Pressure Distribution in the Free Turbulent Jet, by D. R. Miller and E. W. Comings, *Indust. and Engng. Chem.,* vol. 49, June 1957, p. 985.

The Ranque-Hilsch Vortex Tube, by William A. Scheller and George M. Brown,

Manufacturing at Marquardt

by
Roy E. Marquardt
President

Another barrier – the PRODUCIBILITY BARRIER – is currently being penetrated by Marquardt engineers. What do we mean by PRODUCIBILITY BARRIER?

Advanced designs for supersonic ramjet powerplants coming from the drawing boards call for strength to weight ratios and high-precision tolerances previously unobtainable. New high-temperature alloys are meeting the metallurgical demands, but do not readily lend themselves to conventional machining and fabricating techniques.

Those members of the Marquardt team charged with pioneering new production methods comprise our Van Nuys Manufacturing Division. Here—under the direction of John S. Liefeld – creativeness and imagination join forces with a thorough understanding of standard shop practices to produce acceptable hardware. But management realizes that to do his best work the engineer must be supplied with the most up-to-date tools of his trade.

Exemplifying our continuing efforts to this end: a specially designed, half-million dollar roll-former is being added to the company's ever-expanding production facilities. This machine will be capable of spinning conical, tubular, venturi, and parabolic configurations of a size heretofore considered impossible or impractical to fabricate as a single piece. A completely safe, close-up view of the actual metal forming will be afforded the operator by means of two closed-circuit TV cameras mounted on the machine frame.

We are also acquiring other automatic machines – numerically controlled units capable of multiplying the output of their manually operated counterparts several times. Utilizing punched and magnetic tape, these machines are expected to greatly expand the scope of Manufacturing Engineering.

Another of the modern production techniques at Marquardt puts to use modern optics equipment for the construction of prototype engines.

At Marquardt, the engineer will find a broad range of challenging assignments and the opportunity to further his career through supplemental educational programs.

Within this Division, engineering openings exist now for:

METHODS ENGINEERS — PROCESS ENGINEERS
TOOL ENGINEERS — AUTOMATION ENGINEERS
NUMERICAL CONTROL ENGINEERS

For information about these positions and the professional engineering environment at Marquardt, we invite you to write Jim Dale, Professional Personnel, today.

Roy E Marquardt

marquardt AIRCRAFT CO.
VAN NUYS, CALIFORNIA — OGDEN, UTAH
FIRST IN RAMJETS

To Manufacturing Engineers Facing an ENGINEER | BARRIER *

Shown here: John S. Liefeld, Director Van Nuys Manufacturing Division

Marquardt Means Opportunity– Manufacturing engineers no longer need feel stymied because of the lack of up-to-date equipment. At Marquardt Aircraft – the company where an ENGINEER/BARRIER* has never existed – you will find the most advanced tools of your trade. Look to your future by looking to Marquardt, today. Address your inquiries to Jim Dale, Professional Personnel, 16556 Saticoy Street, Van Nuys, California.

marquardt AIRCRAFT CO.

VAN NUYS, CALIFORNIA OGDEN, UTAH

-SUPER-
LaVezzi
SERVICE
REG. U.S. PAT. OFF.
LAVEZZI – Reliable source for high precision machine parts.
Small parts for instruments, missiles, rockets, aircraft components, and other fine units, with close tolerances and fine finishes which are usually considered difficult to produce can be manufactured by LaVezzi strictly according to your specifications. Our years of experience are at your disposal.
Send your drawings for quotation or write for brochure or further details.
Specialists in fine machine work since 1908.
LAVEZZI MACHINE WORKS
4635 WEST LAKE ST. • CHICAGO 44, ILL.

PRECISE CURRENT for your TESTING NEEDS!

VARIABLE FREQUENCY MOTOR GENERATOR SETS ADJUST 360 TO 440 CPS.

Generator mounted controls include reset buttons, limit switch. Motor and generator remain stationary. Vari-drive pulley adjustment controlled by small motor. Remote control panels available

Units can be equipped with synchronous motor starter and magnetic amplifier, automatic voltage regulator.

KATO 400 CYCLE MOTOR GENERATOR SETS
NOW UP TO 250 KW!

KATO MOTOR GENERATOR SETS are available in frequencies, speeds and sizes for every specialized use . . . operating high cycle tools, testing components and electronic equipment

INPUT 60 CYCLES
OUTPUT 400 CYCLES

WRITE FOR NEW FOLDER!

Builders of Fine Electrical Machinery Since 1928
KATO Engineering Company
1498 First Ave., Mankato, Minn.

NORTHAM
DIFFERENTIAL
PRESSURE
TRANSDUCER

Length: 2½"
Weight: 12 oz.

A variable inductance instrument for measurement of differential pressures in ranges ± 200 to ± 5,000 psi and line pressures up to 5,000 psi. Designed for rocket and jet engine testing involving extreme mechanical disturbances, and for general laboratory measurement and industrial control applications.

MODEL DP-15 SPECIFICATIONS:

Pressure Ranges: . . ± 200 to ± 5,000 psid
Maximum Line Pressure: . . . . . 5,000 psi
Accuracy: . . . . . ± 1% full scale
Excitation Frequency: From 60 to 20,000 cps
Natural Frequency: From 2,000 cps to 10,000 cps depending on range
Acceleration Response: Less than 1%/1,000 g along most sensitive axis (range above 1,000 psi)
Less than 1%/1,000 g axial (all ranges)

WRITE FOR BULLETIN NO JP-8

Northam Engineering Facilities Are Available To Assist You With Any Application Problems.

NORTHAM PRODUCTS INCLUDE . . .

Transducers for pressure, acceleration and displacement measurement and auxiliary electronic equipment for complete systems.

NORTHAM ELECTRONICS, INC.
A Subsidiary of Norris-Thermador Corp.
2420 North Lake Avenue, Altadena, Calif.

Indust. Engng. Chem., vol. 49, June 1957, pp. 1013–1016.

Laminar Boundary Layer Flows with Surface Reactions, by Andreas Acrivos and Paul L. Chambré, *Indust. Engng. Chem.*, vol. 49, June 1957, pp. 1025–1029.

Instrumentation, Telemetering, Data Recording

A Nonlinear Instrument Diaphragm, by Fidel Corero, Harry Matheson and Daniel P. Johnson, *J. Res. Nat. Bur. Stands.*, vol. 58, June 1957, pp. 333–338.

Redstone In-Flight Telemetering, by Charles T. N. Paludan, *Missiles and Rockets*, vol. 2, June 1957, pp. 126, 128.

The Design of an Acceleration Insensitive Skin Friction Balance for Use in Free Flight Vehicles at Supersonic Speeds, by Willis Carson Lyons Jr., *Texas Univ., Defense Res. Lab.*, CF-3605 (DRL-397), June 1957, 42 pp., 18 fig.

Ultrasonic Flowmeter Monitors Reactor Heat Exchange Circulation, by M. Koblenz, R. Spiegel, S. Kass and H. Sterling, *ASME Pap.* 57-NESC-84; *Amer. Inst. Elect. Engrs., Pap.* 57-400, March 1957, 8 pp.

A Resistance Temperature Detector for Nuclear Service, by F. Ralph Sias *ASME Pap.* 57-NESC-83; March 1957, 6 pp.

Recent Developments in Nuclear Instrumentation at the Knolls Atomic Power Laboratory, by Richard S. Stone, *ASME Pap.* 57-NESC-70; *Amer. Inst. Elect. Engrs., Pap.* 57-399, March 1957, 5 pp.

A Wire Activation Technique for Reactor Flux Profile Measurements, by Alton E. Klickman and Francis R. DeFalco, *ASME Pap.* 57 NESC-40; *Amer. Inst. Elect. Engrs. Pap.* 57-405, March 1957, 4 pp.

Designing Thermocouples for Response Rates, by R. J. Moffat, *ASME Pap.* 57-GTP-8, March 1957, 8 pp.

Methods of Measuring the Thermal Conductivity of Solids, by G. L. Cooper, *Gt. Brit., Atomic Energy Res. Estab., Rep.* Inf/Bib. 104, 1956, 10 pp.

Radar Video Integrator Study, by Roy W. Hendrick (Internal Research Project 81-011), *Cornell Aeron. Lab., Rep.* CAL-78, Jan. 1957, 51 pp.

Bourdon Elements Require Special Tubing, by Charles C. Mathews, *Instruments & Automation*, vol. 30, May 1957, pp. 891–893.

Precision Automatic Manometer Reader, by J. Farquharson and H. A. Kermicle, *Rev. Sci. Instrum.*, vol. 28, May 1957, pp. 324–325.

Thermistor Thermometer Bridge: Linearity and Sensitivity for a Range of Temperatures, by Kenneth S. Cole, *Rev. Sci. Instrum.*, vol. 28, May 1957, pp. 326–328.

Theory of a New Apparatus for Determining the Thermal Conductivities of Metals, by S. T. Hsu, *Rev. Sci. Instrum.*, vol. 28, May 1957, pp. 333–336.

X-Ray Powder Diffraction Assembly for Studies at Elevated Temperatures and High Gas Pressures, by Edward J. Goon, John T. Mason and Thomas R. P. Gibb Jr., *Rev. Sci. Instrum.*, vol. 28, May 1957, pp. 342–344.

Apparatus for the Measurement of Vapor Pressure and Ignition of Decomposition Temperature at Pressures Above Atmospheric, by A. Greenville Whittaker, *Rev. Sci. Instrum.*, vol. 28, May 1957, pp. 360–364.

Summary of the Computer Amplifier

PRESSURIZING AVIONIC SYSTEMS

Eastern pressurization equipment protects vital electronic gear. A continual program of research and development creates customized pressurization units that keep the performance of avionic systems unaffected by altitude and ambient conditions. Custom units that *meet military specifications* help to solve your problems when recommending electronic components.

When you have a challenging problem to prevent pressure, or heat, or moisture, or dust from affecting electronic performance, come to Eastern for complete and creative engineering help.

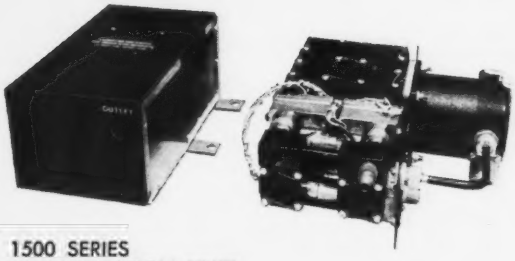

1500 SERIES
PRESSURIZATION UNIT

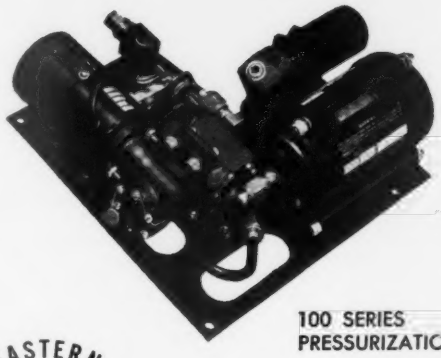

100 SERIES
PRESSURIZATION UNIT

EASTERN PRESSURIZATION UNITS

A variety of capacities accommodates a broad range of requirements and meets appropriate government standards. Typical units operate from zero to over 70,000 feet at temperatures from — 65°F to +160°F. Delivery: 0-3600 cu. in./min. free delivery, Discharge Pressure: 0-60 p.s.i. Standard sub-assemblies and components normally are used to create a custom-made design to fit your exact needs. Units may consist of an air pump and motor assembly, pressure switch, check valve, tank valve, terminal connectors, and dehydrator.

Write for Eastern AVIONICS BULLETIN 340

EASTERN AVIATION PRODUCTS

Eastern INDUSTRIES, INC.
100 Skiff St., Hamden 14, Conn.
West Coast Office: 1608 Centinela Avenue
Inglewood 3, California — Phone ORegon 8-3958

DATA PROCESSING SPECIALISTS!

Get in now—at the beginning of the new era in missiles!

When you join Telecomputing's Engineering Services Division, you will be given full scope to allow you to grow . . . your talents will be used to the fullest . . . recognition and rewards will be yours as a matter of course.

Engineering services is a member of an integrated five-company missile systems corporation which designs and manufactures its own data-processing equipment. Our efforts are directed toward the "systems concept." We are engaged in the reduction of large amounts of flight test data being generated by the daily missile firings on the integrated Holloman-White Sands range.

ATTRACTIVE SALARIES
PROFIT SHARING

RELOCATION PAY
ACCREDITED EDUCATION
GROUP INSURANCE

A NEW LIFE IN NEW MEXICO'S FABULOUS "LAND OF ENCHANTMENT"

MOUNTAIN SKIING AND DESERT RESORTS WITHIN 30 MINUTES!

A WONDERFUL PLACE TO MAKE YOUR HOME — GRAND COUNTRY TO RAISE KIDS!

Send resume to Director of Technical Personnel

TELECOMPUTING CORPORATION
Engineering Services Division

BOX 447 • HOLLOMAN AIR FORCE BASE • NEW MEXICO

MISSILE TEST DATA TRANSCRIPTION AND ANALYSIS

The transcription, analysis, and evaluation of ballistic missile test data is one of the important aspects of R-W's system engineering and technical direction responsibility for the Air Force Ballistic Missile Program. Utilizing the facilities of R-W's Data Reduction Center, test data are transcribed and reviewed to determine performance characteristics and confidence levels.

The following positions in this rapidly expanding field are currently open on the R-W staff:

Senior analyst to direct mathematicians, engineers, and technical aides in missile test analysis projects and to participate in overall evaluation of missile systems performance. The test information originates from optical, radar, and telemetry instrumentation. Particular emphasis is placed upon electronic analysis of vibration data.

Engineer with wide experience in telemetry operations. The position volves planning and directing the conversion of telemetered data into forms appropriate for the analysis of weapon systems performance. Experience in the design, maintenance, and operation of telemetry data transcription and electronic vibration analysis equipment is desirable.

Engineer experienced in the utilization of missile test data transcription equipment. This position involves the planning of equipment schedules, with various research and industrial organizations, for the conversion of missile test data. A thorough knowledge of the capabilities and limitations of telemetry transcription and electronic vibration analysis equipment is desirable.

Inquiries should be addressed to: **Mr. J. H. Armitage**

The Ramo-Wooldridge Corporation

5730 ARBOR VITAE STREET • LOS ANGELES 45, CALIFORNIA

Development for the NATIV Servo System, by W. D. Mullins Jr. and K. R. Jackson, *North American Aviation Inc., Rep.* AL162, March 1947, 15 pp. (Declassified from Confidential by authority of North American Aviation, Inc., letter 54D-6322, citing WADC letter WCSG, 8/6/54.)

Survey of Field Test Range Instrumentation Requirements for NATIV Firings, by Donald H. Jacobs, Warren Kott and Seymour Scholnick, *North American Aviation, Inc., Rep.* AL220, June 1947, 48 pp. (Declassified from Confidential by authority of North American Aviation, Inc., letter 54D-6322, citing WADC letter WCSG, 8/6/54.)

The NAA Telemetering System, by Donald H. Jacobs and Claude W. Chapman, *North American Aviation, Inc., Rep.* AL-371, Nov. 1947, 59 pp. (Declassified from Confidential by authority of North American Aviation, Inc., letter 54D-6233, citing WADC letter WCSG, 8/6/54.)

The NAA Time Standard System, by Donald H. Jacobs and Michael May, *North American Aviation, Inc., Rep.* AL372, Nov. 1947, 35 pp. (Declassified from Confidential by authority of North American Aviation, Inc., Letter 54D-6233, citing WADC letter WCSG, 8/6/54.)

The NAA Plotting Cameras, by Donald H. Jacobs, *North American Aviation, Inc., Rep.* AL378, Dec. 1947, 24 pp. (Declassified from Confidential by authority of North American Aviation, Inc., letter 54D-6233, citing WADC letter WCSG, 8/6/54.)

NAA Radar Recording Systems, by Donald H. Jacobs, *North American Aviation, Inc., Rep.* AL380, Rev. March 1948, 16 pp. (Declassified from Confidential by authority of North American Aviation, Inc., letter 54D-6233, citing WADC letter WCSG, Aug. 6, 1954.)

NAA Radar Modifications, by Donald H. Jacobs, *North American Aviation, Inc., Rep.* AL379, Rev. March 1948, 9 pp. (Declassified from Confidential by authority of North American Aviation, Inc., letter 54D-6233, citing WADC letter WCSG, 8/6/54.)

Semiannual Progress Report for the Period Ending June 30, 1955, *Nat. Bur. Standards, Off. Basic Instrumentation, Rep.* 4264, 68 pp.

A Simply Constructed Contour Gage, by W. W. Oshel and William C. Shaw, *NAVORD Rep.* 5436 (*NOTS* 1704), April 1957, 133 pp.

Astrophysics, Aerophysics

Reduction Methods for Photographic Meteor Trails, by Fred L. Whipple and Luigi G. Jacchia, *Smithsonian Contribs. Astrophys.*, vol. 1, no. 2, 1957, pp. 183–206.

The Method of Reduction of Short-Trail Meteors, by Gerald S. Hawkins, *Smithsonian Contribs. Astrophys.*, vol. 1, no. 2, 1957, pp. 207–214.

A Rapid Graphical Method of Meteor Trial Reduction, by Richard E. McCrosky, *Smithsonian Contribs. Astrophys.*, vol. 1, no. 2, 1957, pp. 215–224.

A Reduction Method for the Motions of Persistent Meteor Trains, by Allan F. Cook and Robert F. Hughes, *Smithsonian Contribs. Astrophys.*, vol. 1, no. 2, 1957, pp. 225–238.

Methods for the Study of Shower Radiants from Photographic Meteor Trails, by Fred L. Whipple and Francis

W. Wright, *Smithsonian Contribs. Astrophys.*, vol. 1, no. 2, 1957, pp. 239–243.

IGY World Warning Agency, *Tech. News Bull. (Nat. Bur. Standards)*, vol. 41, May 1957, pp. 65–66.

Meteor Burst Extends VHF Radio Range, by Philip J. Klass, *Aviation Week*, vol. 66, June 17, 1957, pp. 96–97, 99–101.

Materials of Construction

Influence of Crucible Materials on High-Temperature Properties of Vacuum-Melted Nickel-Chromium-Cobalt Alloy, by R. F. Decker, John P. Rowe and J. W. Freeman, *NACA TN* 4049, June 1957, 34 pp.

Inhibition of Titanium in Fuming Nitric Acid, by John B. Rittenhouse and Cornelius A. Papp, *Calif. Inst. Tech., Jet Propulsion Lab., Mem.* 20-140, -March 1957, 8 pp.

Tabulation, Bibliography and Structure of Binary Intermetallic Compounds, II: Compounds of Beryllium, Magnesium and Calcium, by K. A. Gschneidner, D. J. Beernstsen, R. W. Vest, J. A. Kingston and J. F. Smith, *Atomic Energy Comm.*, ISC-812, Dec. 1956, 36 pp.

Internal Friction and Shear Modulus of Thorium at High Temperatures, by C. E. Dixon and H. Hori, *ASME, Pap.* 57-NESC-6, March 1957, 4 pp. (*Nuclear Engng. and Sci. Conf., 2nd.*, Philadelphia, March 11–14, 1957).

Fabricated Pressure Piping as Related to Nuclear Applications, by J. J. Murphy, C. R. Soderberg Jr., H. S. Blumberg and D. B. Rossheim, *ASME, Pap.* 57-NESC-103, March 1957, 24 pp. (*Nuclear Engng. and Sci. Conf., 2nd.*, Philadelphia, March 11–14, 1957).

The Effect of Oxygen on Zirconium Uranium Epsilon Phase Alloys, by H. A. Saller, F. A. Rough and A. A. Bauer, *ASME, Pap.* 57-NESC-20, March 1957, 8 pp. (*Nuclear Engng. and Sci. Conf., 2nd.*, Philadelphia, March 11–14, 1957).

Bibliography on the Brazing of Mild Steel, by G. L. Cooper, *Gt. Brit., Atomic Energy Res. Estab., Rep.* Inf/Bib 103, 1956, 4 pp.

Thermal Stresses in HRT Pressure Vessel, by R. E. Aven, *Atomic Energy Comm.*, CF-55-2-128, Feb. 1955, 17 pp.

MTR Hot Cell Tests of High Pressure Piping, by M. S. Robinson, F. W. Rider and M. H. Bartz, *Atomic Energy Comm. Res. and Dev. Rep.* IDO-16294, Dec. 1956, 28 pp.

Two Factors Influencing Temperature Distributions and Thermal Stresses in Structures, by William A. Brooks, Jr., George E. Griffith and H. Kurt Strass, *NACA TN* 4052, June 1957, 13 pp.

The Combinations of Thermal and Load Stresses for the Onset of Permanent Buckling in Plates, by George W. Zender and Richard A. Pride, *NACA TN* 4053, June 1957, 10 pp.

Trends in the Use of Materials in the Electronics Industry in the United States, by M. Bousquet, *Fusées et Recherche Aéronautique*, vol. 1, no. 2, Oct. 1956, pp. 129–130 (in French).

Atomic Energy

The Safety Aspects of the Use of Nuclear Energy, by C. R. Russell, *SAE, Prepr.* 4, Jan. 1957, 7 pp., 7 fig.

Unclassified Engineering Materials List, *Atomic Energy Comm., TID* 4100, Jan. 1957.

the

A. W. HAYDON COMPANY'S

ELAPSED TIME INDICATORS

measure a of time . . . for

INDUSTRIAL, AIRCRAFT and MILITARY *applications*

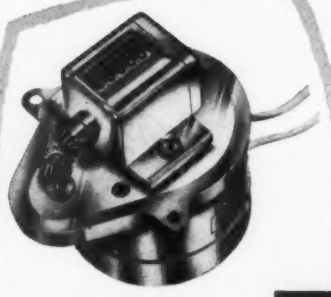

7500 SERIES DC ELAPSED TIME INDICATOR

Send for Bulletins: AWH ET600 Basic Elapsed Time Indicators 7500, 12500, 24200 Series.

Now the Company offers a complete line of timing motors and devices to record the operating time of any electrical or electronic equipment. Compact, minimum weight, each unit has five digits. They can be used to provide daily running time plus a total running record, eliminating estimating or manual totalizing. They increase efficiency and reduce costs, since they provide the quickest way to know when to lubricate, overhaul or replace equipment. They give on-the-spot pictures of idle and waiting periods for machinery. Used with electronic equipment, they tell when to replace tubes, preventing costly failures during essential operating periods.

In both AC and DC, continuous or manual reset for 50 or 60 up to 400 cycle line frequency. Will measure hours or on down to 10ths of seconds. All models can be supplied with Radio Interference Filtering to meet MIL-1-6181B.

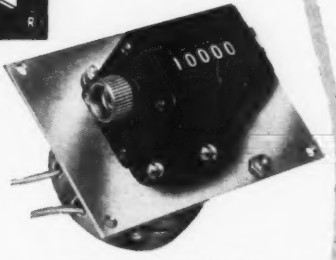

7500 SERIES RESET TYPE ELAPSED TIME INDICATOR

Send for Bulletins: AWH ET601 Reset Type Elapsed Time Indicators 7500, 12500, 24200 Series.

Preferred Where Performance is Paramount.

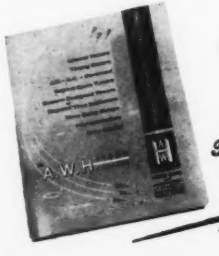

Shown at the left is the new A. W. Haydon Co. catalog describing the complete line of timing motors and devices; if you haven't received your copy write for it on your company letterhead.

The **A.W. HAYDON Company**

248 NORTH ELM STREET, WATERBURY 20, CONNECTICUT

Design and Manufacture of Electro-Mechanical Timing Devices

small, light, reliable
Robertshaw-Fulton
HELIUM
Pressure Regulators

Size, weight, performance—a key consideration in helium pressurization projects. Turn to R-F Aeronautical—a prime source for helium control components. Engineering experience, complete helium testing facilities... combined to meet your pressurization requirements—faster and better.

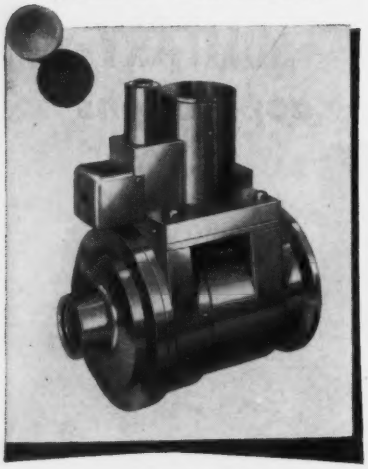

TYPICAL—this missile borne Helium Pressure Regulator with integral shut-off. INLET PRESSURE: 325±25 psig, NOMINAL OUTLET PRESSURE: 20±0.5 psia (or psig), FLOW RATE: 2000 scfm, OPERATING TEMP: AMBIENT: —65° to 165°F, GAS: —80° to 350°F. INITIAL RESPONSE TIME: 20 μsec. WEIGHT: 2.75 lbs. max. DIMENSIONS: 6⅜" x 3⅜" x 5-15/16", no flutter, chatter, overshoot, or instability.

At R-F Aeronautical—a complete line of helium pressure regulators... shelf and to specification... smaller, lighter, more reliable. Write for technical data.

Products for Progress by the Men of the
AERONAUTICAL DIVISION
RF Robertshaw-Fulton
CONTROLS COMPANY
Santa Ana Freeway at Euclid Avenue
Anaheim, California

Sponsor: The Annual Helium Symposium

Index to Advertisers

AEROJET-GENERAL CORPORATION ..... Back Cover
D'Arcy Advertising Co., Los Angeles, Calif.

AMERICAN MACHINE & FOUNDRY CO. 1271
Fletcher D. Richards, Inc., New York, N. Y.

AMERICAN POTASH & CHEMICAL CORPORATION 1221
The McCarty Co., Los Angeles, Calif.

B & H INSTRUMENT CO., INC. 1279
The Kotula Company, New York, N. Y.

BROOKS & PERKINS, INC. 1284
Holden, Chapin, Larue, Inc., Detroit, Mich.

CENTURY ELECTRONICS & INSTRUMENTS, INC. 1272
Gibbons Advertising Agency, Inc., Tulsa, Okla.

COAST MANUFACTURING & SUPPLY COMPANY 1274
Peter Hurst Advertising, Inc., San Francisco, Calif.

CONVAIR, A DIVISION OF GENERAL DYNAMICS CORPORATION ..... Third Cover
Buchanan & Co., Inc., New York, N. Y.

CURTISS-WRIGHT CORPORATION 1224
Burke Dowling Adams, Inc., New York, N. Y.

DIVERSEY ENGINEERING COMPANY 1230
Roark & Colby Advertising, Chicago, Ill.

DOEHLER-JARVIS DIVISION, NATIONAL LEAD COMPANY 1276–1277
Marschalk & Pratt, Div. of McCann-Erickson, New York, N. Y.

THE DOW CHEMICAL COMPANY 1269
MacManus, John & Adams, Inc., Bloomfield Hills, Mich.

DU PONT DE NEMOURS, E. I., AND COMPANY 1281
EXPLOSIVES DEPARTMENT
Charles L. Rumrill & Co., Inc., Rochester, N. Y.
PHOTO PRODUCTS 1219
N. W. Ayer & Son, Inc., Philadelphia, Pa.

EASTERN INDUSTRIES, INC. 1287
Remsen Advertising Agency, Inc., New Haven, Conn.

EXCELCO DEVELOPMENTS, INC. 1228

THE GARRETT CORPORATION, AiRESEARCH MANUFACTURING COMPANY 1273
J. Walter Thompson Co., Los Angeles, Calif.

THE A. W. HAYDON COMPANY 1289
Cory Snow, Inc., Boston, Mass.

HEILAND DIVISION, MINNEAPOLIS-HONEYWELL 1282–1283
Tool & Armstrong Advertising, Denver, Colo.

KATO ENGINEERING COMPANY 1286
Frizzell Advertising Agency, Minneapolis, Minn.

KELLOGG, THE M. W., COMPANY 1222
Fuller & Smith & Ross, Inc., New York, N. Y.

LAVEZZI MACHINE WORKS 1286
R. W. Sayre Co., Chicago, Ill.

LIBRASCOPE, INC. 1278
Western Advertising Agency, Inc., Los Angeles, Calif.

MARQUARDT AIRCRAFT COMPANY 1284–1285
Grant Advertising, Inc., Hollywood, Calif.

NORTHAM ELECTRONICS, INC. 1286
Heintz & Co., Inc., Los Angeles, Calif.

THE NORTON COMPANY 1229
James Thomas Chirurg Co., Boston Mass.

PHILLIPS PETROLEUM COMPANY 1223
Lambert & Feasley, Inc., New York, N. Y.

THE RAMO-WOOLDRIDGE, CORPORATION 1288
The McCarty Co., Los Angeles, Calif.

REACTION MOTORS, INC. ..... Second Cover
Aitkin-Kynett Co., Philadelphia, Pa.

REVERE CORPORATION OF AMERICA 1280
W. L. Towne Advertising, New York, N. Y.

ROBERTSHAW-FULTON CONTROLS COMPANY 1290
Leland Oliver Co., Santa Ana, Calif.

ROCKETDYNE, A DIVISION OF NORTH AMERICAN AVIATION, INC. 1275
Batten, Barton, Durstine & Osborn, Los Angeles, Calif.

SANBORN COMPANY 1227
Culver Advertising, Inc., Boston, Mass.

SOUTHWEST PRODUCTS COMPANY 1278
O. K. Fagan Advertising Agency, Los Angeles, Calif.

STATHAM INSTRUMENTS, INC. 1270
Western Advertising Agency, Inc., Los Angeles, Calif.

TELECOMPUTING CORPORATION 1288
Mogge-Privett, Inc., Los Angeles, Calif.

WESTVACO CHLOR-ALKALI DIVISION, FOOD MACHINERY AND CHEMICAL CORPORATION 1225
James J. McMahon, Inc., New York, N. Y.

WYMAN-GORDON COMPANY 1226
John W. Odlin Co., Inc., Worcester, Mass.

570 7